CHARACTERIZING ANAEROBIC BIODEGRADATION OF GASOLINE WITH LOW MOLECULAR WEIGHT ORGANIC ACID ANIONS AND PHOSPHATE AMENDMENT

A Dissertation Submitted to the College of Graduate and Postdoctoral Studies

in Partial Fulfillment of the Requirements

for the Degree of Doctor of Philosophy

in the Department of Soil Science

University of Saskatchewan

Saskatoon

By

Tingting Chen

PERMISSION TO USE

In presenting this dissertation in partial fulfillment of the requirements for a Postgraduate degree from the University of Saskatchewan, I agree that the Libraries of this university may make it freely available for inspection. I further agree that permission for copying of this dissertation in any manner, in whole or in part, for scholarly purposes may be granted by the professor or professors who supervised my dissertation work or, in their absence, by the Head of the Department or the Dean of the College in which my dissertation work was done. It is understood that any copying or publication or use of this dissertation or parts thereof for financial gain shall not be allowed without my written permission. It is also understood that due recognition shall be given to me and the University of Saskatchewan in any scholarly use which may be made of any material in my dissertation. Requests for permission to copy or make other uses of materials in this dissertation, in whole or part, should be addressed to:

Head of the Department of Soil Science
Agriculture Building
University of Saskatchewan
51 Campus Drive
Saskatoon, Saskatchewan, Canada
S7N 5A8

OR

Dean
College of Graduate and Postdoctoral Studies
University of Saskatchewan
Room 116, Thorvaldson Building, 110 Science Place
Saskatoon, Saskatchewan, Canada
S7N 5C9

DISCLAIMER

Reference in this dissertation to any specific commercial products, process, or service by trade name, trademark, manufacturer, or otherwise, does not constitute or imply its endorsement, recommendation, or favouring by the University of Saskatchewan. The views and opinions of the author expressed herein do not state or reflect those of the University of Saskatchewan, and shall not be used for advertising or product endorsement purposes.

ABSTRACT

Bioremediation is a feasible method to clean up petroleum hydrocarbons (PHC) contaminated soil. But bioremediation is often limited by nutrient bioavailability, PHC bioaccessibility, microbial activity and environmental factors. It was hypothesized low molecular weight organic acid anions (LMOAA) can enhance PHC biodegradation by increasing PHC bioavailability, increasing phosphorus (P) bioavailability, or stimulating hydrocarbon degrader community. A microcosm study and a field study were conducted to evaluate this hypothesis. In the microcosm study, 10-100 mM citrate increased petroleum hydrocarbon bioavailability to enhance *in situ* anaerobic gasoline degradation. Lower citrate addition, 1.0 mM and 1.75 mM, accelerated *ex situ* biodegradation for benzene and gasoline respectively, probably through changing P bioavailability. In the field, two large bore injectors were constructed in a gasoline contaminated cold region calcareous site, for *in situ* biostimulation solution delivery. Two biostimulation solutions were applied. The first solution containing 11 mM $MgSO_4$, 1 mM H_3PO_4, and 0.08 mM HNO_3 (phosphate amendment) stimulated the site for about 4 months. Then, 10 mM citric acid was incorporated into the existing biostimulation solution (phosphate and citrate amendment) for another 8 months. Dissolved P in groundwater and bioavailable organic P in soil were increased after citrate addition, which corresponded to the decrease for benzene, toluene, ethylbenzene, and xylene (BTEX) in groundwater and $F1_{-BTEX}$ (C6-C10 with BTEX subtracted) decrease in soil. Citrate addition also increased benzoate degradation N (*bzdN*, encoding ATP-dependent benzoyl-CoA reductase subunit N) gene prevalence and culturable anaerobic PHC degraders population in soil. After applying phosphate amendment, the bacterial community structure changed in both soil and groundwater. However, the influence of citrate on microbial community differed between soil and groundwater. Citrate selectively stimulated anaerobic hydrocarbon degraders in groundwater, and reversed soil bacterial community structure, which corresponded to the rebounded adsorbed phosphate. In addition, a method trapping $^{13}CO_2$ produced from ^{13}C-labelled contaminates was developed and successfully assessed PHC mineralization rate using the cavity ring-down spectrometry. This research highlights the positive effect of LMOAA on anaerobic PHC biodegradation through increasing PHC/P bioavailability and stimulating PHC degraders.

ACKNOWLEDGEMENTS

I am very grateful for the support, patience, and encouragement from my supervisor, Dr. Steven Siciliano. I would like to acknowledge the helpful input and guidance from my advisory committee, Drs. Derek Peak, Richard Farrell, Darren Korber, and Wonjae Chang. I would also like to thank my external examiner, Dr. Lyle Whyte, for taking time to review and to contribute to this dissertation.

Financial support for this work was provided by the Natural Sciences and Engineering Research Council of Canada (NSERC) and the Federated Co-operatives Limited (FCL) through grants to Dr. Siciliano. Personal support was received from the Chinese Scholarship Council (CSC), the Department of Soil Science, the University of Saskatchewan, and the stipend from Dr. Siciliano.

Much of the work in this dissertation would not have been possible without the help from everyone in 3D13/5E75/5E19/4E05/5C13. I am grateful to Richard Nhan, Alix Schebel, Galen Seilis, Prabhakara Medihala, Alexander Grigoryan, Frank Krijnen, Darin Richman and Gourango Kar for their patience, kindness, and sharing their technical savvy. Thanks to Tanja Wildemann, Martin Brummell, Kyle James, Rachel Peters, Erin Karppinen, Wai Ma, Steven Mamet, and Aimée Schryer for all the help. I am grateful to J. Renato de Freitas, Katherine Stewart, Bobbi Helgason, Bing Si and Angela Bedard-Haughn for advice and resources.

The field campaigns that form the foundation of my work were cooperative ventures among the University, FCL, and SaskPolytech, especially Jay Grosskleg, Kris Bradshaw, and Trevor Carlson. Thanks for all your efforts.

To all the friends I've made in the department, your support and our lively discussions in and outside the soil science world kept me sane; especial thanks to Marc, Kim, Sina, Xiaoyue, Jing, Min, Minghui, Chen, Liting, Katie, Amy, Mark, Courtney, Jordan and David.

DEDICATION

I dedicate this dissertation to the people who made me the person I am today, cared about me, supported me, and believed in me even when I was not sure whether I can do it or not…my parents, Qunxian Chen and Shoufu Zeng; my younger brother, Xuanjia Chen. Thank you for all the support!

TABLE OF CONTENTS

LIST OF TABLES

LIST OF FIGURES

LIST OF ABBREVIATIONS

ANOVA: analysis of variance

BCR: benzoyl-CoA reductase

BTEX: benzene, toluene, ethylbenzene, xylenes

CCME: Canadian Council of Ministers of the Environment

CRDS: cavity ring-down spectrometry

CSIA: compound-specific isotope analysis

D: Simpson's index

F1: fraction 1, petroleum hydrocarbons with equivalent carbon numbers C6 to C10

F2: fraction 2, petroleum hydrocarbons with equivalent carbon numbers >C10 to C16

F3: fraction 3, petroleum hydrocarbons with equivalent carbon numbers >C16 to C34

F4: fraction 4, petroleum hydrocarbons with equivalent carbon numbers C34+

FID: flame ionization detector

GC: gas chromatograph

GC-TCD: gas chromatography-thermal conductivity detector

H: Shannon-Weaver index

HOCs: hydrophobic organic contaminants

IRMS: ratio mass spectrometry

LMOA: low molecular weight organic acid

LMOAA: low molecular weight organic acid anion

MPN: most probable number

$NaHCO_3$-IP: inorganic phosphorus extracted by $NaHCO_3$

$NaHCO_3$-OP: organic phosphorus extracted by $NaHCO_3$

NaOH-IP: inorganic phosphorus extracted by NaOH

NaOH-OP: organic phosphorus extracted by NaOH

NAPL: non-aqueous phase liquids

NMDS: non-metric multidimensional scaling

P: phosphorus

PHC: petroleum hydrocarbons

qPCR: quantitative polymerase chain reaction

RDA: redundancy analysis

Resin-P: P extracted by resin

SBE: sorptive bioaccessibility extraction

SOM: soil organic matter

TDS: total dissolved solid

XANES: X-ray absorption near-edge structure

XRF: X-ray fluorescence

1. INTRODUCTION

The world demand for oil was 86 million barrels per day in 2008 (Duffner et al., 2012). Due to the global transport and use, petroleum hydrocarbon (PHC) is one of the most widespread contaminants in the world, with 600,000 tonnes (± 200,000) of crude oil lost per year (Rohrbacher and St-Arnaud, 2016). As defined by the CABERNET (Concerted Action on Brownfields and Economic Regeneration) network, brownfields are 'sites that have been affected by the former uses of the site and surrounding land; are derelict and underused; may have real or perceived contamination problems; are mainly in developed urban areas; and require intervention to bring them back to beneficial use' (Kley et al., 2011). About a decade ago, a study reported the situation for the urban brownfields redevelopment in Canada (Sousa, 2006), gathering information based on a mail-out survey distributed to 55 Canadian cities and from visits to four cites which take proactive management for their brownfields. The study mentioned that 25% of the Canadian urban landscape is potentially contaminated and the national range for the estimated number of potentially contaminated sites is from 2,900 to 30,000. Many of these brownfields are located on prime land in cities, valuable for redevelopment (Canadian Real Estate Association, 2008). But there are about 80-85% brownfields where cleanup costs would be far outweighed the potential value of the land after cleanup (Canadian Real Estate Association, 2008). Consequently, bioremediation may be a good option for these sites, offering much cheaper costs for PHC contaminated brownfield clean-up than common physical approaches to remediation. Bioremediation uses the ability of some organisms (plants, fungi, and bacteria) to sequester, concentrate, and or degrade pollutants in the environment (Rohrbacher and St-Arnaud, 2016), and is considered to be an environment-friendly, cost-effective technique. Bioremediation can clean up the sites without excavation, resulting in lower costs, less labor requirements and a lower carbon footprint (Hunkelera et al., 1999; Vasudevan and Rajaram, 2001; Yang et al., 2009; Chandra et al., 2013; Fuentes et al., 2014).

However, bioremediation for PHC is often limited by PHC and/or phosphorus (P) bioavailability, and active hydrocarbon degrader community (Das and Chandran, 2011; Chandra et al., 2013; Fuentes et al., 2014; Martin et al., 2014). Low molecular weight organic acid anions (LMOAA) may resolve problems caused by these three limiting factors. The LMOAA may increase the PHC bioavailability, increase P bioavailability, and or stimulate the hydrocarbon-

degrader populations, to enhance the PHC biodegradation (Martin et al., 2014; Rohrbacher and St-Arnaud, 2016). LMOAA, such as oxalate, promoted the desorption of organic contaminants, polybrominated diphenyl ethers, increased their availability, resulted in distinct shifts in soil bacterial communities, and increased the degradation rate (Huang et al., 2016). Citrate can also help P release in the soil (Chatterjee et al., 2015). Citrate enhances dissolution of P minerals caused by acidification and complexation of cations such as calcium (in alkaline soils), aluminum, and iron (in acid soils) from phosphate minerals, and competes with P for adsorption on metal (hydr)oxides (Duffner et al., 2012). Citrate and malonate increase microbial activity in uncontaminated and diesel-contaminated soil microcosms studies (Martin et al., 2016). Most studies on LMOAA on organic contaminants focus on polyaromatic hydrocarbons bioavailability, P desorption or microbial community structure (Ström et al., 2005; Johnson and Loeppert, 2006; Sato and Comerford, 2006; Wei et al., 2010; An et al., 2010, 2011; Kan et al., 2011; Gao et al., 2015; Ling et al., 2015; Raynaud et al., 2016). Relatively little research has focussed on the effect on LMOAA on gasoline (as a complex mixture) bioavailability, P bioavailability or microbial PHC degrader community in a brownfield site.

The overall goal for this dissertation was to assess the influence of LMOAA (mainly citrate) on gasoline bioavailability, P bioavailability, microbial community during gasoline biodegradation, especially under anaerobic conditions. This was accomplished with microcosm studies and field trials, with physical, chemical, and biological strategies.

1.1 Organization of the Dissertation

The research presented in this dissertation was organized in the manuscript format. Following this introduction and the literature review presented in Chapter 2, four studies were presented from Chapter 3 to Chapter 6. The first three research chapters presented the results of studies outlining the influence of LMOAA on PHC bioavailability (Chapter 3), P bioavailability (Chapter 4), and microbial community function and structure for PHC bioremediation amended with phosphate fertilizer (Chapter 5). Chapter 6 developed an approach to assess the mineralization rate for PHC biodegradation.

The goal of the microcosm project in Chapter 3 was to identify a good combination of citrate and phosphate to enhance the anaerobic bioremediation in cold calcareous gasoline

contaminated site. Chapter 3 also tested the effect of LMOAA on PHC bioavailability for phosphate amended anaerobic benzene or gasoline biodegradation under mimicked *in situ* and *ex situ* conditions. Dissipation and distribution of PHC was analyzed in the water and soil phase with microcosm studies, at cold or ambient temperature.

Based on the result of Chapter 3, the objective of Chapter 4 was to explore how citrate addition influenced the P bioavailability and gasoline biodegradation in calcareous cold-region soils in a former gas station. Changes for BTEX and $F1_{\text{-BTEX}}$ concentration were investigated in the soil and groundwater. Sequential P extraction and X-ray fluorescence (XRF) determined the P speciation in the soil samples. Groundwater properties were also analyzed, including dissolved P and iron(II).

To explore how the citrate and phosphate combination influenced the indigenous bacterial community especially the anaerobic hydrocarbon degraders, Chapter 5 constructed 16S metagenomics sequencing library for soil and groundwater samples from the field site. Functional activity was estimated with quantitative PCR and most probable number method. The P K-edge X-ray absorption near-edge structure technique determined the soil phosphate mineral composition to understand the change for bacterial community in soil and groundwater.

Chapter 6 presented the development of a strategy to assess the anaerobic hydrocarbon mineralization rate for indigenous microbial community using stable isotope technique. Benefits and limitations were evaluated for this approach. Benzene and phenanthrene were chosen representative compounds for PHC. The mineralization rate calculation was based on the difference for $^{13}CO_2$ production between ^{13}C labelled substance biodegradation and the normal substance biodegradation. Finally, Chapter 7 synthesized the major findings of the research studies and suggested future work.

2. LITERATURE REVIEW

2.1 Petroleum hydrocarbons (PHC) contamination and bioremediation

Petroleum hydrocarbons (PHC), a wide range of organic compounds, are one of the most widespread soil contaminants in Canada (Canadian Council of Ministers of the Environment [CCME], 2008a). PHC can be divided into four fractions (CCME, 2008b). These fractions are defined based on their equivalent carbon (EC) numbers. The EC of a compound is the corresponding carbon number when the boiling point or retention time of that compound is normalized to the boiling point or retention time of the *n*-alkanes in a boiling point gas-chromatography (GC) column. Compounds with similar leachability and volatility values are grouped into a fraction, represented by an EC range. Fraction 1 (F1) hydrocarbons encompass the range from C_6 to C_{10}. It represents the volatile fraction of most hydrocarbon mixtures. Fraction 2 (F2) is from $>C_{10}$ to C_{16}. Fraction 3 (F3) is from $>C_{16}$ to C_{34}. Fraction 1, 2 and 3 all have aromatic sub-fractions and aliphatic sub-fractions. Fraction 4 (F4) is C_{34+}. PHC could cause a variety of problems for several reasons. First, their reduced nature and volatility pose a fire or explosion hazard. Second, PHC constituents are toxic. Third, lighter hydrocarbons are mobile and can move in groundwater or air. Fourth, larger and branched chain hydrocarbons are persistent in the environment. Fifth, they may create aesthetic problems such as offensive odor, taste or appearance in environmental media. Finally, under some conditions they can degrade soil quality by influencing water retention and transmission, and nutrient supplies (CCME, 2008a).

PHC contamination caused by leakage from underground storage tanks or pipelines and by accidental spills is very common in brownfields areas (Menendez-Vega et al., 2007) of which there are approximately 30,000 in Canada (Lam, 2004). Brownfields, industrial areas that have contaminated soils and groundwater from past chemical leaks, can increase in value and useability if these sites could be safely cleaned (Lam, 2004; Licht and Isebrands, 2005). However, cleaning these brownfields has proven to be difficult and challenging. CCME developed a 3-tiered, risk-based remedial standard, Canada-Wide Standard for Petroleum Hydrocarbons in Soil (PHC CWS), for four generic land uses – agricultural, residential/parkland, commercial and industrial (CCME, 2008c). Tier 1 is for remediation to generic criteria based on

land use; tier 2 is modified based on site-specific parameters; tier 3 is site-specific risk assessment and/or risk management. The common land uses in brownfields are residential/parkland, and commercial. Table 2.1 shows the tier 1 criteria for soils and groundwater based PHC CWS in Saskatchewan and Canada.

There are plenty of remediation techniques for contaminated environmental soil. Traditional technologies include excavation, transport to specialized landfills, incineration, stabilization and vitrification. There are two main classification systems for the remediation techniques (Table 2.2). One is characterized by the discipline principle these techniques utilize, such as physical, chemical, or biological remediation. The other one is based on whether need to remove the contaminated material, including *ex situ* and *in situ* remediation. *Ex situ* remediation involves excavating and removing contaminated soils, which effectively displace rather than address the problem. The disposal of soil material after *ex situ* treatment of contaminated soil also is a problem (van Hees et al., 2008). Relative to *ex situ* remediation, *in situ* remediation attracts more attention recently, due to its environmental-friendly, cheap and convenient characteristics. The remediation strategy selection for a contaminated site mainly depends on the contaminants in the site. For volatile organic contaminants like, e.g. aromatics, the most efficient technique is soil vapor extraction, and for inorganic contaminants like heavy metals, electrokinetic remediation, which can solubilize ionic pollutants from ground and groundwater, is one potential solution (Lageman et al., 2005). The latest developments in remediation technology often involve combination of two or more comprehensive remediation techniques. For example, chemical oxidation can collaborate with aerobic bioremediation techniques, and chemical reduction can be used for anaerobic bioremediation (Sullivan and Sylvester, 2006).

Bioremediation, defined by the United States Environmental Protection Agency (USEPA) as a treatability technology, uses biological activity to reduce the concentration and/or toxicity of a pollutant. Bioremediation of PHC-contaminated soils has been investigated since the late 1940s, but interest increased after the Exxon Valdez oil spill in 1989 (Sarkar et al., 2005). Compared with other technologies, bioremediation technologies are less expensive, less labor intensive, and these techniques have a lower carbon footprint and a higher level of public acceptance. Bioremediation uses microorganisms and plants. However, some chemicals are not

Table 2.1. Tier 1- Risk-based criteria for petroleum hydrocarbons in soil and groundwater.

Petroleum Hydrocarbons	Soils (mg kg^{-1})				Groundwater (mg L^{-1})		Reference
	Coarse-Grained		Fine-Grained		Exposure Pathway		
	Residential	Commercial	Residential	Commercial	Potable Groundwater†	Freshwater/Aquatic Life‡	
Benzene	0.03	0.03	0.0068	0.0068	0.005	0.37	Saskatchewan Ministry of Environment (2009)
Toluene	0.1	0.1	0.08	0.08	0.024	0.002	
Ethylbenzene	0.082	0.082	0.018	0.018	0.0024	0.09	
Xylenes	11	11	2.4	2.4	0.3	NA§	
F1 (C6-C10)	30	240	170	170	NA	NA	CCME (2008c)
F2 (>C10-C16)	150	260	150	230	NA	NA	
F3 (>C16-C34)	300	1700	1300	2500	NA	NA	
F4 (>C34)	2800	3300	5600	6600	NA	NA	

† applies to coarse- and fine-grained soils.
‡ applies to coarse-grained soils only 10 m – 500 m from surface water.
§ NA denotes not available

amenable for bioremediation, for example, radionuclides, some metals and some chlorinated compounds (Boopathy, 2000).Typically, bioremediation is considered a site-specific solution due to the variety of factors that influence bioremediation success.

When using bioremediation technologies, some factors need to be considered, i.e., PHC partitioning, bioavailability of pollutants, electron acceptors, nutrients, and the suitable microorganisms (McGuinness and Dowling, 2009; Schwitzguébel et al., 2011). PHC are water-immiscible contaminants, present in the soil as four phases: soil gas, sorbed to soil materials, dissolved in water, or an immiscible liquid (Huling and Weaver, 1992; Newell et al., 1995; Zytner, 2002). Lighter PHC are volatile as gas phase. Solid phase is adsorbed to the soil organic matter (SOM) and soil colloids. Liquid PHC often exist as non-aqueous phase liquids (NAPL) or dissolved aqueous PHC. NAPL is an immiscible phase. The PHC can partition between any one or all four of these phases. The distribution of PHC between these phases can be represented by partition coefficients such as Henry's Law constant describing partitioning between water and soil gas. The partition coefficients are highly dependent on the properties of the subsurface materials and the NAPL (Newell et al., 1995).

The bioavailability of PHC is determined by absorption and adsorption process (Pignatello and Xing, 1996). The sorption can occur by physical adsorption on a surface, or by partitioning (dissolution) into a phase such as the SOM. Most PHC contaminants in soil and subsurface environments are poorly soluble in water and therefore persist in NAPL, sorbing onto the soil colloids or the SOM. And the sorption partition coefficients normalized to organic carbon content are constant for organic compounds, which implies that the PHC will partition into SOM more than PHC will adsorb to soil mineral surfaces (Heyse et al., 2002). The partitioning between soil and water for PHC is driven by SOM. A study found that biodegradation and partitioning rates of phenanthrene from NAPL to water varied with the NAPL and the concentration of the test substrate. Biodegradation was slow if the partitioning rate was slow (Grimberg et al., 1996). The SOM can form complex with inorganic ions (e.g. Fe^{3+}, Al^{3+}, Ca^{2+} and Mg^{2+}) (Ding et al., 2011). In addition, polyvalent metal ions serve as linking agents binding to the multiple carboxyl or phenolate groups on soil organic matter. The free SOM or dissolved organic matter bind to PHC in the ambient soil solution and reduce its adsorption onto the soil. It was reported that the contribution of clay surfaces to hydrophobic

Table 2.2. Examples for remediation techniques.

Type of technology	Remediation technology	Technology category	References
Physical	Landfilling	*Ex situ*	Gavrilescu et al. (2009)
Physical	Soil washing	*Ex situ*	Sims (1990)
Physical	Thermal desorption	*In situ*/ *Ex situ*	Yao et al. (2012)
Physical	Membrane separation	*Ex situ*	Li and Zhang (2012)
Physical	Solidification	*In situ*/ *Ex situ*	Wang et al. (2012a)
Chemical	Chemical leaching	*In situ*/ *Ex situ*	Tong and Yuan (2012)
Chemical	Chemical fixation	*In situ*/ *Ex situ*	Shi et al. (2009)
Chemical	Electrokinetic remediation	*In situ*	Sun et al. (2012); Barrera-Díaz et al. (2012)
Chemical	Vitrify technology	*In situ*/ *Ex situ*	Yao et al. (2012)
Chemical	Oxidation	*In situ*/ *Ex situ*	Romero et al. (2011)
Biological	Composting	*In situ*/ *Ex situ*	Hashim et al. (2011)
Biological	Plant-assisted microbial remediation	*In situ*/ *Ex situ*	Megharaj et al. (2011)
Biological	Phytoremediation	*In situ*/ *Ex situ*	McGuinness and Dowling (2009); Schwitzguébel et al. (2011)
Biological	Bioremediation	*In situ*/ *Ex situ*	Farhadian et al. (2008); Yang et al. (2009); Lin et al. (2010)
Biological	Animal remediation	*In situ*/ *Ex situ*	Gan et al. (2009b)

sorption in soils can be significant when the OM content is below 6-8% (Ortega-Calvo et al., 1997).

Bioavailability is the portion of a compound that enters a biological organism. As this can be difficult to measure, two endpoints are commonly used to estimate potential bioavailability: bioaccessibility and chemical activity. The bioaccessibility represents the determination of the hydrophobic organic contaminants (HOCs) fraction which are weakly or reversibly sorbed and can be rapidly desorpted from the solid phase into the aqueous phase; the chemical activity means the potential fraction of HOCs which undergo spontaneous processes such as partitioning, at equilibrium according to the Equilibrium Partitioning Theory (Cui et al., 2013). Bioaccessibility quantifies a relative long uptake of available contaminants, which can be determined by partial extraction methods, such as mild solvent extraction, cycoldextrin extraction, Tenax extraction. However, bioaccessiblity is influenced by the sample matrix, properties of contaminants, desorption time, due to the operationally defined conditions of the bioaccessibility test. The chemical activity is the freely dissolved concentration in equilibrium samples. The bioavailability for biodegradation is dependent on the bioaccessibility. The decreasing freely dissolved concentration of PHC during biodegradation can be quickly replenished by the fraction that is reversibly sorbed, which is a limitation for some extraction methods. Gouliarmou and Mayer developed a sorptive bioaccessibility extraction (SBE) method with an absorption sink, which avoids underestimating bioaccessibility (Gouliarmou and Mayer, 2012; Gouliarmou et al., 2013). The principle for the SBE is providing an infinite sink without phase separation steps under the addition of diffusive carrier to enhance desorption process (Gouliarmou and Mayer, 2012), and it can be used as a passive dosing method to estimate the biodegradation of PHC with low water solubility for biodegradation kinetic data (Birch et al., 2017).

The electron acceptor determines the pathway for bioremediation of PHC (Haritash and Kaushik, 2009). Aerobic PHC bioremediation is the preferred way, because many common degraders are aerobic and oxygen provides the greatest amount of energy per unit of PHC degraded (Menendez-Vega et al., 2007). It is assumed that the soil has sufficient oxygen content (air volume fraction is from 40% to 50%) when the gravimetric water contents are within the range of 3-11% and the bulk densities are between 1.0 and 1.2 g mL^{-1} (Powell et al., 2006). The anaerobic condition is present in water submerged soil such as paddy field, swamps and deep underground soil, and even exists in anoxic microsites in aerobic soils. As a result, oxygen

limitation is a common problem for PHC bioremediation. Chemical amendments are usually applied to oxygenate the groundwater and soil. For instance, both solid and liquid peroxides have been used in hydrocarbon bioremediation. Aerobic treatment is easy to use, cheap, non-persistent, and safe. However, sometimes the delivery of oxidants is difficult and expensive. Nitrate, manganese, iron, sulfate can act as electron acceptors for anaerobic bioremediation. The reduction of NO_3^-, Fe(III), Mn(IV), SO_4^{2-}, and CO_2 can also be coupled with the mineralization of PHC. Based on the Gibbs free energies, the anaerobic toluene biodegradation potential follows the order nitrate reducing > iron reducing > sulfate reducing > methanogenic (Heider et al., 1998), and benzene biodegradation follows the similar order (Table 2.3). The rate for degradation of PHC varies under different redox states (Foght, 2008).

Table 2.3. Stoichiometric equations and standard free energy changes ($\Delta G^{0\prime}$) for benzene biodegradation.

Electron Acceptor	Stoichiometric Equation	$\Delta G^{0\prime}$ (kJ mol^{-1})	Reference
CO_2	$C_6H_6 + 6.75\ H_2O \rightarrow 2.25\ HCO_3^- + 3.75\ CH_4 + 2.25\ H^+$	-116	Burland and Edwards (1999)
SO_4^{2-}	$C_6H_6 + 3\ H_2O + 3.75\ SO_4^{2-} \rightarrow 6\ HCO_3^- + 1.875\ H_2S + 1.875\ HS^- + 0.375\ H^+$	-185	Kleinsteuber et al. (2008)
Fe^{3+}	$C_6H_6 + 18\ H_2O + 30\ Fe^{3+} \rightarrow 6\ HCO_3^- + 30\ Fe^{2+} + 36\ H^+$	-3070	Burland and Edwards (1999)
NO_3^-	$C_6H_6 + 6\ NO_3^- \rightarrow 6\ HCO_3^- + 3N_2$	-2978	Vogt et al. (2011)
O_2	$C_6H_6 + 7.5\ O_2 + 3\ H_2O \rightarrow 6\ HCO_3^- + 6\ H^+$	-3173	Weelink et al. (2007)

Many pure cultures of aerobic and anaerobic bacterial strains are proven to be able to degrade PHC, such as benzene, toluene, ethylbenzene, and xylene (BTEX) (Das and Chandran, 2011; Sarkar et al., 2017). Isolated from a hydrocarbon-contaminated industrial area, *Serratia sp.* (HCS1) and *Pseudomonas sp.* (HCS2) could degrade gasoline compounds, including benzene, toluene, and ethylbenzene, under aerobic conditions (Avanzi et al., 2015). Anaerobic strains, GS-15 and *Geobacter metallireducens* could mineralize aromatic hydrocarbons, like toluene (Lovley and Lonergan, 1990; Zhang et al., 2010). Most BTEX degraders belonged to the genera *Pseudomonas*, *Pseudoxanthomonas*, *Burkholderia*, *Sphingomonas*, *Thauera*, *Dechloromonas*, *Rhodococcus*, *Janibacter*, *Acinetobacter*, and *Comamonas* (Jiang et al., 2015a, b; Qu et al., 2015; Morales et al., 2016; Zhou et al., 2016; Khodaei et al., 2017; Wongbunmak et al., 2017).

2.2 Mechanisms for biodegradation of PHC

Alkanes and aromatic hydrocarbons are the most common PHC (Fuentes et al., 2014). Alkanes can be classified into linear, branched and cyclic alkanes (Mbadinga et al., 2011). Aromatic hydrocarbons often are divided into monocyclic and polycyclic aromatic hydrocarbons (PAHs). Because PHC are one of the most widespread soil contaminants and have caused various environmental problems, there are thousands of papers focusing on pathways for biodegradation of alkanes and aromatic hydrocarbons.

2.2.1 Alkanes

Under aerobic conditions, there are four pathways identified for the initial attack on alkane biodegradation (Fig. 2.1): monoterminal oxidation, biterminal oxidation, subterminal oxidation, and Finnerty pathway (Ji et al., 2013). The monoterminal oxidation pathway and subterminal oxidation pathway are regarded as major pathways (Fuentes et al., 2014).

(1) Monoterminal oxidation pathway (Fuentes et al., 2014). Alkanes are initially attacked at the terminal methyl group to form the corresponding primary alcohols by an oxygenase, carried out by either a multimeric monooxygenase or a cytochrome P450 monooxygenase which hydroxylates the substrate at terminal position. Then, primary alcohols are oxidized into aldehydes by alcohol dehydrogenases, and aldehydes are subsequently oxidized by aldehyde dehydrogenases to fatty acids. The fatty acids are further degraded by β-oxidation. The monooxygenase complex for the initial attack consists of a particulate membrane-bound hydroxylase (pAH), a rubredoxin (AlkG), and a rubredoxin reductase (AlkT). The AlkB from *Pseudomonas putida* GPo1 is a well-characterized model pAH enzyme that oxidizes propane, n-butane, and C_5–C_{13} alkanes. Substrate range and specificity for pAHs and Alk among alkane-degrading bacteria.

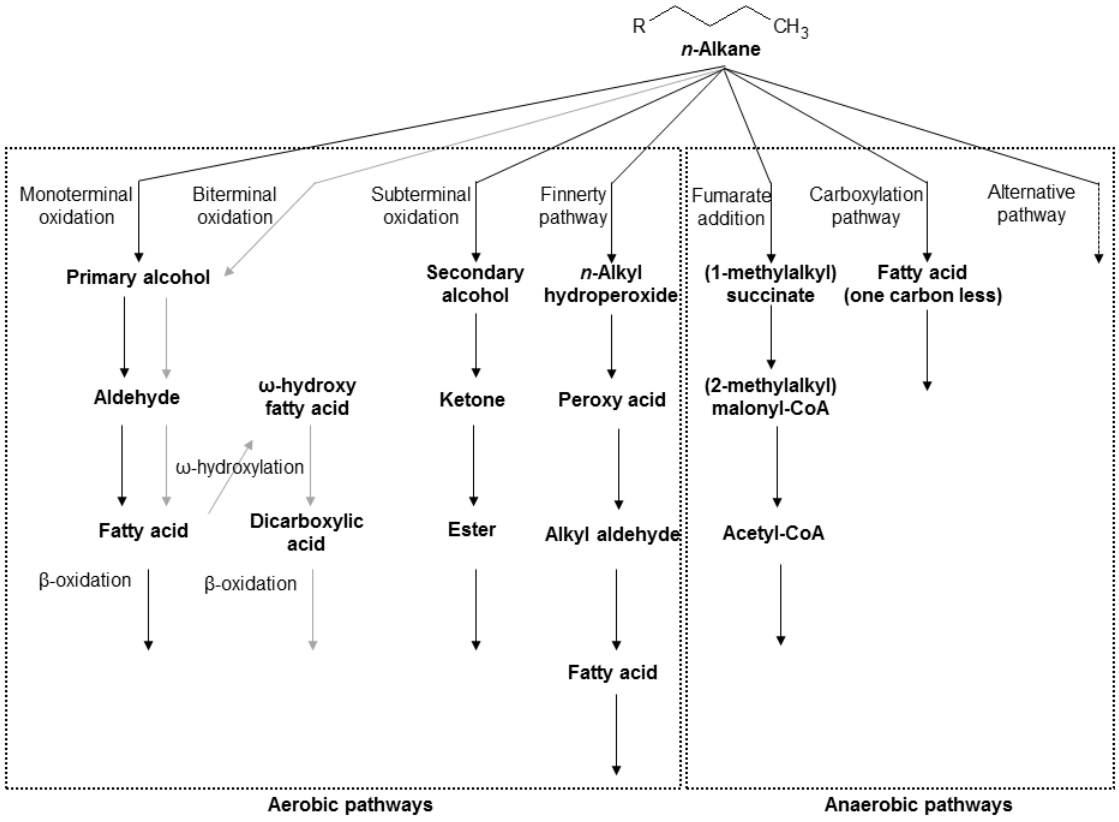

Fig. 2.1. Pathways for aerobic and anaerobic bacterial degradation of n-alkanes.

(2) Biterminal oxidation (Ji et al., 2013). The fatty acid produced in the monoterminal oxidation pathway undergoes ω-hydroxylation at the terminal methyl group (the ω position), yielding a ω-hydroxy fatty acid (rather than an aldehyde like the monoterminal pathway) that is further converted to a dicarboxylic acid, which then also enters β-oxidation.

(3) Subterminal oxidation (Wentzel et al., 2007). Alkanes are oxidized at the subterminal position and form a primary alcohol and a secondary alcohol or methyl acetone with the same chain length as the substrate. The secondary alcohol is converted to the corresponding ketone, and then oxidized by a Baeyer–Villiger monooxygenase to form an ester. The ester then is hydroxylated by an esterase to form an alcohol and a fatty acid.

(4) Finnerty pathway (Ji et al., 2013). This is a long-chain *n*-alkane oxidation pathway, which is unique to *Acinetobacter* sp. strain HO1-N. In this pathway, it is proposed that *n*-alkanes are oxidized to form *n*-alkyl hydroperoxides and then peroxy acids, alkyl aldehydes, and finally fatty acids by alcohol dehydrogenase and aldehyde dehydrogenase. The first step involves a dioxygenase, which has been reported to be common in *n*-alkane-using *Acinetobacter* spp.

The fumarate addition pathway and carboxylation pathway are two common proposed reaction mechanisms for the activation of alkane biodegradation under anaerobic conditions (Wentzel et al., 2007). Bacterial strains can conduct degradation of alkanes under nitrate, sulfidogenic, chlorate and methanogenic conditions (Grossi et al., 2008; Mbadinga et al., 2011). Nitrate-reducers and sulfidogenic microorganisms are the major contributors detected (Table 2.4). Anaerobic alkane degradation has been mainly described in sulfate-reducing *Deltaproteobacteria*.

(1) Fumarate addition pathway (Fuentes et al., 2014). Addition of fumarate to n-alkane is catalyzed by anaerobic glycyl radical enzymes (the extracted hydrogen from the parent substrate is recovered) to form (1-methylalkyl) succinate, after which the activation metabolite undergoes a carbon skeleton rearrangement to form (2-methylalkyl) malonyl-CoA that allows decarboxylation to 4-methylalkanoyl- CoA. The produced fatty acid then is degraded via "conventional" β-oxidation to yield intermediates such as (2-methylalkyl)-CoA, a linear fatty acid containing two carbon atoms less than the parent n-alkane, propionyl-CoA and acetyl-CoA. Acetyl-CoA is further oxidized to CO_2. Fumarate can be regenerated from propionyl-CoA (via methylmalonyl-CoA and succinyl-CoA) or alternatively from acetyl-CoA. The fumarate addition pathway has been found in sulfate-reducing bacteria, denitrifying bacteria, and a nitrate-reducing consortium. The mentioned glycyl radical enzymes is termed alkylsuccinate synthase or (1-methylalkyl) succinate synthase (ASS or MAS).

Table 2.4. Distribution of anaerobic alkanes degraders.

Microbes	Affiliation	Mechanism involved	Strains	References
Nitrate reducer	β-, γ-, δ-Proteobacteria	Fumarate, Carboxylation	Strain HxN1, Strain OcN1, *Marinobacter* sp. BC36, *Marinobacter* sp. BP42, *Pseudomonas balearica* strain BerOc6	Grossi et al. (2008); Mbadinga et al. (2011)
Sulfate reducer	δ-Proteobacteria, Clostridia	Fumarate, Carboxylation	Strain AK-01, Strain Hxd3	Grossi et al. (2008); Mbadinga et al. (2011)
Chlorate reducer	γ- Proteobacteria	Alternative Pathway	*Pseudomonas chloritidismutans* AW	Mbadinga et al. (2011)

(2) Carboxylation pathway. The initial steps to activate alkanes in carboxylation pathway include carboxylation with inorganic bicarbonate and the removal of two carbon atoms from the alkane chain terminus, forming a fatty acid that is shorter by one carbon than the original alkane. The carboxylation pathway can transform C-odd alkane substrates to C-even fatty acids and vice versa. This activation strategy was mainly developed based on the sulfidogenic strain Hxd3, which is the only isolated and identified strain that anaerobically degrades via carboxylation pathway. But Hxd3 enzymes involved in anaerobic alkane catabolic pathways have not been identified.

(3) Anaerobic biodegradation of alkanes may proceed via alternative activation mechanisms (Mbadinga et al., 2011). For instance, *Pseudomonas chloritidismutans* AW-1T can produce its own oxygen via chlorate respiration for degradation of alkanes, which is referred to as “unusual oxygenation” of alkane because it occurs at the absence of air. There is another recently proposed strategy involved anaerobic hydroxylation of oil alkanes. The result of pyrosequencing of total genomic DNA for methanogenic enrichment cultures degrading crude oil showed the presence of genes encoding the β-oxidation pathway, alcohol and aldehyde dehydrogenase genes. However, no *assA*-like genes (related to encoding alkylsuccinate synthase) and metabolites were found.

2.2.2 Aromatic hydrocarbons

Compared with alkane, aromatic hydrocarbons have limited chemical reactivity because of the stabilizing resonance energy of aromatic ring (Fuchs et al., 2011). The major principle of aromatic hydrocarbon biodegradation is that a broad range of reactions (peripheral pathways) that activate substrates, which are transformed to a restricted range of central intermediates (Fig. 2.2). Central intermediates are converted to intermediary metabolites by ring-cleavage, and further funnel into the Krebs cycle (Pérez-Pantoja et al., 2010; Fuchs et al., 2011).

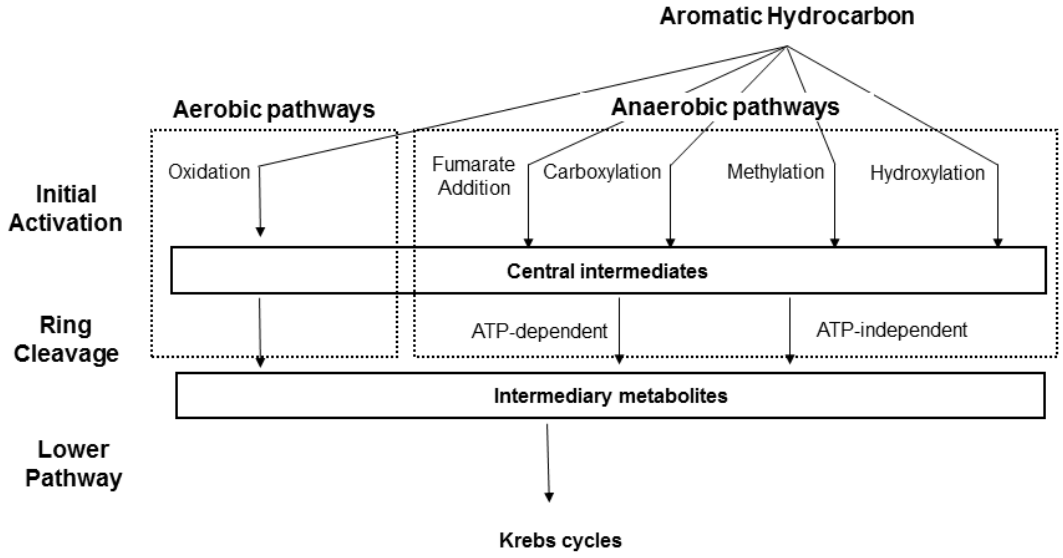

Fig. 2.2. Pathways for aerobic and anaerobic bacterial degradation of aromatic hydrocarbons.

Under aerobic conditions, O_2 works as both the terminal electron acceptor and an dispensable reactant (Widdel and Rabus, 2001). Microbes initiate degradation by activation of the aromatic nucleus through oxygenation reactions. By the action of monooxygenases or dioxygenases, one or two oxygen atoms, respectively, are directly incorporated from O_2 leading to hydroxylated products, which are called central intermediates, such as catechols and protocatechuates (Pérez-Pantoja et al., 2010; Díaz et al., 2013). There are two pathways for aerobic aromatic-ring cleavage process.

(1) For classical aerobic catabolism, the oxygenolytic cleavage of central intermediates is carried out by ring-cleavage dioxygenases, which cleave the ring either between the two hydroxyl groups (*ortho*-cleavage) or next to one of the hydroxyl groups (*meta*-cleavage) with intradiol or extradiol dioxygenases (Fuchs et al., 2011; Díaz et al., 2013).

(2) For the second strategy for ring cleavage under aerobic condition (called aerobic hybrid pathway), some aromatic hydrocarbons can be metabolized through the corresponding CoA thioesters (activated by CoA ligase), which are subjected to non-oxygenolytic ring cleavage to form non-aromatic epoxides by hydrolysis (Díaz et al., 2013).

Under anaerobic conditions, four reactions for initial activation of aromatic are recognized: (1) fumarate addition; (2) carboxylation; (3) methylation; (4) hydroxylation (Foght, 2008). These activation reactions feed into pathways that result in ring saturation, β-oxidation and/or ring cleavage reactions, producing central metabolites such as benzoyl-CoA that eventually incorporated into biomass or completely oxidized.

(1) Fumarate addition. Anaerobic toluene biodegradation is known to be initiated via fumarate addition in nitrate-reducing, sulfate-reducing, ferric iron-reducing, and fermenting bacteria (Heider, 2007), which forms (*R*)-benzylsuccinate. This reaction is carried out by benzylsuccinate synthases, which are complex glycyl radical enzymes composed of different subunits. This degradation reaction is conserved among various types of anaerobic microorganisms utilizing toluene and other substituted monoaromatic contaminants (Tierney and Young, 2010). The gene encoding the α-subunit of benzylsuccinate synthases, *bssA*, was used in PCR assays to detect anaerobic hydrocarbon degraders. Through a series of reactions, (*R*)-benzylsuccinate is then metabolized to benzoyl-CoA, which is further metabolized to acetyl-CoA via a series of β-oxidation-like reactions (Parales et al., 2008).

(2) Carboxylation. Non-substituted aromatic hydrocarbons like benzene, naphthalene or phenanthrene seem to be activated by direct carboxylation of the respective aromatic compounds (Zhang and Young, 1997; Fuchs et al., 2011; Luo et al., 2014). Proposed carboxylation of benzene produces benzoate by anaerobic benzene carboxylase, and

the benzoate-CoA ligase further catalyses benzoate to benzoyl-CoA (Coates et al., 2002; Abu Laban et al., 2010). The carboxylation of benzene seems to occur in iron- and nitrate-reducing bacteria (Dong et al., 2017).

(3) Methylation. Methylation has been proposed for anaerobic activation of unsubstituted aromatic hydrocarbon, such as benzene, naphthalene (Safinowski and Meckenstock, 2006; Weelink et al., 2010). The initial methylation of benzene to toluene was supported by stable isotope labelling method (Ulrich et al., 2005), and the produced toluene could be further activated by fumarate addition (Kunapuli et al., 2008; Vogt et al., 2011). The naphthalene activation by methylation converts naphthalene to 2-methylnaphthalene, which is consequently metabolized by fumarate addition and β-oxidation to succinyl-CoA and naphthoyl-CoA (Heider, 2007).

(4) Hydroxylation. The first case of anaerobic hydroxylation of aromatic hydrocarbon was for ethylbenzene and *n*-propylbenzene (Heider, 2007). The metabolism is initiated by hydroxylating the alkyl substituent at the carbon atom proximal to the ring with water, which is catalysed by ethylbenzene dehydrogenase. Ethylbenzene dehydrogenase could hydroxylate a wide spectrum of ethyl- and propyl- substituted aromatic and heteroaromatic substrates (Fuchs et al., 2011). The hydroxylation of ethylbenzene forms (*S*)-1-phenyethanol, which is further oxidized to acetophenone. Subsequently, acetophenone is carboxylated to benzoylacetate by an ATP-dependent carboxylase. Finally, benzoylacetate is activated to benzoylacetyl-CoA and cleaved to acetyl-CoA and benzoyl-CoA (Heider, 2007).

All four initial activation reactions can produce benzoyl-CoA as a central intermediate. Under anaerobic conditions, most aromatic hydrocarbons are channeled to benzoyl-CoA, which is the substrate for dearomatization and ring cleavage (Kuntze et al., 2008). There are two strategies for aromatic ring reduction (Fuchs et al., 2011).

(1) ATP-dependent reduction of the aromatic ring. Predominantly found in facultative anaerobes, benzoyl-CoA reduction is driven by stoichiometric ATP hydrolysis catalyzed by class I benzoyl-CoA reductases (BCR), producing non-aromatic dienoyl-CoA (Fuchs et al., 2011). A class I BCR enzyme has been isolated and studied in a nitrate-reducing, facultative anaerobe *Thauera aromatic* K172 (Boll and Fuchs, 1995;

Boll et al., 2000). The class I BCR is comprised of four subunits encoded by *bcrABCD* genes.

(2) ATP-independent reduction of the aromatic ring. Not homologous to class I, the class II BCR was found in the iron-reducing bacteria, *Geobacter metallireducens* (Philipp and Schink, 2012). The class II BCR has eight subunits, BamBCDEFGHI (Fuchs et al., 2011). Class II BCR are present in obligately anaerobic bacteria (Löffler et al., 2011; Boll et al., 2014).

2.3 Soil phosphorus (P) and PHC bioremediation

Phosphorus (P) is present in many different forms in soil. But only a small fraction of total soil P is in a bioavailable form, which closely equates to orthophosphate ($H_2PO_4^-$ and HPO_4^{2-}) or low molecular organic P in soil solution (Doolette and Smernik, 2011; Jones and Oburger, 2011). Many remaining soil P forms can be converted to the directly available form, but the conversion rate varies (Doolette and Smernik, 2011). The weakly sorbed orthophosphate is constantly coming into and out of soil solution and is in rapid equilibrium with solution orthophosphate. For other forms of P, this conversion can be very slow. Consequently, the ability of the soil to provide bioaccessible P depends on what forms of P are present and their relative amounts. The most commonly used differentiation of soil P is between inorganic and organic forms. The inorganic P comprises 35-70% of total soil P, which in top soil (0-15 cm) ranges 50-3000 mg kg^{-1}(Jones and Oburger, 2011). The parent material, soil pH, vegetation cover, and the soil development influence the chemical forms of P. Inorganic forms vary greatly in solubility and chemical reactivity (Jansa et al., 2011). Common inorganic P forms include: crystalline apatites; amorphous phosphates of calcium, potassium, iron and aluminum, and other phosphates; inorganic polyphosphates; and orthophosphates. Calcium-phosphates (mainly different forms of apatites) are the primary inorganic P in unweathered or moderately weathered soils with neutral to alkaline pH. But iron and aluminum phosphate and inorganic P bound and/or occluded by iron and aluminum oxy(hydr)oxides predominate in acidic and more progressively weathered soils (Jansa et al., 2011). Organic P forms present in the soil are thought to be composed of nucleic acids, phospholipids, inositol phosphates, and many metabolic intermediates (Jansa et al., 2011).

Three major processes of the soil P cycle have been identified to influence available P in soil solution: (1) dissolution-precipitation (mineral equilibria), (2) sorption-desorption (interactions between soil solution and soil solid surfaces), and (3) mineralization-immobilization (biological conversions between inorganic P and organic P) (Jones and Oburger, 2011). In acidic soils, most P is readily adsorbed on the surfaces of iron and aluminum (hydr)oxides. Phosphate adsorption takes place by ligand exchange reactions, oxygen bridging between Fe and Al and P. Phosphate can be adsorbed by one bond or stronger bidentate bonds (formed two oxygen bridges with the same Fe/Al atom). In calcareous soils, oxide surfaces for P sorption also exist. However, P is mainly adsorbed on calcite surfaces or precipitated as calcium phosphates, in which most phosphate are not in the solution (Yli-Halla, 2016). For example, dicalcium phosphate ($CaHPO_4 \cdot H_2O$) is precipitated, and further converted gradually to less soluble compounds such as octacalcium phosphate, $Ca_8(HPO_4)_2(OH)_2$, and hydroxyapatite, $Ca_{10}(PO_4)_6(OH)_2$.

Soil P bioavailability may be the most challenging factor to enhance PHC bioremediation. The nutrient level at a site influences the microbial activity and biodegradation. The ratio of C:N:P is a governing factor. The introduction of PHC disturbs the natural C:N:P ratio of the soil by dramatically increasing the amount of C available. Thus, additional N and P are required to maintain the balance. Amendments of N or P enhance hydrocarbon mineralization (Aislabie et al., 2006). For example, an oleophilic fertilizer, S200 (urea, phosphoric ester, water, oleic acid, and glycol ether) has been applied in marine oil spills and been proposed to treat hydrocarbon-polluted groundwater and soil (Menendez-Vega et al., 2007). The common N fertilizers, urea, ammonium chloride, ammonia salt or ammonium nitrate are highly water soluble, which are all readily assimilated in bacteria metabolism (Liebeg and Cutright, 1999). However, the P, which is needed by the organisms, unfortunately forms a large number of insoluble chemical complexes with mineral fraction, such as calcium, iron, and aluminum, then the P becomes unavailable to microorganism (Sashidhar and Podile, 2010). The most readily available state for P is around neutral pH. As a result, the availability of P often becomes the rate-limiting step in effective bioremediation (Paliwal et al., 2012). There are several kinds of classification for the P forms to analyze the availability. Some researchers use water soluble P (WSP), readily desorbable P (RDP), algal available P (AAP) and $NaHCO_3$ extractable

phosphorus (Olsen-P), or the sum as the total bioavailable P (Zhou et al., 2001). The dissolved phosphorus (DP), aluminum-bound phosphorus (Al–P), iron-bound phosphorus (Fe–P), calcium-bound phosphorus (Ca–P), and organic phosphorus (OP) have also been used to determine the P speciation and P bioavailability (Jiang et al., 2011).

2.4 Low molecular weight organic acids and PHC bioremediation

Low molecular weight organic acids (LMOA) normally contain 1-6 carbon atoms and 1-3 carboxyl groups, and constitute only a minor part of the total organic carbon in soil (van Hees et al., 2005b). Common LMOA include oxalic acid, citric acid, tartaric acid, aconitic acid, succinic acid, salicylic acid, *p*-hydroxybenzoic acid, malonic acid, fumaric acid, which can be sorted into three types: mono-carboxylic, di-carboxylic and tri-carboxylic based on their chemical structures (Fig. 2.3). The LMOA are produced from the decomposition of organic matter, dead plants or exudates of plants and microbes, ubiquitous in soil (van Hees et al., 2002). The concentration of mono-carboxylic acids in soil solution are usually higher than those of di- and tri-carboxylic acids (Collins, 2004). But the concentration varies with soil types, vegetation types (Table 2.5).

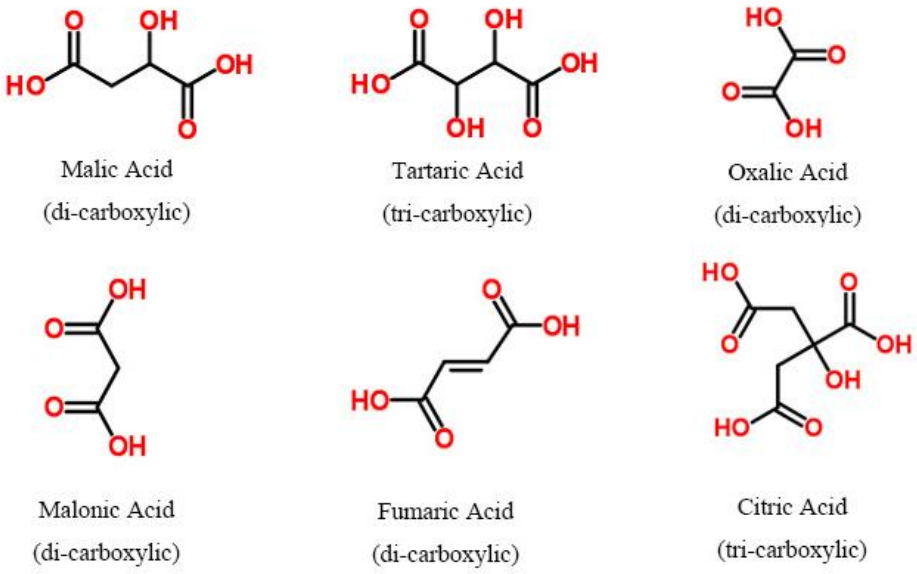

Fig. 2.3. Chemical structures for some low molecular weight organic acids.

Table 2.5. Concentrations of some common low molecular weight organic acids (LMOA) in soil solutions and soil extracts literature.

Type	LMOA	Soil Solution Concentration (µM)	Soil Extract (mmol kg^{-1})	Reference
Mono-carboxylic	Acetic	0-2000	0-300	Strobel (2001)
	Butyric	0-100	-	Strobel (2001)
	Formic	0-400	0-100	Strobel (2001); van Hees et al. (2002)
	Lactic	0-200	0-1000	Strobel (2001)
	Propionic	0-800	0-100	Strobel (2001); van Hees et al. (2002)
	Valeric	0-300	-	Strobel (2001)
Di-carboxylic	Fumaric	0-10	0-300	Strobel (2001)
	Malic	0–3000	0-9000	Strobel (2001); van Hees et al. (2005b)
	Maleic	0-80	0-300	Strobel (2001)
	Malonic	0-80	-	Strobel (2001)
	Oxalic	0-600	0-2000	Strobel (2001); van Hees et al. (2002, 2003, 2005a; b)
	Succinic	0-7000	0-6000	Strobel (2001)
	Tartaric	0-100	-	Strobel (2001)
Tri-carboxylic	Aconitic	0-10	0-100	Strobel (2001)
	Citric	0-700	0-1000	Strobel (2001); van Hees et al. (2002, 2003, 2005a)

LMOA play an important role in soil chemistry and rhizosphere processes (Bolan et al. 1994; Kpomblekou-A and Tabatabai 2003). LMOA can form complexes with aluminum and iron with high stability constants (Bergelin et al., 2000; van Hees and Lundström, 2000; Strobel, 2001). The complexation is important for the podzolization by enhancing the weathering rate of minerals and facilitating of transport through the soil profile (Bergelin et al., 2000). The presence of LMOA anions could increase the negative charge and decrease the positive charge on the soil surface. The influence of LMOA anions on surface charge typically follows the order: citrate> malate> oxalate> acetate (Xu et al., 2004). It is noteworthy that LMOA can be rapidly decomposed in the soil due to microbial consumption (Fujii et al., 2013). The microbial mineralization may affect the earlier mentioned processes, however, this depends on soil properties, vegetation, and microbial community structure (van Hees et al., 2003). For example,

in the mineral phase, the LMOA biodegradation rate was low because of strong sorption to the soil matrix, which prevented microbial uptake (van Hees et al., 2002).

There are conflicting results regarding the relationship between LMOA and PHC biodegradation. The LMOA in the root exudates from the rhizosphere of ryegrass, may inhibit PHC biodegradation (Corgié et al., 2006). In addition, the repression of phenanthrene degradation activity of *Pseudomonas putida* ATCC 17484 was observed in the presence of acetate, lactate (Rentz et al., 2004). The LMOA in root exudates, acetate, citrate, lactate, malate, oxalic, may inhibit the gene expression related to naphthalene dioxygenase transcription (Kamath et al., 2004). But, LMOA can also enhance the microbial activity to increase the degradation of PHC, acting as a direct and easily degradable energy source (Martin et al., 2014).

Some LMOA can facilitate PHC degradation by enhancing bioavailability of PHC (Ding et al., 2011). It was reported that the addition of LMOA may cause the partial dissolution of the soil structure by chelating with inorganic structural ions to enhance the bioavailability of soil contaminants (White et al., 2003). Some LMOA in root exudates can enhance the desorption of phenanthrene and pyrene, such as citric, malic and oxalic acid (Gao et al., 2010b; a). In addition, the tartaric acid, lactic acid, and acetic acid can also inhibit the adsorption and promote the desorption of pyrene in soil-water system, which is also affected by the pH (An et al., 2010).

LMOA can increase P bioavailability, a key factor for PHC biodegradation, through three ways: (1) LMOA (citric, oxalic, tartaric, malic, lactic, formic, and acetic acid) can release P from phosphate rocks and P compounds, complex metal ions in phosphate rocks and release P, due to various functional groups of the LMOA (Bolan et al. 1994; Kpomblekou-A and Tabatabai 2003); (2) LMOA (citric, oxalic, tartaric, malic, lactic, formic, and acetic acid) can prevent adsorption of phosphate by competing for adsorption sites on soil minerals, dissolution of absorbents and changing the surface charge on adsorbents. LMOA decreased the adsorption of P by soils in the order tri-carboxylic acids > di-carboxylic acids > mono-carboxylic acids (Staunton and Leprince, 1996; Wang et al., 2012b); (3) LMOA (maleic, oxalic and citric acids) can mobilize organic P by enhancing the solubilisation of organic P (Wei et al., 2010). The effect of LMOA on mobilizing P was reported mostly from the rhizosphere under P-limited conditions (Jones and Darrah, 1994, 1995). And the production of LMOA in the rhizosphere is influenced by the availability of P. In contrast, in some cases, LMOA may actually decrease P bioavailability. This occurs by Ca-aided

co-adsorption of phosphate and citrate under low citrate concentrations, which is a function of the soil mineralogy, phosphate loading, and soil solution composition (Oburger et al., 2011; Duputel et al., 2013).

2.5 Techniques to evaluate PHC bioremediation and the stable carbon isotope technique for PHC bioremediation

For successful *in situ* bioremediation, the first two steps are to assess whether the contaminants can be mineralized by the indigenous microbes and whether the mineralization can be improved by stimulation or augmentation (Höhener et al., 1998). The fate of PHC in a contaminated site involves complicated processes, including dissolution, partitioning, volatilization, oxidation, and biodegradation (Dutta and Harayama, 2000; Coulon et al., 2010). This complicated dissipation for PHC results in challenges for precise estimation for PHC bioremediation. There are many strategies based on chemical, and biological properties to evaluate the PHC bioremediation potential with various experimental approaches including microbial cultures, microcosms, laboratory aquifer columns, field observations, and field experiments (Höhener et al., 1998). The chemical monitoring characteristics include concentrations for contaminants (PHC fractions or biomarkers), end products (dissolved inorganic carbon), reaction metabolites, electron acceptors (e.g. O_2, Fe^{3+}, NO_3^-, SO_4^{2-}), reduced products (e.g. Mn^{2+}, Fe^{2+}, H_2S, CH_4), essential nutrients (e.g. C, N, and P sources), and isotopic element composition of the involved compounds (e.g. hydrogen, carbon, oxygen, nitrogen, and sulfur) (Hunkelera et al., 1999; Kirtland et al., 2000; Hunkeler et al., 2001; Johnson et al., 2006; Höhener and Aelion, 2010; Sihota and Ulrich Mayer, 2012; Su et al., 2013). The biological parameters for monitoring include the population of total organisms (plate counts, most probable number [MPN]), population for functional microbes with culturable and non-culturable means (selected plate counts, MPN counts with specific substrates, enrichment cultures, and *in situ* hybridization targeting RNA or DNA) (Höhener et al., 1998; Bekins et al., 1999). There are various analytical methods determining these parameters. Each method has its advantages and disadvantages. Among them, the isotope techniques are attractive tools to track or estimate the mineralization of the contaminants.

Isotopes are molecules of different masses of the same element, which are nuclides having the same number of protons but different neutrons. Carbon is one of the most used elements for isotope techniques. The delta (δ) notation is usually used to report the stable isotope variations, which are relative variations comparing element isotope composition in the sample with that in a known reference material (Hoefs, 2015). For global comparison of stable isotope data, international standards were developed. The National Institute of Standards and Technology (NIST) and the International Atomic Energy Agency are the two major organizations distributing the international standards. For carbon, the international standard for $^{13}C/^{12}C$ is the Pee Dee Belemnite (PDB), which was introduced based on the internal calcite structure (rostrum) of the fossil *Belemnitella americana* from the Cretaceous Pee Dee Formation in South Carolina (Höhener and Aelion, 2010). The abundance ratio $^{13}C/^{12}C$ for PDB is 0.011237.

Stable isotope techniques offer some advantages and specific information for biodegradation and bioremediation studies (Höhener and Aelion, 2010). Stable isotope techniques can track biodegradation processes which reduce the uncertainty for simple concentration measurements due to complicated fate for contaminants. Isotope ratios are not affected by dilution, evaporation or sorption during sampling process. The variation for stable isotopes abundance in compounds can provide information for different assessments to: identify sources of compounds; diagnose the origin of a specific compound formed in a given specific environment; assess the transformation pathway; distinguish between abiotic and biotic processes; quantify the extent of transformation; verify reactive transport models for the prediction of contaminant plumes (Höhener and Aelion, 2010; Hoefs, 2015). Therefore, labeling PHC with ^{13}C could be a good option to assess the PHC mineralization rate, which provides a more accurate measure of the contribution of biodegradation to PHC dissipation.

3. CITRATE ENHANCES BIOREMEDIATION BY INCREASING HYDROCARBON BIOAVAILABILITY UNDER *IN SITU* CONDITIONS AND PHOSPHATE BIOAVAILABILITY UNDER *EX SITU* CONDITIONS

3.1 Preface

Petroleum hydrocarbons (PHC) often contaminate soil and groundwater from spills, leakages, and seepage. Bioremediation use biological activity to degrade or detoxify PHC, and it is typically more economical than physical or chemical remediation. Adding nutrients, such as nitrogen and phosphate, is a common strategy for bioremediation. But, the availability of PHC also plays an important role for bioremediation. Low molecular weight organic acid anions (LMOAA) was found to increase polyaromatic hydrocarbons desorption. However, few researchers have studied the influence of LMOAA on PHC bioremediation. It is not clear whether LMOAA can change PHC bioavailability to affect PHC bioremediation. The goal for this chapter was to investigate whether LMOAA could increase PHC bioavailability to further influence PHC bioremediation which was amended with phosphate.

3.2 Abstract

Hydrocarbon bioavailability is a major factor limiting *in situ* petroleum hydrocarbon bioremediation. Low molecular weight organic acid anions (LMOAA) can enhance organic contaminant desorption and diffusion in the soil, which may increase the hydrocarbon bioavailability and related biostimulation. The hypothesis was LMOAA would increase the distribution of hydrocarbons in water, and presumably bioavailability, in cold region calcareous soils. Three microcosm tests were conducted to evaluate the influence of citrate addition on anaerobic biodegradation for a simple hydrocarbon compound, benzene, or a complicated hydrocarbon mixture, gasoline, with phosphate amendment, under *ex situ* (soil was dried and sieved) or *in situ* (soil was left intact) conditions. As expected, citrate addition increased petroleum hydrocarbon bioavailability at concentrations between 10-100 mM. However, citrate concentrations of only 1.0 mM paired with 0.1 mM phosphate enhanced anaerobic benzene dissipation in soil under *ex situ* conditions. Similarly, anaerobic gasoline remediation under *ex situ* conditions was enhanced at 1.75 mM citrate with 0.1 mM phosphate. In contrast, for mimicked *in situ* biostimulation, 10 mM citrate (with 1.0 mM phosphate) enhanced anaerobic gasoline biodegradation. Thus, citrate increased *ex situ* anaerobic gasoline biodegradation at low concentrations which did not alter gasoline partitioning, but under *in situ* conditions, citrate concentrations that enhanced anaerobic degradation also increased gasoline mobilization.

3.3 Introduction

Hydrocarbon distribution throughout the soil matrix is a key factor for effective petroleum hydrocarbons (PHC) bioremediation. PHC distribution in soil is thought of as a three-phase system in which (i) PHC are strong-absorbed to soil organic matter (SOM) and clay particles, (ii) PHC are dissolved in soil water, and (iii) PHC exist as droplets of non-aqueous phase liquids (NAPL) dispersed in the soil matrix. NAPL droplets occur when the soil matrix's ability to adsorb PHC is exceeded, such as 3,400 µg g^{-1} methyl *tert*-butyl ether in gasoline for soil containing pooled NAPL (Feenstra, 2005). The dominant soil matrix phase that sorbs PHC is SOM. The SOM can be envisioned as an organo-metallic polymer in which inorganic ions (e.g. Fe^{3+}, Al^{3+}, Ca^{2+}, and Mg^{2+}) serve as linking agents binding to the multiple carboxyl or phenolate groups on organic compounds (Ding et al., 2011). In addition to organic matter, clay surfaces are also important contributors to hydrophobic sorption in soils, especially when organic matter

content is below 6-8% (Ortega-Calvo et al., 1997). Typically, biodegradation is thought to occur only in the aqueous phase (Grimberg et al., 1996), and thus altering PHC partitioning may increase biodegradation rates.

Low molecular weight organic acid anions (LMOAA) can alter partitioning of PHC. LMOAA are produced from the decomposition of organic matter, dead plants or exudates of plants and microbes, ubiquitous in soil. The concentration of mono-carboxylic acids in soil solution are usually higher than those of di- and tri-carboxylic acids (Collins, 2004). Even though LMOAA are not stable due to consumption by soil microbes (Fujii et al., 2013), LMOAA play an important role in soil chemistry and rhizosphere processes (Bolan et al., 1994; Kpomblekou-A and Tabatabai, 2003). Addition of LMOAA could disrupt the sequestering processes occurring in the soil matrix, thereby enhancing the desorption of organic pollutants such as pesticides or PHC in soils (Ding et al., 2011). Because root exudates are a large natural source of LMOAA, many researchers have explored LMOAA in the context of phytoremediation (Sun et al., 2010; Wang et al., 2014; Rohrbacher and St-Arnaud, 2016). In technosols and active urban centers, phytoremediation is often not a suitable remediation strategy, but it may still be possible to remediate a site with LMOAA.

LMOAA, such as citrate, malate, and oxalate, can mobilize polyvalent metal ions (Fe^{3+}, Al^{3+}, Ca^{2+}, and Mg^{2+}) in the soil through disrupting the humic-metal-mineral linkages, which may increase the organic pollutants bioavailability to stimulate remediation (Yang et al., 2001a; White et al., 2003; Subramaniam et al., 2004; Un et al., 2005; Luo et al., 2006; Ouvrard et al., 2006; Gan et al., 2009a; Yanhong et al., 2009; Gao et al., 2010b; An et al., 2010; Ling et al., 2015). This disruption results in mobilization of SOM and the accompanying PHC into the aqueous phase, and reduces the degree of cross-linking in the SOM phase to accelerate PHC diffusion. However, the desorption for PHC is pH-dependent. For example, polyaromatic hydrocarbons had minimal release occurring at pH 2-3 and maximal release at pH 7-8 (Yang et al., 2001a). The increase for PHC desorption with increasing pH is possibly due to expansion of the humic structure as acidic groups become deprotonated and charged, thereby facilitating diffusion of PHC molecules through the organic matrix and to the water interface. The effect of LMOAA on PHC availability is different based on LMOAA structure. Citrate can enhance polyaromatic hydrocarbons desorption to a greater degree than oxalate (Ling et al., 2009), and

LMOAA inhibit the adsorption and promote the desorption of pyrene in the order of citric acid > oxalic acid > tartaric acid > lactic acid > acetic acid (An et al., 2010). For bound PHC residues in soils, citric acid with three carboxyl groups, always generated greater release than oxalic and malic acids with two carboxyl groups (Gao et al., 2015). It is thought that LMOAA with more carboxyl groups have a greater ability to chelate metal cations and promote the dissolution of soil minerals.

Under field conditions, citrate stimulates gasoline remediation by increasing phosphorus bioavailability (Chen et al., 2017); here additional mechanisms by which this occurred was investigated. The effect of citrate (with three carboxylic groups) and malate (with two carboxylic groups) on PHC biodegradation and PHC bioavailability was evaluated, under anaerobic conditions. Previous work identified the optimal citrate to phosphate ratio to maximize phosphate bioavailability (D. Bulmer, personal communication, 2015). The hypothesis was that citrate or malate, would also increase PHC bioavailability as a second mechanism by which citrate enhances remediation. *In situ* bioremediation is one of the cheapest remedial alternatives applicable for both soil and groundwater, but it is difficult to spread the water-based biostimulation solution throughout the treatment area due to tight and impermeable subsurface for some cases (Kuppusamy et al., 2016a). Despite the high cost, *ex situ* bioremediation achieves more uniformity and requires shorter time to reach efficient remediation with a larger surface area for microbial attachment (Kuppusamy et al., 2016b). The effect of LMOAA on *ex situ* and *in situ* anaerobic biostimulation was tested by mimicking these soil conditions (disturbed versus undisturbed) in two microcosm studies. Relatively clean and contaminated soil samples were collected for anaerobic assessment. Benzene was used for a PHC simple compound, which is resistant to biodegradation, and gasoline was used for a complicated mixture but typical for PHC sites. Other work exploring LMOAA influences on PHC availability are focused on polyaromatic hydrocarbon, not gasoline or BTEX (benzene, toluene, ethylbenzene, and xylenes) (Ling et al., 2009, 2015, Gao et al., 2010a, 2015, An et al., 2010, 2011). This research is the first to evaluate how LMOAA influence the bioavailability of benzene and gasoline under biostimulation conditions.

3.4 Materials and Methods

3.4.1 Evaluation of LMOAA effectiveness on a simple PHC under ex situ remediation conditions

3.4.1.1 Soil source

Two soil sample (Table 3.1) were collected from a former gasoline station, located in an active urban area (Broadway and 8th Street) in Saskatoon, SK, Canada, on April 15 and 16, 2015. Soil samples were air-dried and sieved to 2 mm, then stored at room temperature.

Table 3.1. Information on soil samples (prior to being air-dried and sieved) used for anaerobic benzene bioremediation.

Soil	Sample ID	BTEX (mg kg^{-1})†	$F1_{-BTEX}$ (mg kg^{-1})‡	Soil Depth (m)
A	15-01-06	111	136	6
B	15-09-05	54	0	5

† BTEX are six compounds, benzene, toluene, ethylbenzene, and ortho, meta and para-xylene.
‡ $F1_{-BTEX}$ was defined by Canadian Council of Ministers of the Environment (CCME) (2001), and has the equivalent normal straight-chain hydrocarbon (nC) from nC6 to nC10, from which the results of a BTEX analysis have been subtracted.

3.4.1.2 Experimental design

In a soil solution (1 mM PO_4, pH >6), the optimal ratio for citric acid: 50% desorbed phosphate was within the range from 5:1 to 50:1 (D. Bulmer, personal communication, 2015). So, three ratios, 7.5:1, 10:1 and 17.5:1 were used to test the optimal concentration of phosphate and citrate for petroleum hydrocarbons biostimulation. A 1:1 ratio of soil (6 g) to autoclaved medium (6 mL) for biostimulation was added to a 20 mL serum bottle. The basic medium contained 11 mM $MgSO_4$, 10 mM $NaNO_3$. Biostimulation treatments were designed at different phosphate concentrations (0.01 M, 0.001 M, 0.0001 M KH_2PO_4) with different ratios for citric acid to phosphate (0, 7.5, 10.0, 17.5). No phosphate addition treatments were set with 0 mM, 7.5 mM, 10 mM, and 17.5 mM citrate. The abiotic control for the whole design contained 0.02% sodium azide, 1 mM KH_2PO_4, 10 mM citric acid, 11 mM $MgSO_4$ and 10 mM $MgNO_3$. All biostimulation media were adjusted to neutral pH. There were 17 biostimulation treatments (Table 3.2). Each treatment was run in triplicate. Each sample was spiked with 4.2 μL of benzene

for a concentration of 940-980 mg kg^{-1}. In an anaerobic chamber (Forma Scientific Inc., Ohio, USA; Model 1025, 80% N_2 and 20% CO_2), 10 mL of filter-sterilized 2.9% Na_2S solution was added to 1 L of autoclaved medium, and the medium was transferred to the serum bottle containing soil. Serum bottle microcosms were shaken at 100 rpm for 28 days in the dark at 10°C. After incubation, benzene concentration was determined for the slurry (5 g, 1000 rpm cannot separate water and soil phases), and an additional 1 g was used for moisture content. Benzene concentration was determined using a gas chromatograph (GC) equipped with a flame ionization detector (FID) (SCION 436-GC, Bruker, ON, Canada).

Table 3.2. Phosphate and citrate concentrations for anaerobic, low temperature, benzene degradation treatments.

Phosphate Concentration (mM)	0 X Citrate†	7.5 X Citrate	10 X Citrate	17.5 X Citrate
0	√‡	√	√	√
0.1	√	√	√	√
1	√	√	√; AC§	√
10	√	√	√	√

† "0 X Citrate" means no citrate; "7.5 X Citrate" means the ratio for citrate: phosphate is 7.5 (concentration in mM); "10 X Citrate" means the ratio for citrate: phosphate is 10.0; "17.5 X Citrate" means the ratio for citrate: phosphate is 17.5.
‡ √: the biostimulation treatment with this combination of phosphate and citrate was used; for 0 mM phosphate treatment, the concentration for citrate is the amount mM at the number for citrate treatment.
§ AC: applied abiotic control with 0.02% sodium azide.

3.4.2 Evaluation of LMOAA effectiveness on a PHC mixture under ex situ conditions

Soil samples were sampled at 3-6 m depth ($F1_{-BTEX}$: 0-878 mg kg^{-1}; BTEX: 0-239 mg kg^{-1}; before air-dried and sieved), from the Broadway and 8th street site, on September 9, 2015. Soil (5 g, air-dried, sieved to 2 mm) was placed into a 20 mL serum bottle and was mixed with 15 mL of sterile anaerobic biostimulation medium (the same medium compositions described in section 3.4.1) in the anaerobic chamber. The abiotic control set-up differed from that in section 3.4.1. The first abiotic control contained 0.2% sodium azide, 1 mM KH_2PO_4, 10 mM citric acid, 11 mM $MgSO_4$ and 10 mM $NaNO_3$. The second abiotic control used gamma radiation (four days at 2.5 gray per hour) with the same amendment medium as the first abiotic control. Each sample

was spiked with 20 μL of gasoline, and serum bottle microcosms were shaken at 100 rpm for 21 days in the dark at 10°C. After incubation, serum bottles were centrifuged (1000 rpm for 15 mins). Then, 5 mL of water was taken for headspace analysis to determine F1 content in the water. For soil F1 content, about 2.5 g of the soil was weighed for extraction, and the remaining soil was used for moisture content determination. The BTEX, Canadian Council of Ministers of the Environment (CCME) PHC fraction $F1_{-BTEX}$ and total F1 in the water (W_{BTEX}, $W_{F1\text{-}BTEX}$, and W_{F1}) and soil phase (S_{BTEX}, $S_{F1\text{-}BTEX}$, and S_{F1}) were determined using the GC-FID after 0, 7, 14, and 21 days. The F1 has the equivalent normal straight-chain hydrocarbon (nC) from nC6 to nC10. $F1_{-BTEX}$ is simply BTEX subtracted from F1 (CCME, 2001). The distribution factor for F1 between soil and water (K_{SW}: $K_{SW\text{-}BTEX}$, $K_{SW\text{-}F1\text{-}BTEX}$, and $K_{SW\text{-}F1}$) was calculated by dividing the F1 concentration in the soil phase (mg kg^{-1}) from the F1 concentration in the water phase (mg L^{-1}).

3.4.3 Evaluation of LMOAA effectiveness on a PHC mixture under in situ conditions

Soil samples were collected from a depth of 6.75 m to 7.50 m from the soil core S16-12 at a former bulk fuel site (11^{th} street) in Saskatoon, SK, Canada, on December 15, 2016. Approximately 5 g of wet soil was weighed into a 20 mL serum bottle, and mixed with 15 mL of sterile biostimulation medium containing 11 mM $MgSO_4$, 10 mM $NaNO_3$, and different phosphate and LMOAA (Table 3.3) at neutral pH. To keep anaerobic incubation, 10 mL of filter-sterilized 2.9% Na_2S solution was added to 1 L of autoclaved medium. Each treatment had three replicates. Sodium azide at 0.2% was used for the abiotic control. Each sample was spiked with 20 μL of gasoline. Microcosms were incubated at 100 rpm (shaker) for 28 days at room temperature. The concentration for BTEX in the water and soil phase was analyzed with a GC-FID after 7, 14, 21, and 28 days.

Table 3.3. Phosphate and low molecular weight organic anions (LMOAA, citrate or malate) concentrations used for analysis of different amendment treatments on gasoline bioavailability at 22ºC during anaerobic biodegradation.

Phosphate Concentration (mM)	0 X LMOAA†	10 X Citrate	10 X Malate
0	√; AC‡	NA	NA
0.1	√	√	√
1	√	√	√
10	√	√	√

† "0 X LMOAA" means no citrate and malate; "10 X Citrate" means the ratio for citrate: phosphate is 10 (concentration in mM); "10 X Malate" means the ratio for malate: phosphate is 10.0.
‡ √: the biostimulation treatment with this combination of phosphate and citrate (or malate) was used; AC: applied abiotic control with 0.2% sodium azide; NA: not applied.

3.4.4 Analysis of hydrocarbon compounds

The concentration of benzene, BTEX, and $F1_{-BTEX}$ was determined based on CCME protocol (CCME, 2001). For soil hydrocarbon determination, soil was weighed in a 20 mL Teflon tube, and mixed with methanol (methanol:wet solid ratio = 2), shaken for 2 hours at 100 rpm, then centrifuged at 1000 rpm for 20 minutes. Then, 1 mL of the extract was added to a 20 mL headspace vial containing 9 mL of DDI water for headspace analysis by GC-FID with a PAL Combi-xt autosampler. Each set of ten samples had one duplicate (a randomly chosen sample), one method blank, one blank spike, and one matrix spike, which were carried through the complete extraction process with samples. Method blank and blank spike used clean sand. The blank spike and matrix spike for a random sample were extracted after adding 0.5 mL of 200 mg L^{-1} commercial standard for F1, which had hexane (C6), BTEX, and decane (C10). Recovery for blank spike and matrix spikes was from 70 to 130%. To determine moisture content for soil, wet soil was air dried overnight in the fume hood, then was oven-dried at 105 °C overnight. For water, 5 mL of the water sample was added to a 20 mL headspace vial that had 4 mL of DDI water and 1 mL methanol. Each set of ten water samples had a random duplicate. Chemical standards (BTEX, hexane, and decane) were purchased from Sigma-Aldrich.

3.4.5 Statistical design and analysis

All statistical analyses were performed using R (R Core Team, 2016). Linear mixed-effect models evaluated the influence of treatment and time. All tests were declared significant at $p < 0.05$. For the first microcosm study in section 3.4.1, a linear mixed-effect model with the restricted maximum likelihood (REML) method tested the effect of phosphate plus citrate (fixed effect); contamination status was included as a random effect. For the second microcosm study in section 3.4.2, a linear mixed-effect model tested the effect of treatment (fixed effect), and time with or without citrate addition concentration (random effect), using the maximum likelihood (ML) method. For section 3.4.3, a linear mixed-effect model with the ML method determined the effect of treatment (fixed effect), and time with or without anion addition concentration (random effect).

3.5 Results

3.5.1 Identification of the optimal concentration of phosphate and citrate amendment for anaerobic benzene bioremediation at 10°C temperature under ex situ conditions

Low concentrations of phosphate enhanced benzene bioremediation. The lowest residual benzene concentration among treatment groups after 28 days was 102 ± 53 mg kg^{-1}, found in the 0.1 mM phosphate + 1.0 mM citrate treatment (Fig. 3.1 panel (1), $p < 0.001$ for the phosphate and citrate interaction in the linear mixed model). Across all citrate concentrations, the phosphate addition of 0.1 mM had the lowest residual benzene concentration (Fig. 3.1 panel (2), 144 ± 26 mg kg^{-1}). In contrast, 1.0 mM citrate concentration (102 ± 53 mg kg^{-1}) was close to 0 mM citrate (122 ± 23 mg kg^{-1}) and was different from increased citrate concentrations (Fig. 3.1 panel (3), $p < 0.001$ for the citrate factor in the linear mixed model).

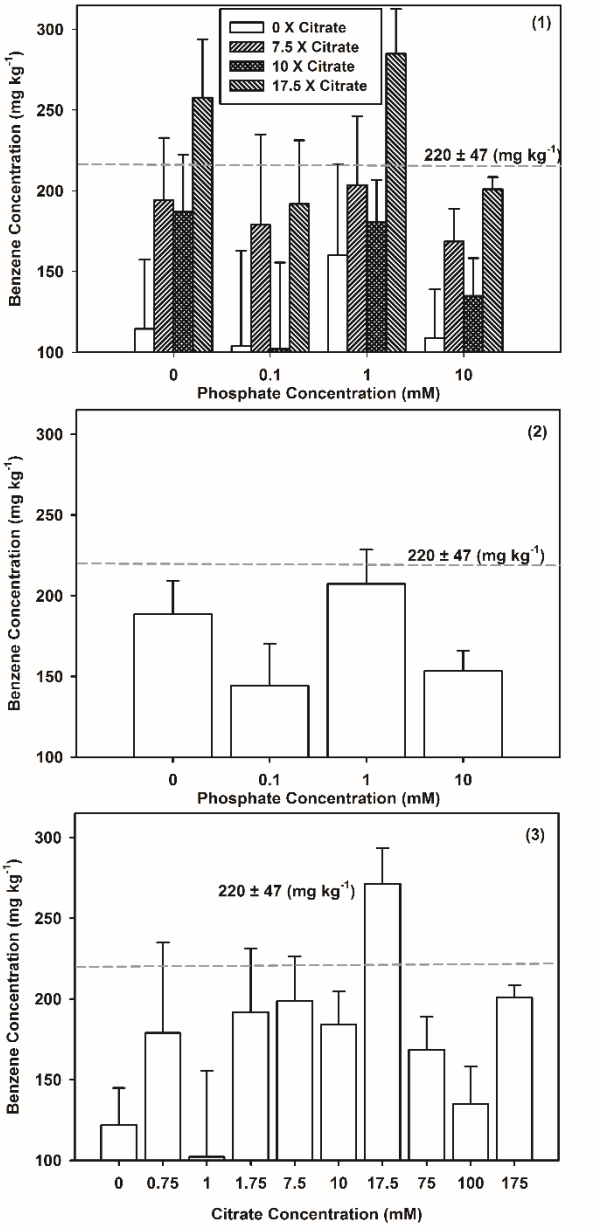

Fig. 3.1. Residual benzene concentration after 28 days, (1) for different amendment treatments, (2) for different phosphate additions, and (3) for different citrate additions, under anaerobic conditions. For panel (1), averages of 6 replicates (three replicates per each soil, two soils) are denoted by bars with the error bars representing the standard error (SE) from the mean; patterns on bars correspond to the same ratio of citrate:phosphate (the 0 X citrate represents 0 times of phosphate concentration for citrate added in that treatment) treatment. The grey dash line indicates the average benzene concentration in the abiotic control treatment (0.02% sodium azide, 1 mM phosphate, and 10 mM citrate, 6 replicates). Sample size for panel (2) was 24, but sample size for panel (3) were different among treatments (6-24).

3.5.2 Identification of the optimal concentration of phosphate and citrate amendment for anaerobic gasoline bioremediation at 10°C temperature under ex situ conditions

The addition of phosphate and citrate increased the BTEX dissipation in microcosms under anaerobic conditions (Fig. 3.2). BTEX was positively correlated with $F1_{\text{-BTEX}}$ (Spearman's correlation coefficient, *rho* = 0.91) and F1 (*rho* = 0.95) (Table A1.1) and provided a convenient means of tracking gasoline bioremediation. The residual BTEX content (also called T_{BTEX}) had the lowest value, 938 ± 108 µg, in the treatment with 0.1 mM phosphate plus 1.75 mM citrate (a ratio of 1:17.5 phosphate:citrate, Fig. 3.2 panel (1)). For the phosphate addition, the lowest addition group, 0.1 mM, had the lowest residual BTEX (Fig. 3.2 panel (2), 1017 ± 47 µg). Similarly, for the citrate addition the 1.75 mM addition of citrate reached the lowest residual BTEX content (panel (3) in Fig. 3.2). The best treatment for benzene and $F1_{\text{-BTEX}}$ dissipation in gasoline was also 0.1 mM phosphate plus 1.75 mM citrate.

Whereas citrate increased hydrocarbons bioremediation, enhanced BTEX bioavailability did not correspond to optimal remediation conditions. Instead, 17.5 mM citrate and 1 mM phosphate had the lowest $K_{SW\text{-}BTEX}$ (0.43 ± 0.19 L mg^{-1}, panel (1) in Fig. 3.3) which is 10X the phosphate (1.0 mM) and citrate (17.5 mM) concentrations that stimulated hydrocarbon remediation. Other measures of gasoline bioavailability also had the lowest distribution factor between soil and water for benzene (0.22 ± 0.39 L mg^{-1}) and $F1_{\text{-BTEX}}$ (1.06 ± 1.57 L mg^{-1}).

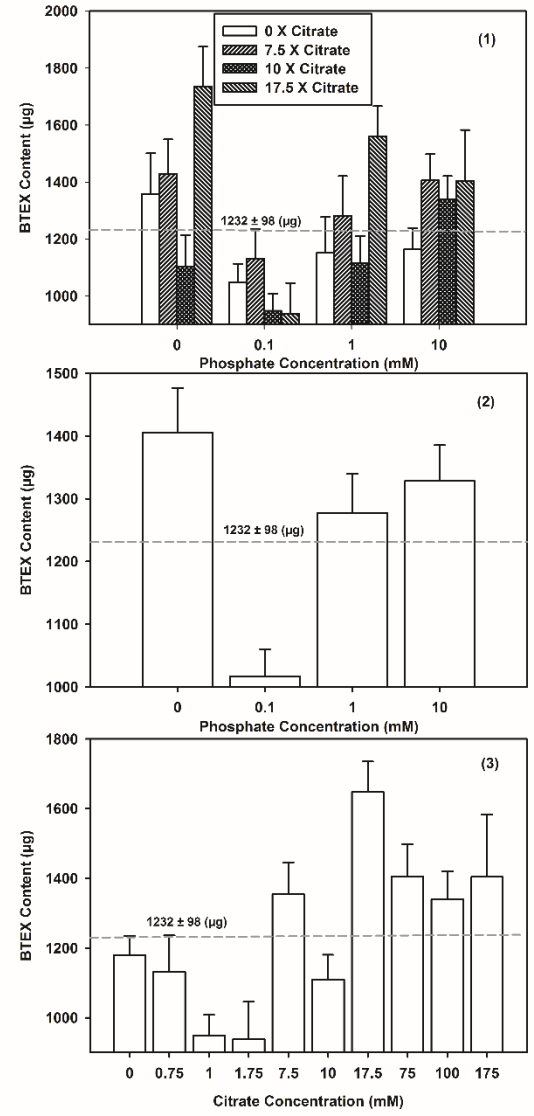

Fig. 3.2. Anaerobic gasoline remediation under cold (10°C) conditions after 21 days. The residual content of BTEX (T_{BTEX}) in the microcosm, (1) across all amendment treatments, (2) for different phosphate additions, and (3) for different citrate additions. For panel (1), averages of 12 replicates (three replicates per each soil, four soils) are denoted by bars with error bars representing the standard error (SE) from the mean; patterns on bars correspond to the same ratio for citrate:phosphate (the 0 X citrate means 0 times of phosphate concentration for citrate added in that treatment) treatment. The grey dash line indicates the average T_{BTEX} in the abiotic control treatment (0.2% sodium azide, 1 mM phosphate, and 10 mM citrate, 12 replicates). Another abiotic control (supplemented with 1 mM phosphate and 10 mM citrate addition), not represented on the figure, was gamma irradiated, and had 1281 ± 122 µg residual BTEX. Sample size for panel (2) was 48. But for panel (3), sample size (12-48) varied among treatments, which depends on the citrate concentration.

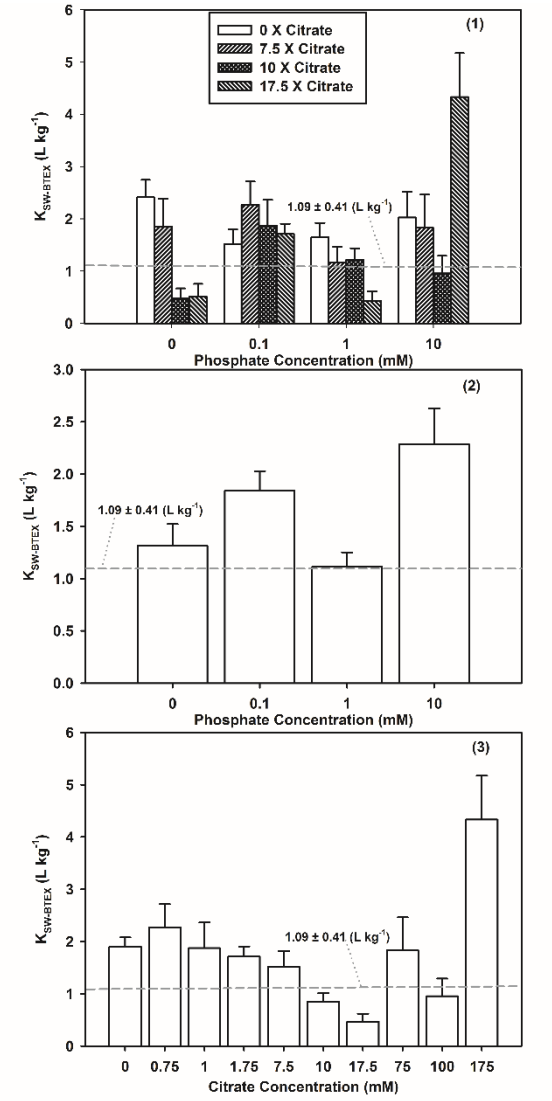

Fig. 3.3. Gasoline partitioning under cold (10°C), anaerobic conditions after 21 days. The distribution factor of BTEX between soil and water ($K_{SW-BTEX}$) in the microcosm, (1) for different amendment treatments, (2) for different phosphate addition, and (3) for different citrate addition. In panel (1), averages of 12 replicates (three replicates per each soil, four soils) are denoted by bars with the vertical bars marking the standard error (SE) from the mean; the same type of bar is for the same ratio for citrate: phosphate (the 0 X citrate means 0 times of phosphate concentration for citrate added in that treatment) treatment. The grey dash line indicates the average $K_{SW-BTEX}$ in the abiotic control treatment (0.2% sodium azide, 1 mM phosphate, and 10 mM citrate, 12 replicates). Another abiotic control (amended with 1 mM phosphate and 10 mM citrate addition) was gamma irradiated and had 0.83 ± 0.26 L mg^{-1} value for $K_{SW-BTEX}$. Sample size for panel (2) was 48. But for panel (3), sample size was determined the citrate concentration, from 12 to 48.

3.5.3 Effect of phosphate and LMOAA amendment on gasoline bioavailability under anaerobic conditions for in situ biodegradation

At room temperature, 1 mM phosphate and 10 mM citrate (1.0P10.0C), a ratio of 1:10 phosphate:citrate had the lowest residual BTEX content of 1932 ± 78 µg (Fig. 3.4). In contrast, only at much higher malate concentrations (100 mM) was malate effective in biostimulation. Citrate additions with 10-100 mM citrate increased gasoline bioavailability (panel (1) in Fig. 3.5). All the phosphate addition groups had lower residual BTEX content than the abiotic control and the no phosphate addition group. For $K_{SW\text{-}BTEX}$, the two lowest values were 9.6 ± 1.4 L kg^{-1} (10P100C, 10 mM phosphate and 100 mM citrate) and 10.5 ± 1.1 L kg^{-1} (1.0P10.0C, 10 mM phosphate and 10 mM citrate). The 10 mM phosphate addition group had lower $K_{SW\text{-}BTEX}$ than other phosphate addition groups (panel (2) in Fig. 3.5).

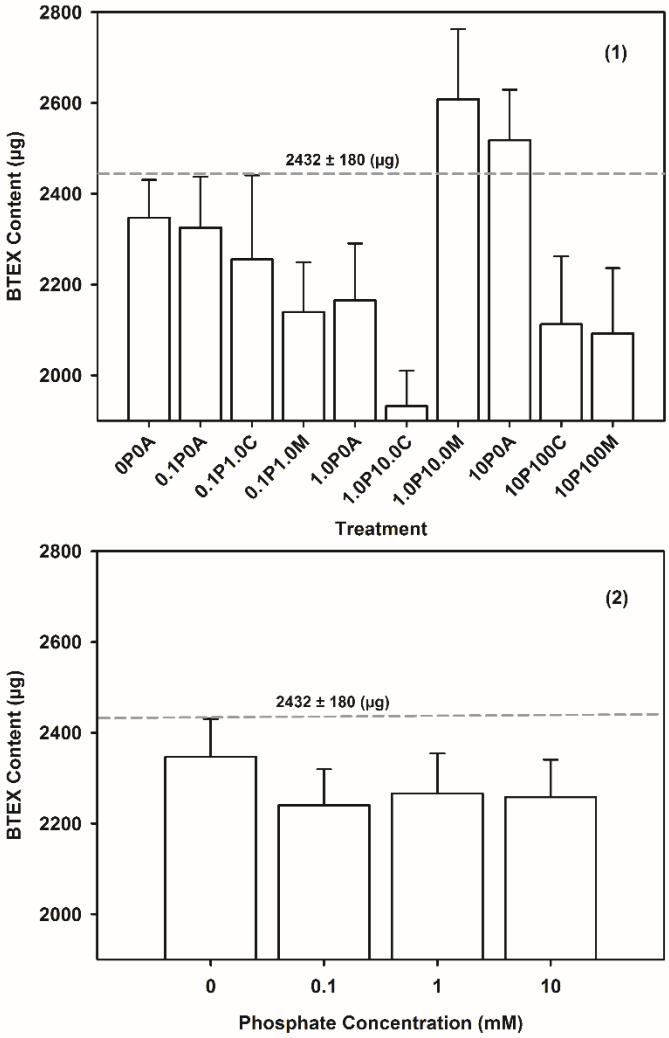

Fig. 3.4. Gasoline remediation under warm (21°C), anaerobic conditions for 28 days comparing citrate to malate effectiveness. The residual BTEX content (T_{BTEX}) in the microcosm, (1) for different amendment treatments, (2) for different phosphate addition. For panel (1), averages of 12 replicates (three replicates per each soil, four soils) are denoted by bars with the error bars representing the standard error (SE) from the mean. The "i" and "j" for the treatment label "iPjA (C/M)" are concentrations (mM) for the phosphate (P) and anion (A)/ citrate (C)/ malate(M) added for the treatment. And 0A means no anion was added for biostimulation. The grey dash line indicates the average T_{BTEX} in the abiotic control treatment (0.2% sodium azide, 0 mM phosphate, and 0 mM citrate/malate, 12 replicates). Sample size for panel (2) was 36.

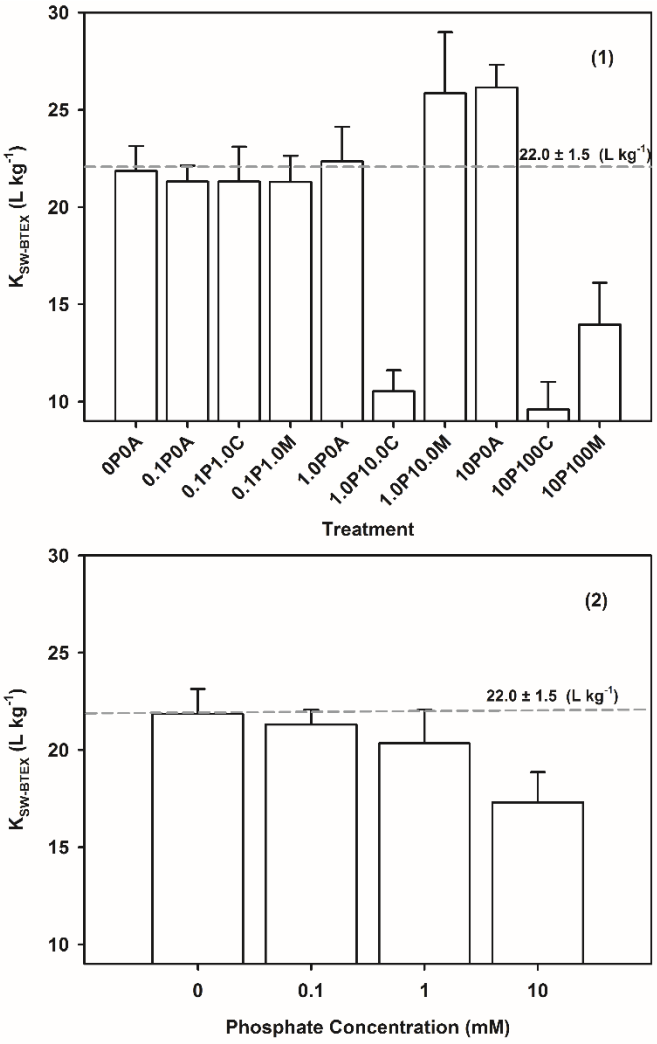

Fig. 3.5. Gasoline partitioning under warm (21°C), anaerobic conditions for 28 days after citrate or malate additions. The distribution factor of BTEX between soil and water ($K_{SW\text{-}BTEX}$) in the microcosm, (1) for different amendment treatments, (2) for different phosphate addition. For panel (1), averages of 12 replicates (three replicates per each soil, four soils) are denoted by bars with the vertical bars marking the standard error (SE) from the mean. The "i" and "j" for the treatment label "iPjA (C/M)" are concentrations (mM) for the phosphate (P) and anion (A)/ citrate (C)/ malate(M) added for the treatment. And 0A means no anion was added for biostimulation. The grey dash line indicates the average $K_{SW\text{-}BTEX}$ in the abiotic control treatment (0.2% sodium azide, 0 mM phosphate, and 0 mM citrate/malate, 12 replicates). Sample size for panel (2) was 36.

3.6 Discussion

Low concentrations of phosphate (0.1 mM), coupled with low citrate concentrations increased anaerobic benzene biodegradation when benzene was present as a single contaminant

(1.0 mM citrate) and in a gasoline mixture (1.75 mM citrate). However, at the concentration of 0.1 mM phosphate and 1.0-1.75 mM citrate, benzene remained strongly partitioned to soil. Thus, it is unlikely that citrate's enhancement of anaerobic benzene biodegradation is from increased benzene bioavailability. Other experiments which found that LMOAA enhanced PHC (e.g. phenanthrene or pyrene) bioavailability used 10-1000 mM citrate, malate and other LMOAA (Ling et al., 2009, 2015; Gao et al., 2010a,b; An et al., 2010, 2011). In my third microcosm study, less citrate was needed to increase gasoline bioavailability than malate, which is similar to that seen by others in which PHC desorption from soil decreased in the order of citric acid > oxalic acid > malic acid present in solution (Ling et al., 2015). There are three other potential mechanisms by which LMOAA enhance PHC biodegradation: activation of microbial enzymatic pathways, acting as a selective nutrient source to the microbial PHC degrader community (Martin et al., 2014), or by increasing phosphate bioavailability. Under field conditions, using large bore injectors, adding 1 mM phosphate and 10 mM citrate enhanced anaerobic gasoline bioremediation by increasing phosphorus bioavailability (Chen et al., 2017).

The major mechanism for citrate to enhance PHC biodegradation for anaerobic biostimulation differs between *ex situ* and *in situ* conditions. The influence of citrate was assessed in three replicate studies designed to assess *ex situ* conditions (air-dried, sieved, contaminated saturated soil) with either a single pollutant or a gasoline mixture, and *in situ* conditions (intact, contaminated saturated soil) polluted with a gasoline mixture. In soils such as these, it is not clear why benzene is persisting; however, it has been postulated this is due to the lack of appropriate microbes, nutrients or electron acceptors (Edwards and Grbić-Galić, 1992). Benzene and BTEX were elected as chemicals of concern, and benzene was used in either a mixture or as a sole source for PHC contaminant. Under all these conditions, citrate increased PHC bioavailability when used between 7.5 and 100 mM under both cold and ambient temperature. Under *ex situ* conditions, citrate enhanced anaerobic PHC biodegradation but at concentrations that did not increase PHC bioavailability. Under *in situ* conditions, citrate increased anaerobic gasoline biodegradation at concentrations that also increased PHC bioavailability. The difference between these conditions likely arises because under *ex situ* conditions PHC biodegradation is mostly limited by phosphorus bioavailability as soil structure is disrupted releasing PHC (Rojas-Avelizapa et al., 2007). In contrast, under *in situ* conditions,

PHC biodegradation is likely limited by PHC bioavailability due to limited PHC mobilization in condensed soil (Pandey et al., 2009). These microcosm experiments used different soils and soil processing from across a site, and thus, comparing partitioning values between studies is fraught with difficulties because soil texture is a well-known determinant of PHC partitioning (Amellal, 2001; Conte et al., 2001; Falciglia et al., 2011; Bielská et al., 2012). Partitioning values here are 0-34.2 L kg^{-1} for $K_{SW\text{-}BTEX}$, within the range reported 0-95.3 L kg^{-1} by others (Ranck, 2003; Lee et al., 2004), and similar that seen in the field study (0.25-11.7 L kg^{-1} for $K_{SW\text{-}BTEX}$, unpublished data).

Under field conditions, citrate was applied for eight months before assessing effectiveness and others have incubated their microcosms for 100-200 days (Phelps and Young, 1999; Philp et al., 2002; Townsend et al., 2004). In contrast, experiments in this chapter were limited to a 28 day period, and a 30-100 day lag time sometimes occurs for anaerobic benzene degradation in microcosms (Edwards and Grbić-Galić, 1992). The rationale for the short time period was that citrate would not persist in the microcosms for longer than 28 days. Under field conditions, citrate was non-detectable throughout the field site demonstrating the labile nature of LMOAA in soil ecosystems. To increase the sensitivity of microcosm assay, 10,000 µg of F1 was added to each microcosm that initially contained approximately 1,000 mg kg^{-1} (5,000 µg). Maximum residual BTEX content in the microcosm of 2500 µg, soil BTEX concentration of 300 mg kg^{-1}, and water BTEX concentration of 200 mg L^{-1} were detected. Thus, after 28 days, only approximately 16-32% percent of the original F1 spiked content was detected. These high spike concentrations suggest that to fully evaluate citrate effectiveness, multiple sites should be assessed for citrate based biostimulation of hydrocarbon remediation. Citrate concentrations between 2 and 10 mM in concert with between 0.1 and 1 mM phosphate will likely be effective under field conditions.

3.7 Conclusion

The LMOAA, citrate, increased anaerobic PHC biodegradation at lower concentrations, which did not alter PHC partitioning for *ex situ* biostimulation, and at higher concentrations enhancing PHC mobilization for *in situ* biostimulation. The wide range of citrate found to stimulate biodegradation reflects the robustness of this experimental design in which different

soils, under different conditions, were exposed to citrate. It also highlights that, depending on the nature of the soil, citrate's mechanism of action may differ from what was presented here for a cold region calcareous soil. Practioners should follow best practices, and determine the optimal citrate effectiveness for their respective sites' soils before applying citrate in large quantities.

4. CITRATE ADDITION INCREASED PHOSPHORUS BIOAVAILABILITY AND ENHANCED GASOLINE BIOREMEDIATION[1]

4.1 Preface

Gasoline bioremediation is often limited by the phosphorus bioavailability, which could be increased by citrate addition. The previous chapter tested the effect of different low weight molecular organic acid anions including citrate on hydrocarbon bioavailability and anaerobic gasoline biodegradation in microcosm studies. However, it is not clear how citrate addition would influence phosphate amendment for *in situ* gasoline biodegradation due to environmental heterogeneity. In order to evaluate the effect of citrate under field conditions, a field study was conducted, with tracking physical and chemical properties in groundwater and soil during biostimulation.

[1] Chapter 4 of this dissertation has been previously published (with minor changes for formatting) as: Chen, T., C. Philips, J. Hamilton, B. Chartbrand, J. Grosskleg, K. Bradshaw, T. Carlson, K. Timlick, D. Peak, and S.D. Siciliano. 2017. Citrate addition increased phosphorus bioavailability and enhanced gasoline bioremediation. J. Environ. Qual. 46(5): 975–983. Tingting Chen is the major contributor and author of the manuscript. Courtney Philips, Jordan Hamilton, Blaine Chartbrand, Jay Grosskleg, Kris Bradshaw, Trevor Carlson, Karen Timlick and Derek Peak helped with experimental design, implementation, sampling and analazing. Steven D. Siciliano is the supervisor and helped throughout this study.

4.2 Abstract

Phosphorus (P) bioavailability often limits gasoline biodegradation in calcareous cold-region soils. One possible method to increase P bioavailability in such soils is the addition of citrate. Citrate addition at the field scale may increase hydrocarbon degradation by: (i) enhancing inorganic and organic P dissolution and desorption, (ii) increasing hydrocarbon bioavailability, and/or (iii) stimulating microbial activity. Alternatively, citrate addition may inhibit biodegrading activity due to competitive effects on carbon metabolism. Using a field-scale *in situ* biostimulation study, it was evaluated whether citrate could stimulate gasoline degradation and what the dominant mechanism of this stimulation will be. Two large bore injectors were constructed at a site contaminated with gasoline, and a biostimulation solution of 11 mM $MgSO_4$, 1 mM H_3PO_4, and 0.08 mM HNO_3 at pH 6.5 in municipal potable water was injected at ~5000 L d^{-1} for about 4 mo. Following this, 10 mM citric acid was incorporated into the existing biostimulation solution and the site continued to be stimulated for 8 mo. After citrate addition, the bioavailable P fraction in groundwater and soil increased. Iron(II) groundwater concentrations increased and corresponded to decreases in benzene, toluene, ethylbenzene, xylenes (BTEX) in groundwater, as well as a decrease in $F1_{\text{-BTEX}}$ in the soil saturated zone. Overall, citrate addition increased P bioavailability and may stimulate anaerobic microbial activity, resulting in accelerated anaerobic gasoline bioremediation in cold-region calcareous soils.

4.3 Introduction

The storage, transport, and use of gasoline and diesel fuel often results in inadvertent hydrocarbon releases into soil and groundwater. There are many different approaches for remediating the released hydrocarbons; bioremediation is one cost-effective approach (Zhao et al., 2014; Masy et al., 2016; Mitra and Mukhopadhyay, 2016). Bioremediation uses microorganisms to convert chemical compounds, such as gasoline, into energy, cell mass, and biological waste products (Rahman et al., 2002). Two major strategies for bioremediation are bioaugmentation (addition of contaminant-degrading microorganisms) and biostimulation (providing nutrients or other supplementary components to support microbial growth) (Tyagi et al., 2011). There are numerous microorganisms that can degrade hydrocarbons by catalyzing electrons transfer from gasoline to electron acceptors such as oxygen, nitrate, Fe(III) minerals, or

sulfate (Tiehm and Schulze, 2003; Yakubu, 2007). However, optimization of *in situ* conditions for anaerobic hydrocarbon biodegradation remains a challenge. The simple addition of electron acceptors and nutrients often fails for a variety of reasons likely linked to limited microbial populations (Bento et al., 2005), poor dispersion of the biostimulation solution (Liang et al., 2009), or nutrient inaccessibility (Mills and Frankenberger, 1994).

Phosphorus (P) can readily become a rate-limiting factor for hydrocarbon biodegradation (Jin and Fallgren, 2007; Yang et al., 2009). Phosphorus is needed at an approximate ratio of 100:1 C (as hydrocarbon) to P to allow microorganisms to assimilate the energy released during hydrocarbon degradation (Thompson et al., 1954). However, simple addition of P to soils rarely works because P is almost always added as phosphate (PO_4), which readily precipitates with Ca, Fe, and Al, resulting in low P bioavailability (efficiency to take up P) to microorganisms. In calcareous soils, P ions typically precipitate as Ca and Mg phosphate, such as octacalcium phosphates and hydroxyapatite, which are largely unavailable (Hinsinger, 2001; Ström et al., 2005). Furthermore, the formation of certain phosphate mineral phases, such as brushite, can inhibit microbial populations that degrade hydrocarbons (Siciliano et al., 2016). It is possible to design biostimulation solutions to prevent mineral formation, but adsorption processes can also severely limit PO_4 bioavailability. Thus, what is needed is a method of maintaining PO_4 in soil solution, even in calcareous soils. Such an adjunct to biostimulation solutions would then allow the PO_4 to disperse across a contaminated site into areas of peak bioremediation activity, which are themselves acting as a strong biological sink for available P (Sato and Comerford, 2006).

Citrate is one possible adjunct to increase P bioavailability through three distinct mechanisms: (i) competitive ligand exchange, (ii) mineral dissolution, or (iii) organic P dissolution (Wei et al., 2010). Citrate provides a ligand that has a higher affinity for some soil surfaces than does PO_4 (Sato and Comerford, 2006), which can thus displace adsorbed P from the soil surface. Citrate can also chelate Fe, Mn, or Ca to enhance Ca-P mineral dissolution (Bolan et al., 1994; Kpomblekou-A and Tabatabai, 2003; Ström et al., 2005). Citrate mobilizes organic P by similar mechanisms to inorganic P, because the organic P can react with metal ions like free phosphate ion, that is, via the P oxygen bonds (Wei et al., 2010). Recent work has suggested that organic P release by citrate may not be due to chelating effects but instead arises from other unknown mechanisms (Wang et al., 2015). In addition to effects on P bioavailability, citrate can also facilitate biodegradation by enhancing bioavailability of hydrocarbons (Gao et

al., 2010b; a; Wang et al., 2015). The increase in hydrocarbon bioavailability is thought to occur by enhancing hydrocarbon desorption via disruption of the organic matter caused by chelation of metals within the organo-metallic polymer complex (Yang et al., 2001b; Rohrbacher and St-Arnaud, 2016).

Citrate, however, may not be a panacea. First, under some soil conditions, citrate may actually decrease P bioavailability. This occurs by Ca-aided coadsorption of phosphate and citrate under low citrate concentrations (Duputel et al., 2013), which is a function of the soil mineralogy, phosphate loading, and soil solution composition (Oburger et al., 2011; Duputel et al., 2013). Second, citrate can act as an energy source for microorganisms (Jana and Ghosh, 1995; Knight et al., 1996; Polen et al., 2007), thereby reducing their hydrocarbon degradation activity. Microbial uptake for citrate is quick in soil, and reported half-life for citrate is <2 d (Owen et al., 2001). However, when citrate is chelated to other ions, thereby increasing P or hydrocarbon bioavailability, the citrate may not be a readily available energy source (Martin et al., 2014).

Here, the objective was to assess the effect of citrate addition on *in situ* P bioavailability and petroleum hydrocarbon bioremediation at a contaminated field site. The research site was impacted with gasoline- and diesel-related petroleum hydrocarbons largely related to its operation as a retail gasoline station over a time span of >40 yr. As part of this research, the site was exposed to PO_4 amendment delivery for 17 weeks, after which the amendment was altered to PO_4 with citrate addition. Site impacts in the soil are smeared across the unsaturated capillary fringe and saturated soil zones, providing an ideal living laboratory to evaluate the effect of citrate across a variety of redox environments.

4.4 Materials and Methods

4.4.1 Field site and design

The study site is at a former gasoline station located in an active urban setting in Saskatoon, SK (Fig. 4.1). Based on the previous site assessment results, a comingled plume may exist beneath the adjacent street originating from both the former and an existing gasoline station located across the street from the study site. The groundwater flow direction in this area is to the northwest toward to the South Saskatchewan River. Due to historic site disturbance and development, utilities, plume size and shape, site flow may not always be in that direction. Two

infiltrators, denoted as the North and East Infiltrator, for amendment solution delivery were installed (Fig. 4.1). Detailed information about infiltrators can be found in Siciliano et al. (2016). This study used two amendment treatments to test the effect of citrate addition on P bioavailability. The first amendment delivery containing 1 mM H_3PO_4, 0.08 mM HNO_3, and 11 mM $MgSO_4$ in municipal potable water (100,000 L in the tank) was pumped into infiltrators 0.5 m below ground at a rate at ~5000 L d^{-1} on 15 May 2015. The second amendment delivery including 10 mM citric acid, 1 mM H_3PO_4, 0.08 mM HNO_3, and 11 mM $MgSO_4$ began on 25 Sept. 2015.

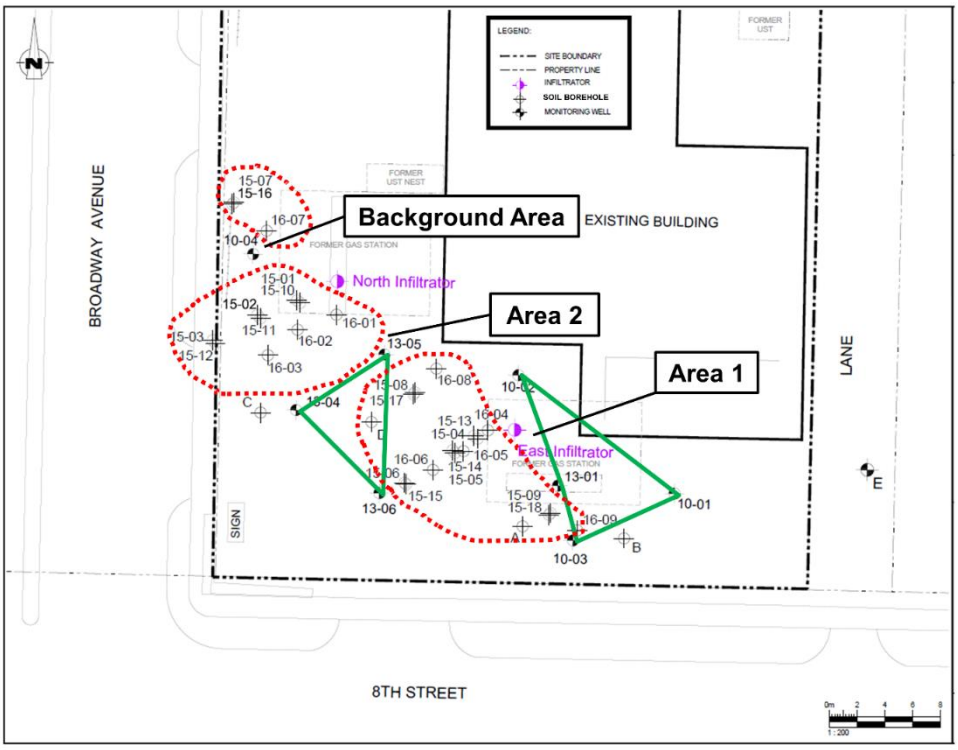

Fig. 4.1. Locations of groundwater monitoring wells and soil boreholes for different areas at Broadway and 8th street (adapted from a site map provide by Federated Co-operatives Limited). The scale is 1:200. Green triangles link up groundwater monitoring wells in each area. The red dash circles group the soil boreholes for each area.

4.4.2 Groundwater sampling and analysis

Eight monitoring wells (as spatially arranged in Fig. 4.1) were installed in 2010 and 2013. Groundwater samples (about 1 L) were collected monthly from each well and analyzed by Saskatchewan Polytechnic from December 2014 to July 2016. Groundwater parameters determined included conductivity, pH, manganese(II), iron(II), chloride, bromide, fluoride,

nitrate, nitrite, sulfate, calcium (total), magnesium (total), sodium (total), phosphorous (total), manganese (total), iron (total), calcium (dissolved), magnesium (dissolved), potassium (dissolved), sodium (dissolved), phosphorous (dissolved), manganese (dissolved), iron (dissolved), sulfide, total dissolved solids (at 180°C), benzene, toluene, ethylbenzene, xylenes (BTEX), and Canadian Council of Ministers of the Environment (CCME) petroleum hydrocarbon (PHC) fractions $F1_{-BTEX}$, F2, and F3. F1 has the equivalent normal straight-chain hydrocarbon (nC) from nC6 to nC10. $F1_{-BTEX}$ is the content of F1 with BTEX subtracted. F2 has nC10 to nC16, and F3 has nC16 to nC34.

The whole period for groundwater determination process has three treatments: no amendment (seven sampling points: 1 Oct. 2014, 30 Oct. 2014, 15 Dec. 2014, 13 Jan. 2015, 13 Feb. 2015, 3 Mar. 2015, and 10 Apr. 2015), phosphate amendment (six sampling points: 30 Apr. 2015, 28 May 2015, 17 June 2015, 15 July 2015, 12 Aug. 2015, and 17 Sept. 2015), and phosphate plus citrate amendment (seven sampling points: 14 Oct. 2015, 16 Nov. 2015, 7 Dec. 2015, 13 Jan. 2016, 9 Feb. 2016, 2 Mar. 2016, and 7 Apr. 2016). According to the dissolved P change and position, eight monitoring wells were divided into three areas (Fig. 4.1). Background area is represented by 10-04. Area 1 includes 10-01, 10-02, 10-03, and 13-01. Area 2 embraces 13-04, 13-05, and 13-06. The mean for all the monitoring wells in the same area in the same amendment treatment was used for analysis.

4.4.3 Soil sampling and analysis

According to the time for different amendment solution deliveries, nine soil boreholes were drilled at three time points (Fig. 4.1): 15-01 to 15-09 on 15 and 16 Apr. 2015 (for no amendment); 15-10 to 15-18 on 9 Sept. 2015 (for phosphate amendment), the position for soil boreholes was the same as that in April 2015; 16-01 to 16-09 on 26 and 27 Apr. 2016 (for phosphate and citrate amendment), on subsequent samples boreholes were placed with 0.5 m of the previous sampling boreholes. The 15-01, 15-02, 15-03 boreholes were drilled in a southwest line of the North Infiltrator, at distances of 3, 6, and 9.5 m from the infiltrator. The 15-04, 15-05, 15-06 boreholes were drilled in a southwest line of the East Infiltrator, at distances of 2.5, 4.5, and 8.5 m from the infiltrator. The 15-07, 15-08 and 15-09 boreholes were drilled northwest of the North Infiltrator, between the North and East infiltrators, and southeast of the East Infiltrator. All boreholes were backfilled with bentonite and capped at the surface with cold-patch asphalt.

All nine boreholes were drilled to 6.0 m deep and soil samples were collected at 1.0-m intervals to the final depth. The upper three samples for each borehole (1, 2, and 3 m) represented the unsaturated zone and the lower three samples (4, 5, and 6 m) stood for the saturated zone (Fig. 4.2). However, during biostimulation, portions of the unsaturated zone, especially those near the injectors, received biostimulation solution because the injectors were filled to 0.5 m below the surface. Similarly, the whole area was divided into three treatment areas: background area had one borehole for each time point (15-07/15-16/16-07, three replicates for each zone); Area 1 was grouped by five boreholes (15-04/15-13/16-04, 15-05/15-14/16-05, 15-06/15-15/16-06, 15-08/15-17/16-08, and 15-09/15-18/16-09; 15 replicates for each zone); Area 2 was grouped by three boreholes (15-01/15-10/16-01, 15-02/15-11/16-02, and 15-03/15-12/16-03; nine replicates for each zone).

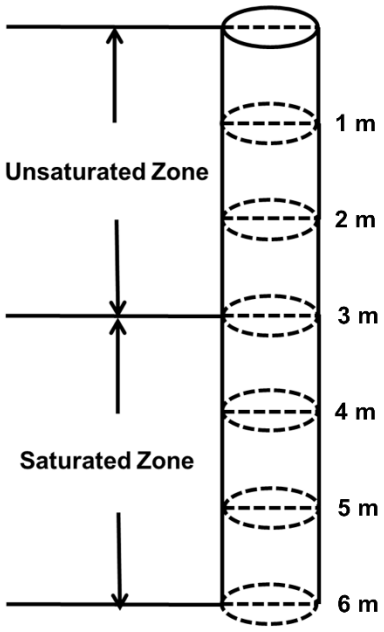

Fig. 4.2. Structure for a soil borehole.

Total elemental concentrations were determined with X-ray fluorescence (XRF) using a Thermo Fisher Scientific ARL OPTIM'X X-ray Analyzer. Soil samples were dried, sieved (0.850 mm), hand ground to a uniform particle size with mortar and pestle to reduce X-ray shadowing effects of large soil aggregates, and then analyzed as powders under helium X-ray chamber conditions. Elemental counts per second were converted to milligrams per kilogram

concentrations using the Thermo Fisher Scientific OPTIQUANT software package. This software package provides an accuracy to within 10% of each element. A known standard reference soil (NIST 2711) was periodically measured to verify that OPTIQUANT was providing consistent results. Only 12 samples that may have been influenced by the citrate addition were analyzed.

Phosphorus speciation was conducted via sequential chemical extractions performed on 0.5 g air-dried 0.850-mm-sieved soil. For this fractionation, 62-mm × 27-mm anion-exchange membrane resin strips (Qian et al., 2006), 0.5 M $NaHCO_3$ (Schoenau and O'Halloran, 2006), and 0.1 M NaOH were used to determine P extracted by resin (Resin-P), $NaHCO_3$–extracted inorganic ($NaHCO_3$–IP) and organic P ($NaHCO_3$–OP), and NaOH-extracted inorganic (NaOH-IP) and organic P (NaOH-OP) using a common sequential extraction methodology (Tiessen and Moir, 2006). Inorganic P was analyzed by 0.9 M H_2SO_4. Total P was determined via an ammonium persulfate and 0.9 M H_2SO_4 autoclaving digestion. Organic P was calculated by subtracting total P with inorganic P. All extracts were analyzed by the compact dual-channel AA1 auto analyzer (Folio Instruments) with continuous flow analysis. Each set of 10 samples had one sample duplicate for quality control.

The PHC fractions were determined based on CCME protocol (CCME, 2001). To determine moisture content, 7 g of wet soil for each sample was air dried overnight in the fume hood, then oven dried at 105°C overnight. Wet soil (7 g) was weighed in 30-mL Teflon tubes to extract $F1_{-BTEX}$ and BTEX. Soil was mixed with 14 mL methanol, shaken for 2 h at 25 *g*, then centrifuged at 700 *g* for 20 min. One milliliter of this extract as mixed with 9 mL of water for headspace analysis by gas chromatograph (GC) equipped with a flame ionization detector (FID) (SCION 436-GC, Bruker, ON, Canada) using a PAL Combi-xt autosampler. Samples were incubated for 5 min at 82°C and agitated at 14 *g* (2 s on and 4 s off). The GC, equipped with a split-splitless injector, was operated with a split 20:1 for the whole run. The injector temperature was 200°C with a constant column flow of 1 mL min^{-1}. The column used was Bruker-BR86092 (30 m × 0.25 mm) with helium carrier gas at a flow rate of 27.5 mL min^{-1}, hydrogen gas at a flow of 30 mL min^{-1}, and air at a flow of 300 mL min^{-1}. The oven temperature program used was initially 60°C, then increasing 15°C min^{-1} to 150°C. Detector temperature was 300°C. Each set of six samples had one method blank, one blank spike, and one matrix spike, which were carried through the complete extraction process with samples. Method blank and blank spike

used 7 g clean sand. The blank spike, and matrix spike which used 7 g soil for a random sample, were extracted after adding 0.5 mL of 50- to 200-mg L^{-1} commercial standard for $F1_{-BTEX}$ and BTEX. Recovery for blank spike and matrix spikes were from 70 to 130%.

The F2 and F3 of PHC were extracted by modified shaking method (Schwab et al., 1999; Siddique et al., 2006), and *o*-terphenyl was used as surrogate. Soil (2 g) was mixed with 2 g oven-dried sodium sulfate and 30 mL of 50:50 hexane/acetone in a 40-mL Teflon tube. The tube was shaken at 25 *g* for 2 h and then centrifuged at 700 *g* for 10 min. The supernatant was evaporated to 1.5 mL by Pierce Reacti-Therm III NON-stirring heating module at room temperature under nitrogen flow and then passed through 9 g of oven-dried sodium sulfate in a column, which was then rinsed with 10 mL of hexane. The eluent was then evaporated to 1.5 mL again. The samples were analyzed quantitatively by GC-FID (CP-3800 GC, Varian, CA, USA) equipped with BD-1HT column (Agilent Technologies, CA, USA), 30 m × 0.25 mm. The oven temperature was programmed at 40°C for 1.0 min with 30°C min^{-1} increments to 350°C. The constant column flow was 10 mL min^{-1}. The detector was kept at 350°C with helium carrier gas at a flow rate of 50 mL min^{-1}, hydrogen gas at a flow of 20 mL min^{-1}, and air at a flow of 300 mL min^{-1}. Each set of 20 samples had a method blank, a blank spike, a matrix spike, and a sample duplicate. The blank spike and matrix spike, which were added 1 mL of 100 to 200 mg L^{-1} standard, had 70 to 130% recovery.

All commercial standards for PHC fractions were purchased from Chromatographic Specialties. For the standard mixture of $F1_{-BTEX}$, BTEX, the stock solution had 2000 mg L^{-1} of *n*-decane, *n*-hexane, toluene, benzene, ethylbenzene, *o*-xylene, *m*-xylene, and *p*-xylene. The stock F2 and F3 standard contained 5000 mg L^{-1} of phytane, pristine, *n*-octadecane, *n*-heptadecane, *n*-decane, *n*-hexadecane, *n*-tetratriacontane, and *o*-terphenyl. Soil pH was measured in 20 mL of 0.01 M $CaCl_2$ with 4 g air-dried 2-mm sieved soil (Hendershot et al., 2008) only for soil samples collected in September 2015 and April 2016. Soil particle size analysis was conducted by a modified pipette procedure (Indorante et al., 1990). Soil organic carbon content was determined by dry combustion using a carbon analyzer (Bisutti et al., 2004).

4.4.4 Statistical analysis

Normality of residuals was tested using the Shapiro–Wilk statistic. The groundwater and soil were zero-inflated data, so a Kruskal–Wallis rank sum test was used to test the effects of

area and treatment on groundwater measures and treatment, area, and soil zone on soil measures. The *t* test was performed to compare different treatments in the same area for groundwater samples and different treatments in the same soil zone and same area for soil samples. All tests were completed at the $p < 0.05$ significance level. The Pearson correlation coefficient was calculated to estimate correlation between hydrocarbon biodegradation and P fractions. Statistical analyses were performed using R version 3.3.2 (R Core Team, 2016).

4.5 Results

4.5.1 Groundwater dissolved P and iron(II)

Citrate addition increased dissolved P and iron(II) in the groundwater (Fig. 4.3, Table 1). The effect of citrate addition on P and iron(II) was limited to Areas 1 and 2, with background groundwater remaining unaffected. For example, in Area 1, dissolved P was undetectable when only phosphate was added but increased to 0.1 mg P L^{-1} after addition of citrate with phosphate. In Area 2, dissolved P jumped from 0.1 to 0.4 mg L^{-1} after adding citrate. Soil pH was stable in the background area, 7.12 (SE = 0.04). However, pH decreased slightly in Areas 1 and 2, from 6.97 (SE = 0.07) to 6.76 (SE = 0.03) and from 7.02 (SE = 0.06) to 6.75 (SE = 0.03), respectively. Iron(II) increased from 20 to 80 mg L^{-1} in Area 1 and from 60 to 80 mg L^{-1} in Area 2 after citrate addition. In contrast with iron(II), sulfate increased ($p < 0.05$) after citrate addition, increasing from 1991 (SE = 172) to 2670 mg L^{-1} (SE = 170) in Area 1 and from 814 (SE = 101) to 1549 mg L^{-1} (SE = 451) in Area 2. For the whole site, sulfide decreased from 3.24 (SE = 2.73, before amendment delivery), to 0.33 (SE = 0.18, before citrate addition), and then to 0.14 (SE = 0.04, after citrate addition).

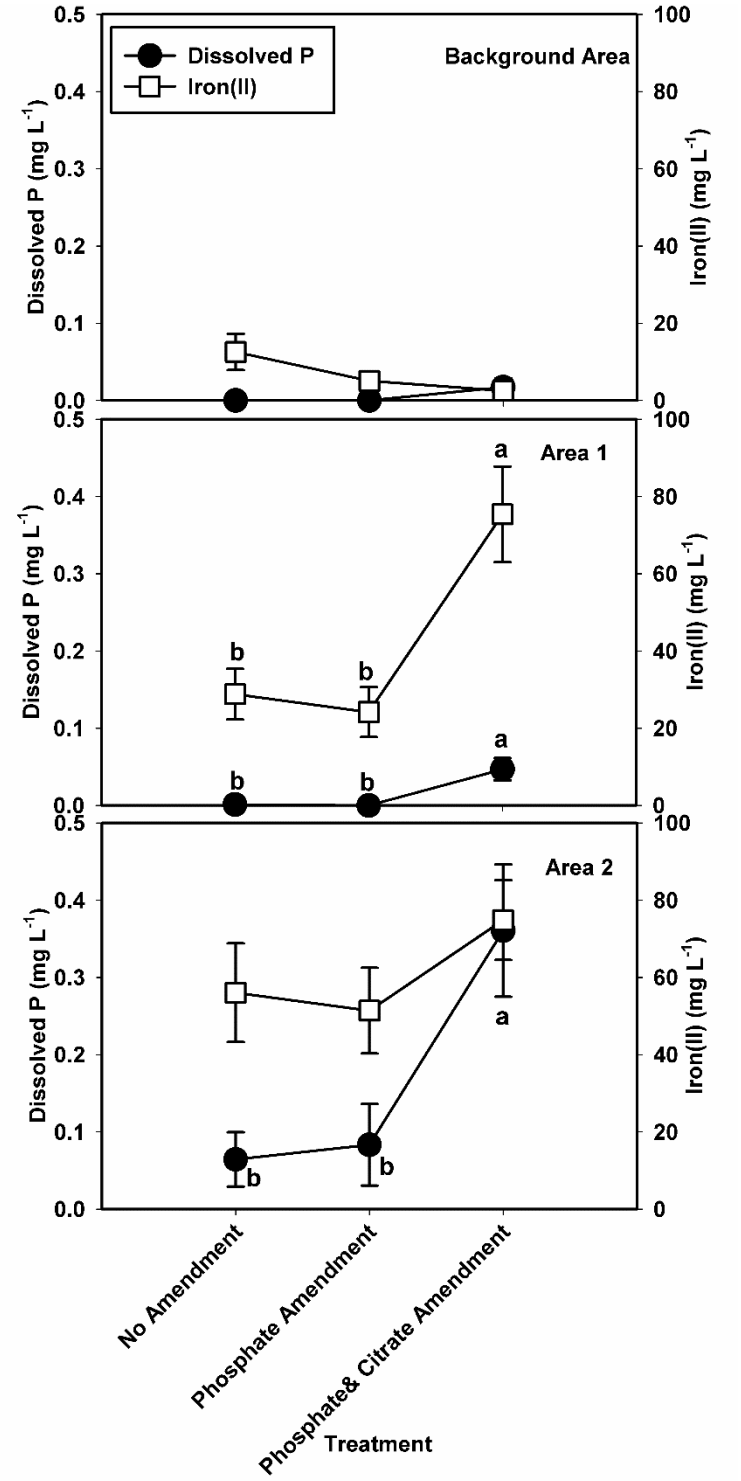

Fig. 4.3. Dissolved phosphorus (circles) and iron(II) (squares) in groundwater across three site treatment areas. Symbols indicate the average of four wells for Area 1, three wells for Area 2, and one well for the background area, with error bars indicating the standard error of the estimate. Different letters indicate significant differences among amendment treatments for the same area.

Table 4.1. The p-values from the Kruskal-Wallis rank sum test for variables in groundwater.

Variables	Types	Area[§]	Treatment
Nitrate	Electron acceptor	3.72E-04	5.59E-01
Sulfate		<2.2E-16	3.91E-02
Manganese(II)	Potential product from anaerobic respiration	5.95E-02	7.12E-01
Nitrite		1.32E-03	1.21E-01
Iron(II)		5.83E-05	1.12E-02
Sulphide		4.26E-01	6.36E-03
Phosphorous (T[†])	Nutrient of interest	7.94E-16	1.64E-01
Phosphorous (D[‡])		2.62E-05	2.30E-09
Benzene	Petroleum hydrocarbon	6.50E-02	3.52E-04
Toluene		4.07E-01	1.09E-02
Ethylbenzene		4.05E-02	1.08E-02
Total xylene		2.66E-03	8.87E-02
BTEX		2.25E-02	2.76E-03
$F1_{-BTEX}$		3.77E-01	1.92E-08
F2 (C_{10}-C_{16})		4.77E-01	3.77E-05
F3 (C_{16}-C_{34})		3.14E-01	2.38E-10
pH	Normal water property	2.83E-06	7.08E-05

† T, concentration for all phases in total; ‡ D, concentration for the dissolved phase

§ Comparison within factor Area having three levels: Background Area, Area 1 and Area 2

4.5.2 Soil P

Citrate addition increased soil P concentrations in what are typically considered the bioavailable fractions, Resin-P, $NaHCO_3$–OP, and $NaHCO_3$–IP, in selective areas (Fig. 4.4, Fig. A2.1). For Resin-P, an increase was observed in both unsaturated zone and saturated zone for background area (unsaturated zone: from 13 to 19 mg kg^{-1}; saturated zone: from 1 to 2 mg kg^{-1}) and Area 1 (unsaturated zone: from 22 to 30 mg kg^{-1}; saturated zone: from 4 to 7 mg kg^{-1}) after

adding citrate in the amendment solution. Citrate addition reacted differently in Area 2, mainly increasing $NaHCO_3$–OP in the unsaturated zone (from 5 to 12 mg kg^{-1}) and saturated zone (from 5 to 8 mg kg^{-1}). The $NaHCO_3$–OP also was slightly enriched in Area 1 for the unsaturated zone (from 9 to 12 mg kg^{-1}). In addition, $NaHCO_3$–IP for Area 2 in the unsaturated zone increased from 23 to 25 mg kg^{-1}. Total P, as measured via XRF (Table A2.1), showed no consistent trend over time and had little variability (930–1240 mg kg^{-1}).

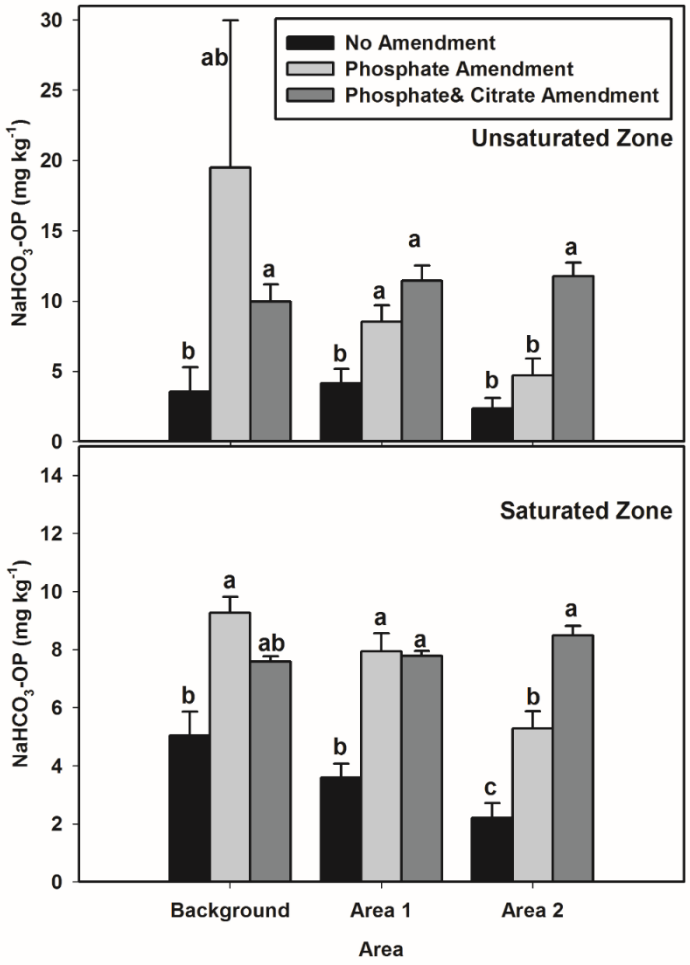

Fig. 4.4. $NaHCO_3$–extracted organic phosphorus ($NaHCO_3$–OP) in different soil zones across three site treatment areas. Averages are denoted by bars, with the vertical bars marking the standard error from the mean. Different letters indicate significant differences among amendment treatments for the same area in the same soil zone.

4.5.3 Hydrocarbon biodegradation and its correlation with P bioavailability

Citrate addition enhanced F1 and benzene biodegradation in the soil, which was related to the P bioavailability. As soil P increased, soil concentrations of benzene decreased. For example, soil benzene concentration was negatively correlated with P for Resin-P (n = 159, rho = −0.187, p = 0.018), $NaHCO_3$–IP (n = 159, rho = −0.209, p = 0.008), and NaOH-IP (n = 159, rho = −0.164, p = 0.038). Hydrocarbon reductions were dependent on the site location, with the largest decrease in Area 2 (Fig. 4.5), which was between the two injectors. For example, in Area 2, $F1_{\text{-BTEX}}$ decreased from 418 (SE = 232) to 12 mg kg^{-1} (SE = 6) for the unsaturated zone and from 495 (SE = 184) to 122 mg kg^{-1} (SE = 46) for the saturated zone. In Area 1, south of the injectors, $F1_{\text{-BTEX}}$ also decreased, but only from 453 (SE = 178) to 331 mg kg^{-1} (SE = 151) in the saturated zone. Groundwater BTEX concentrations were more variable (Fig. S2.2). Benzene and $F1_{\text{-BTEX}}$ in groundwater significantly decreased after the amendment deliveries in the whole site (Table 4.1), from 6.35 (SE = 1.46) then 1.90 (SE = 0.57) to 0.96 (SE = 0.20), and from 7.36 (SE = 3.60) then 4.25 (SE = 0.39), to 0.96 mg L^{-1} (SE = 0.21), respectively. For the saturated zone in Area 2 (Fig. 4.6), the correlation between $F1_{\text{-BTEX}}$ and $NaHCO_3$–OP is negative (−0.23).

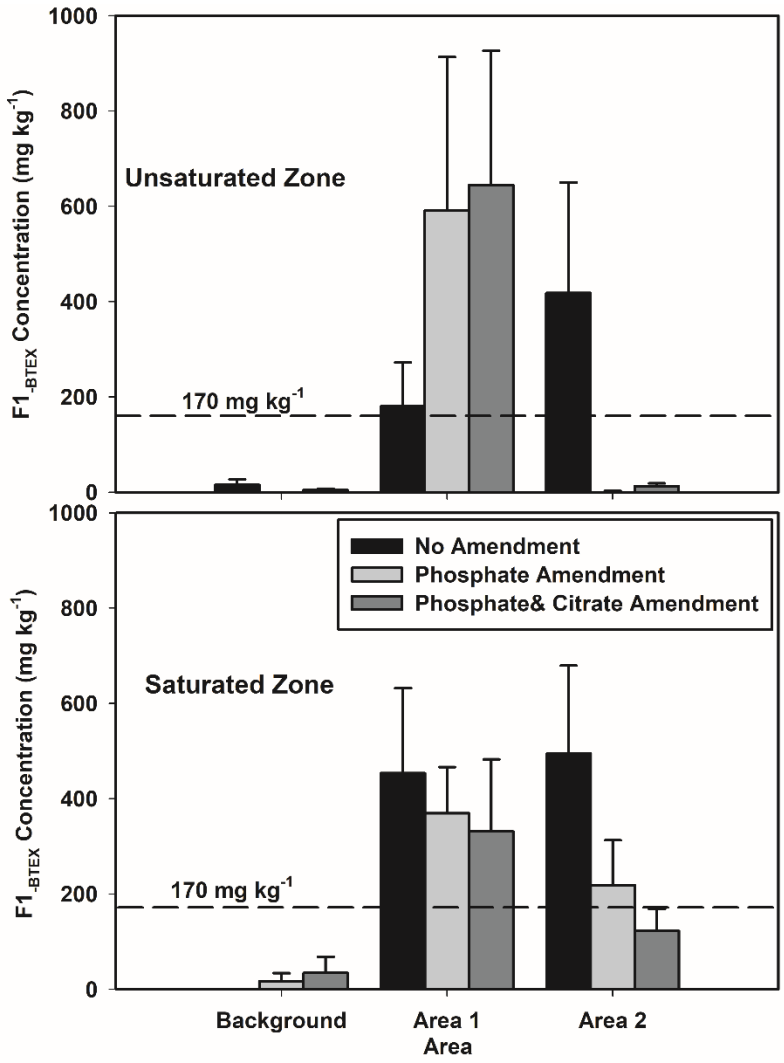

Fig. 4.5. $F1_{-BTEX}$ concentration in unsaturated and saturated zone across three site treatment areas. $F1_{-BTEX}$ is the content of the F1 petroleum hydrocarbon fraction with benzene, toluene, ethylbenzene, and xylenes subtracted. Averages are denoted by bars with the standard error bars. The dash line indicates the Tier 1 risk-based criteria for fine-grained, commercial land use in RBCA (Saskatchewan Ministry of Environment, 2009).

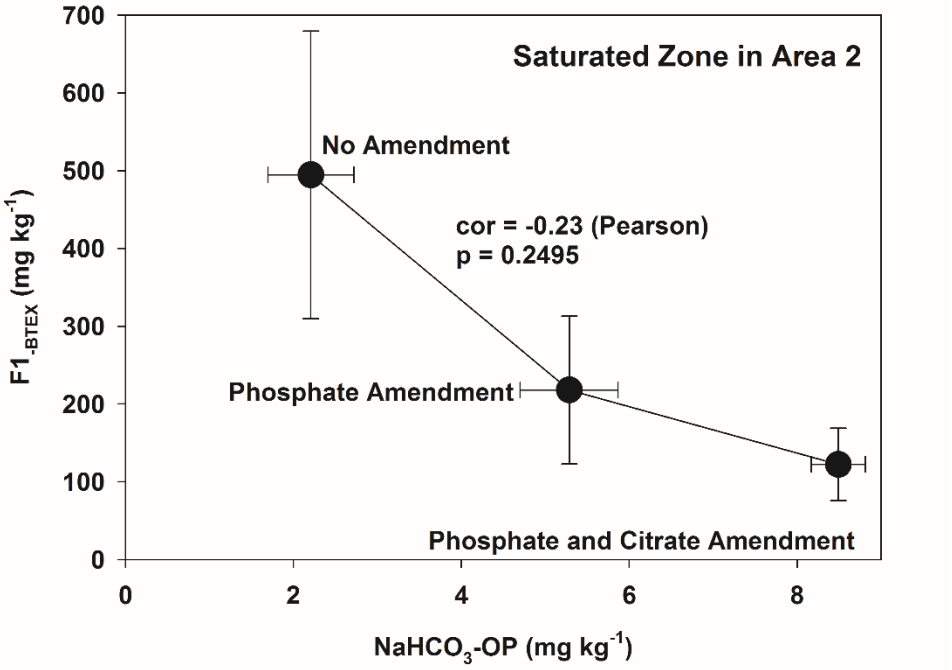

Fig. 4.6. The correlation between $F1_{-BTEX}$ concentration and $NaHCO_3$–extracted organic phosphorus ($NaHCO_3$–OP) in the saturated zone in Area 2 during three amendment treatments. $F1_{-BTEX}$ is the content of the F1 petroleum hydrocarbon fraction with benzene, toluene, ethylbenzene, and xylenes subtracted. The value for cor is Pearson's product moment correlation coefficient.

4.6 Discussion

Citrate addition increased the efficiency of P amendment for gasoline- and diesel-related petroleum hydrocarbon bioremediation. The combined addition of P and citrate did provide more bioavailable P for bioremediation, which indicates that the P amendment could be more effective if it was applied with citrate. Increases in dissolved P (bioavailable) was immediately observed in groundwater after the second amendment delivery containing citrate. No change for dissolved P occurred in the background area. Without citrate addition, dissolved P was not detectable in Area 1 before September 2015 and was ~0.1 mg L^{-1} in Area 2. The strongest effect of citrate addition occurred in the site area located between two infiltrators.

The increased soil P bioavailability by citrate appeared to be linked to the dissolution of exchangeable organic P in soil. The resin- and $NaHCO_3$–extracted P has been shown to contribute to soluble and exchangeable P (Schoenau and O'Halloran, 2006; Tiessen and Moir, 2006), which was selectively increased in certain area but did not change significantly during the

two amendment stages (Table A2.2). The $NaHCO_3$–OP significantly increased after the second amendment delivery in Areas 1 and 2. Particularly for both the unsaturated and saturated zones in Area 2, $NaHCO_3$–OP was raised, corresponding to the dissolved P change in groundwater. Others have also found that citrate induced labile organic P ($NaHCO_3$–OP) release in acidic, neutral, and calcareous soil (Wei et al., 2010; Wang et al., 2015). Alternatively, organic P content may have been overestimated (Turner et al., 2005; Tiessen and Moir, 2006). The potential association between inorganic phosphate and humic substances, which prevents the detection for inorganic phosphate by molybdate colorimetry, will lead to the underestimation of inorganic P. The presence of complex inorganic phosphates was analyzed as organic P because only the free phosphate can be determined by molybdate colorimetry. However, one would expect to observe similar trends in the background samples if interference were to blame, which was not the case in this study.

Citrate addition enhanced anaerobic gasoline dissipation. This gasoline-contaminated site had low content for F2 and F3 (Fig. A2.3). The major contaminant was F1 (represented with BTEX and $F1_{\text{-BTEX}}$). For example, $F1_{\text{-BTEX}}$ decreased after the amendment deliveries in Area 2 were below the criteria in Fig. 4.5 (Saskatchewan Ministry of Environment, 2009). Similarly, BTEX concentrations in groundwater eventually decreased to the baseline (Fig. A2.2). The fluctuation for BTEX was likely due to fractured flow onsite, and BTEX remained below criteria for a 3-mo period. This decrease may be linked to biostimulation of iron-reducing microorganisms during citrate addition. Iron(III) was reported to be the most abundant potential elector for anaerobic BTEX biodegradation (Lovley, 1997). The amendment treatment significantly influences the iron(II), iron (dissolved), and iron (total) in the groundwater (Table 4.1, Table A2.3), especially iron(II). Iron(II) concentrations stayed consistently low throughout the study period in the background area, as well as in Areas 1 and 2, before citrate amendment. The addition of citrate immediately increased iron(II) in Areas 1 and 2. The increase of iron(II) in the groundwater was mainly due to the biological reduction of iron(III), which is a sign for increased activity for iron reducers. Iron-reducing and sulfate-reducing bacteria are well-known anaerobic degraders of gasoline (Phelps and Young, 1999; Philp et al., 2002; Townsend et al., 2004). Confirmation that the loss of gasoline was biological and not abiotic through the use of the diastereomers of acyclic isoprenoids (McIntyre et al., 2007) was unsuccessful, because almost all samples had undetectable levels of phytane, pristine, *n*-octadecane, and *n*-heptadecane. Citrate was not

detected in the groundwater, likely because the biological half-life for citrate in water is short and adsorption processes are rapid (Owen et al., 2001). Thus, it is unclear if the citrate is increasing the iron-reducing bacterial activity mainly by acting as a carbon source for the bacterial growth or primarily through its effects on P availability. Many iron reducers, such as *Shewanella alga*, *Pseudomonas fluorescens*, and *Azotobacter vinelandii* have been reported to degrade citrate (Joshi-Tope and Francis, 1995; Knight et al., 1996; Ganesh et al., 1997). It is unlikely that sulfate-reducing organisms were the primary hydrocarbon degraders at this site, as sulfate concentrations increased and sulfide concentrations decreased at the site during stimulation. This is consistent with competitive processes described with PO_4; citrate will dissociate $CaSO_4$ (gypsum) minerals if present via chelation of Ca and will also desorb SO_4 due to having a much higher affinity for mineral surfaces than does SO_4. Alternatively, citrate addition may be increasing degradation activity by enhancing hydrocarbon bioavailability rather than biological activity, but there was no evidence to evaluate this mechanism (Gao et al., 2010b; a) and the data is consistent with an increase in P bioavailability.

Biostimulation in the field site was mainly constrained by the high clay content of the soils (Table A2.4), which not only limits biostimulation solution dispersion but also is linked to low P bioavailability (Halajnia et al., 2009). Thus, the only decrease in unsaturated zone for BTEX and $F1_{-BTEX}$ was in Area 2, which lies between the two infiltrators. It is notable that this active urban area site had a concrete floor, which blocked influence from rainfall. A tracer study was undertaken, but due to fractured flow, it was unable to delineate an area of infiltrator influence. The temperature recorded by the loggers from monitoring wells did not change much during the whole study (Table A2.5), so the influence from time-depend environmental factors was eliminated. In the future, delivery design with more infiltrators or surfactant addition may improve the phosphate amendment efficiency for bioremediation. Even though Ca-P dominates the soil P sorption in this calcareous soil (Table A2.6) (Hinsinger, 2001), NaOH-OP, which is operationally defined as Fe/Al bound P, reached the maximum content throughout the entire site after citrate addition and was significantly influenced by the amendment treatment (Table A2.2). There is not an obvious link between citrate addition and increased Fe/Al-bounded organic P in the literature; this change in P speciation may be due to a biological effect.

One key finding of this study is that organic P in both the $NaHCO_3$ and NaOH extraction was a relatively small proportion (2–6%) of total P in these soils but was quite important in

microbial remediation activity. Phosphorus species present in such small quantities would be missed by current spectroscopic techniques, which typically observe mineral forms of P and inorganic adsorption species. It appears that citrate is more effective at desorbing organic-P from these soils, which leads to an increase in biodegradation without changing the bulk speciation or mineralogy of P in these samples.

The use of citric acid as an amendment has some specific operational challenges. In this study, free citric acid, which was largely neutralized by the alkalinity of the amendment solution, was used. In prairie regions, this neutralization is practical due to high alkalinity and hardness (due to Mg, Ca, and SO_4). In other regions, other alternatives to maintain pH may be required. In addition to neutralization, biofouling of amendment tanks and injection lines should be considered. In this case, an ultraviolet sterilizer was installed directly in the reservoir tank to prevent microorganisms from using the citrate as an available electron donor while in the amendment tank. We'd recommend that practitioners use a similar system or consider inline injection systems to inject amendment components directly into injection lines to minimize the potential of biofouling. Further, as noted in the previous publication (Siciliano et al., 2016), P levels in the amendment should be maintained at relatively low concentrations of 1 mM to prevent mineral deposition.

4.7 Conclusion

Citrate addition offered several advantages for phosphate biostimulation in gasoline- and diesel-contaminated sites. First, and most importantly, citrate addition enhanced organic P desorption and thus enhanced the bioavailability of P onsite. Second, citrate addition enhanced anaerobic iron-reducing activity. As a consequence, hydrocarbon concentrations in the groundwater and soil decreased significantly. Future work should focus on further delineating the mechanisms by which citrate acid is stimulating degradation: (i) P availability, (ii) C source, or (iii) hydrocarbon bioavailability to determine whether there are general trends that can be used to improve biostimulation solution performance.

5. Diverging Soil and Groundwater Bacterial Community: The Role of Adsorbed Phosphorus in Maintaining Active Hydrocarbon Degradation in Cold Region Soils

5.1 Preface

Citrate addition increased phosphorus bioavailability, enhanced hydrocarbon degradation and stimulated iron-reducing activity in gasoline contaminated brownfield site in Chapter 4. However, it is not clear whether the stimulation of iron-reducing activity was due to functional anaerobic hydrocarbon degraders. In order to evaluate the effect of citrate on the bacterial community, the composition and function for the microbial community were analyzed by culturable-dependent and culturable-independent techniques, in groundwater and soil for three amendment treatments. Professor Derek Peak determined major phosphorus (P) species with P K-edge XANES (X-ray absorption near-edge structure) for some soil samples in the influenced soil area.

5.2 Abstract

Citrate can increase phosphorus and hydrocarbon bioavailability to enhance hydrocarbon bioremediation. Yet, how citrate addition influences the structure and function of microbial communities is unclear. Here, how citrate mediates microbial community response to amendment was investigated during *in situ* remediation of gasoline in a calcareous cold region soil. Three biostimulation treatments (no amendment, phosphate amendment, and a phosphate and citrate amendment) were applied over an 18-month period using large bore infiltrators. Microbial community was assessed in groundwater and soil. Using amplicon sequencing libraries, catabolic gene (*bcrC* and *bzdN*) and culturable hydrocarbon degrader prevalence, this study compared groundwater and soil bacterial communities to phosphorus XANES speciation and sequential extraction distribution. Hydrocarbon degradation was strongly stimulated by phosphate and citrate addition and closely linked with increases in organic phosphorus availability. Phosphate and citrate increased *bzdN* prevalence but not *bcrC*, while simultaneously increasing culturable anaerobic hydrocarbon degraders population. However, while phosphate shifted both soil and groundwater bacterial communities, the further addition of citrate caused differential effects in groundwater compared to soil. In groundwater, citrate increased bacterial diversity as well as altered community structure with specific bacteria stimulated that are known hydrocarbon degraders. In contrast, in soil, citrate increased the amount of adsorbed phosphate and reversed bacterial community structure shifts to be more like the pre-amendment control communities, but still caused increases in selective hydrocarbon degraders. In conclusion, groundwater and soil microbial communities responded differently to biostimulatory treatments largely because changes in phosphorus mineralogy dominated community response in soil, but not in groundwater.

5.3 Introduction

Biostimulation, a common strategy for bioremediation, usually adds electron acceptors, co-substrate, and nutrients to stimulate indigenous microbes that can degrade contaminants such as petroleum hydrocarbons (PHC) (Zhang and Lo, 2015). Low molecular weight organic acid anions (LMOAA), such as citrate and acetate, comprise a significant proportion of root exudates. LMOAA can enhance anaerobic hydrocarbon bioremediation by increasing bioavailability of phosphorus (P) or hydrocarbons, or by stimulating hydrocarbon-degrading anaerobes (Zhang and

Lo, 2015; Martin et al., 2016; Rohrbacher and St-Arnaud, 2016). Recently, it was demonstrated citrate enhanced organic P desorption, iron-reducing bacteria activity, and hydrocarbon degradation in contaminated soils (Chapter 4). However, the effect of LMOAA on microbial community composition and function has received relatively little attention, especially in PHC contaminated cold calcareous soils.

The first microorganism found to degrade aromatic hydrocarbons under strict anaerobic condition was an iron-reducing bacterium, *Geobacter metallireducens* (Lovley et al., 1993). Since then, anaerobic microbial communities that degrade PHC under manganese-reducing (Lovley, 1997), nitrate-reducing (Burland and Edwards, 1999), iron-reducing, sulfate-reducing, and methanogenic conditions (Edwards and Grbić-Galić, 1992, 1994; Lovley and Woodward, 1996) have also been described. The majority of detected anaerobic hydrocarbon bacterial degraders belong to the phyla of *Actinobacteria*, *Bacteroidetes*, *Chlorobi*, *Chloroflexi*, *Firmicutes*, and *Proteobacteria* (Edwards, 2003; Robertson et al., 2007; Yergeau et al., 2009; Weelink et al., 2010; Zhang et al., 2012; van der Zaan et al., 2012; Kleinsteuber et al., 2012; Herbst et al., 2013; Fathepure, 2014; Luo et al., 2014, 2016; Zhang and Lo, 2015; Sheng et al., 2015; Quadros et al., 2016). Within these taxa, two catabolic genes, *bzdN* and *bcrC*, are associated with BTEX (benzene, toluene, ethylbenzene, and xylene) degradation. The *bzdN* gene is associated with the *Azoarcus* type of ATP-dependent class I Benzoyl coenzyme A (benzoyl-CoA) reductases (BCR class I) (Kuntze et al., 2011), and *bcrC* gene is related to the *Thauera* type BCR, which catalyzes the reduction of anaerobic central intermediates benzoyl-CoA (a common intermediate in the anaerobic metabolism of most aromatic compounds) (Fuchs et al., 2011; Fuentes et al., 2014). *Geobacter* species also contain *bzdN* and *bcrC* genes (Kleinsteuber et al., 2012). All three genera: *Azoarcus* (Edwards, 2003; Kasai et al., 2006; Weelink et al., 2010; van der Zaan et al., 2012; Kleinsteuber et al., 2012; Luo et al., 2014), *Thauera* (Weelink et al., 2010; Kleinsteuber et al., 2012) and *Geobacter* (Robertson et al., 2007; Weelink et al., 2010; Zhang et al., 2012; Kleinsteuber et al., 2012) are well known n-alkane and BTEX degraders.

Microbial communities are strongly influenced by soil mineralogy, which can be altered by phosphate and citrate addition. Total phosphate influences microbial community phenotypes whereas the relative percentages of phosphate minerals influences microbial community genotype composition. For example, the amount of adsorbed phosphate was strongly linked to both mineralization activity and *bzdN* prevalence, whereas the relative proportions of brushite

($CaHPO_4 \cdot 2H_2O$) and adsorbed phosphate had strong determining effects on bacterial community composition (Siciliano et al., 2016). Other groups found apatite mineral ($Ca_{10}(PO_4)_6(OH,F,Cl)_2$) dissolution was positively correlated to the abundance of the genus *Burhkolderia* (in the order *Burkholderiales,* class *Betaproteobacteria*) colonization (Lepleux et al., 2012). Therefore, providing the desired P phase for PHC-degrading bacteria may be imperative for maintaining effective biostimulation treatments.

Maintaining available P in the calcareous soils undergoing bioremediation is especially challenging; typically, investigators monitor groundwater to assess the success of their biostimulation treatment. Implicit in this monitoring is the assumption that groundwater chemistry reflects shifts in soil chemistry. However, in cold calcareous soils, this assumption may not hold due to the strong adsorption and mineral forming processes occurring in these soils (Kar et al., 2012; Weyers et al., 2016; Hamilton et al., 2017). This study evaluated how phosphate and citrate amendments altered soil P minerals and microbial activity as well as groundwater microbial activity, and community structure with a focus on anaerobic hydrocarbon degraders, at a gasoline contaminated field site. The hypothesis was that citrate addition would lead to shifts in structure and function across groundwater and soil microbial communities.

5.4 Material and Methods

5.4.1 Site description

A former gasoline station located in an active urban area in Saskatoon, SK, Canada, was selected as the research site (Fig. A3.1). A co-mingled plume may exist in the southeast area due to an active gasoline station close to the study area. Two infiltrators (5.5 m) were drilled at the site in the areas of the former pump islands, using a 1.0 m diameter auger drill rig. Each infiltrator has one injection well, one float pump well connected to the injection well, and one monitoring well, and was backfilled with a silica sand. The injection wells were connected to the underground storage tanks which were charged with biostimulation. Submersible pumps in the underground storage tank were connected to injection lines, with floats and auto shutoff switches installed in the tanks and injection wells. The biostimulation solution delivery was controlled by float switches which resulted in a pseudo-steady elevated hydraulic head in the injector to encourage outward radial flow and nutrient transport. Biostimulation solution was pumped into infiltrators at a rate 5000 L day^{-1}. Three biostimulation treatments were applied: no amendment (October

2014 - April 2015), phosphate amendment (May 2015 - September 2015), phosphate and citrate amendment (October 2015 - April 2016). Delivery of the phosphate amendment (1 mM H_3PO_4, 0.08 mM HNO_3, and 11 mM $MgSO_4$) began May 15, 2015. The phosphate and citrate amendment (10 mM citric acid, 1 mM H_3PO_4, 0.08 mM HNO_3, and 11 mM $MgSO_4$) began delivery September 25, 2015.

5.4.2 Sample collection

Sterile Tenax beads (5 g of 60-80 mesh, porous polymers, Sigma-Aldrich Canada Co., ON, Canada) were placed in a 12.5 cm × 4 cm 60 μm mesh Nitex membrane bag (Dynamic Aqua-Supply Ltd., BC, Canada), zip-tied onto Tygon tube (Fisher Scientific, ON, Canada), and suspended 3 m underground (2.5 m below water surface in the two infiltrators). For one-month cycles starting October 28, 2014, each infiltrator had one bag of Tenax beads, and the bag was replaced each month for DNA extraction until March 24, 2016 (14 bags per infiltrator, two subsamples per bag, sample size n = 56). Three soil boreholes (0-6 m deep; one subsample per m depth, 6 subsamples per borehole) close to the two infiltrators represented the area of influence. Control boreholes were drilled on April 15-16, 2015 (15-01 to 15-03; no amendment); phosphate amendment boreholes on September 9, 2015 (15-10 to 15-12); phosphate and citrate amendment boreholes on April 26-27, 2016 (16-01 to 16-03).

5.4.3 Soil PHC and P analysis

Soil samples were collected following CCME protocol (Canadian Council of Ministers of the Environment, 2001). Soil (7 g) aliquots were weighed for moisture content and $F1_{-BTEX}$ determination (Chapter 4). The bioavailable P fraction, $NaHCO_3$ extracted organic P ($NaHCO_3$-OP), was extracted from 0.5 g of air-dried, 0.850 mm sieved soil subsample with 0.5 M $NaHCO_3$, based on a common sequential extraction methodology (Schoenau and O'Halloran, 2006; Tiessen and Moir, 2006).

All P K-edge XANES for soil samples from influenced soil area (15-01-5 m, 15-10-5 m, 16-01-5 m) were collected at the CLS SXRMB beamline (08-B1-1) in partial fluorescence mode, using a 4-element solid-state detector following methods previously reported (Siciliano et al., 2016).

5.4.4 DNA extraction and microbial community analysis

Groundwater and soil subsamples for DNA extraction were stored at -20°C. DNA was extracted from Tenax beads with PowerLyzer PowerSoil DNA Isolation Kit (MO BIO Laboratories, Inc., CA, USA) and from soil with FastDNA SPIN Kit for Soil (MP Biomedicals Canada, QC, Canada). Qubit Fluorometer (Life Technologies, CA, USA) measured DNA concentration and purity. The 16S metagenomics sequencing library was constructed using the Illumina guide with primers 926F and 1392R (Illumina, 2013). For the initial amplification step, Tenax beads samples were annealed at 61 °C and soil samples were at 55 °C. DNA was sequenced on an Illumina Miseq using V3 chemistry on a 600 cycle kit, then sequencing data was processed by EBI Metagenomics Pipeline version 3.0 (Mitchell et al., 2016). *Aliivibrio fischeri* DNA (0.1 ng: 2-3% w/w DNA extract) was used as an internal standard after DNA extraction for sequencing (Smets et al., 2016).

5.4.5 Catabolic gene prevalence and most probable number (MPN)

Quantitative PCR (qPCR) for *bcrC* and *bzdN* was performed following the published reaction details (Siciliano et al., 2016). Briefly, qPCR was performed on the 7500 Real-Time PCR System (Applied Biosystems, CA, USA). The qPCR mixtures contained 10 μL SYBR Green master mix (Qiagen, ON, Canada), 1 μL of 10 μM primer pairs, 6 μL of water, and 2 μL of template DNA, with a final volume of 20 μL. Primers were ordered from Integrated DNA Technologies (Table A3.1). For *bzdN* and *bcrC*, touchdown qPCR reactions were performed as follows: 95 °C × 10’ for 1 cycle; 95 °C × 1’, 65 °C × 1’ (decreasing 1 °C per cycle), and 72 °C × 1’ for 11 cycles; 95 °C × 1’, 58 °C × 1’ (for *bzdN*, 65 °C for *bcrC*), and 72 °C× 1’ for 35 cycles; followed by a melt curve. Clone libraries for *bzdN* and *bcrC* were created with *E. coli* cells by the TOPO TA Cloning Kit (Invitrogen, CA, USA) from environmental DNA. DNA was then extracted from clones and standardized to 10^9 copies as a stock for the standard curve. Facultative diesel degraders were anaerobically cultivated and enumerated with the MPN method (Siciliano et al., 2016). About 1 g of soil (store at 4 °C, within 1 week after collected) was firstly diluted with 9 mL of sterile KH_2PO_4 buffer in the anaerobic chamber, as the 10^{-1} dilution. Sealed plates for 10^{-1}-10^{-14} dilution series were incubated for 14 days in the dark at 4 °C. Iodonitrotetrazolium violet was chosen as an indicator.

5.4.6 Statistical analysis

The operational taxonomic unit (OTU) abundances were adjusted based on the 16S rRNA gene reads of *A. fischeri* in each sample (Smets et al., 2016), with assumed 16S rRNA gene copy number of eight and a weight of 4.49×10^{-15} g per *A. fischeri* genome. Next, the OTU abundances were normalized by the weight of the sample DNA extract added (typically 3 ng for groundwater samples and 5 ng for soil samples). For diversity analysis, rarefaction (the smallest sample size is 108711 for groundwater samples and 14918 for soil samples) standardized the bacterial community data to calculate richness, Chao, Simpson's index (D), Simpson's Evenness, Shannon-Weaver index (H), E-evenness and J-evenness (Gardener, 2014). OTU abundance (not rarified) was normalized by DESeq2 (Love et al., 2014) with the treatment as the factor for the taxonomy analysis and ordination analysis (McMurdie and Holmes, 2013). The top 100 most abundant OTUs were used to plot the relative abundance for different treatments based at the phylum level.

For the groundwater samples, a Kruskal-Wallis rank with Bonferroni rule, was performed to compare the influence of different treatments on 1607 OTUs abundance. There were 69 OTUs differed among treatments. These OTUs were used to construct a phylogenetic tree with corresponding FASTA files in Greengenes reference database. The evolutionary history was inferred by using the Maximum Likelihood method based on the Tamura-Nei model (Tamura and Nei, 1993). Initial tree (s) for the heuristic search were obtained automatically by applying Neighbor-Join and BioNJ algorithms to a matrix of pairwise distances estimated using the Maximum Composite Likelihood approach, and then selecting the topology with superior log likelihood value. All positions with less than 95% site coverage were eliminated. That is, fewer than 5% alignment gaps, missing data, and ambiguous bases were allowed at any position. There were 1222 positions in the final dataset. Evolutionary analyses were conducted in MEGA7 (Kumar et al., 2016). The phylogenetic tree was combined with the absolute abundance for those OTUs with ggtree v1.6.10 package in R (Yu et al., 2017).

One-way analysis of variance (ANOVA) determined the effect of three treatments: no amendment, phosphate amendment, phosphate and citrate amendment. Statistical analyses were performed using R v 3.3.2 (R Core Team, 2016). Normality of residuals was tested using the Shapiro-Wilk statistic. Means comparisons were made using Tukey's Honestly Significant Differences, if the dataset was normal distributed. When the dataset was non-normal, a t-test was

performed to compare different treatments. All tests were completed at the $p < 0.05$ significance level.

Non-metric multidimensional scaling (NMDS) ordination was performed to examine the microbial relationships among treatments, on the Bray-Curtis distances from the OTU abundance matrix. The OTU abundance matrix for groundwater comprised the 69 OTUs which differ among treatments analyzed by the Kruskal-Wallis rank test with Bonferroni rule. And for soil, 70 OTUs which have the lowest p-value with the Kruskal-Wallis rank analysis were used to test the influence of treatment. Redundancy analysis (RDA) on the Hellinger-transformed OTU matrix (same 70 OTUs described above) was applied to determine the relationship between environmental parameters and bacterial community compositions (Ramette, 2007). The significance of the relationship between explanatory variables and community composition was tested using Monte Carlo permutation tests (999 unrestricted permutations, $p < 0.05$).

5.4.7 Sequence data deposition

The project name was ERP021254 for groundwater sequencing data and ERP020729 for soil sequencing data in EMBL Nucleotide Sequence Database.

5.5 Results

5.5.1 Effect of citrate addition on P and PHC

Citrate addition increased the bioavailable P fraction and enhanced F1 biodegradation in soil. In the influenced soil area, bioavailable $NaHCO_3$-OP (mg kg^{-1}) increased from 2.27 ± 0.45 (SE) to 5.01 ± 0.63 after phosphate amendment, then to 10.14 ± 0.63 following phosphate and citrate amendment (Fig. 5.1). There were two principal soil phosphate phases: adsorbed phosphate and Ca-P (Fig. 5.2). Adding phosphate resulted in a slight increase in Ca-P (an apatite standard was used) and an overall loss of adsorbed P. When the phosphate and citrate amendment was added, apatite was essentially unchanged, but adsorbed P level returned close to its initial state. Simultaneously, $F1_{\text{-BTEX}}$ decreased from 456 ± 144 mg kg^{-1} to 116 ± 56 mg kg^{-1} after phosphate amendment, then to 67 ± 26 mg kg^{-1} after citrate application. The reduction for $F1_{\text{-BTEX}}$ may be due to the stimulated anaerobic hydrocarbon degrader activity.

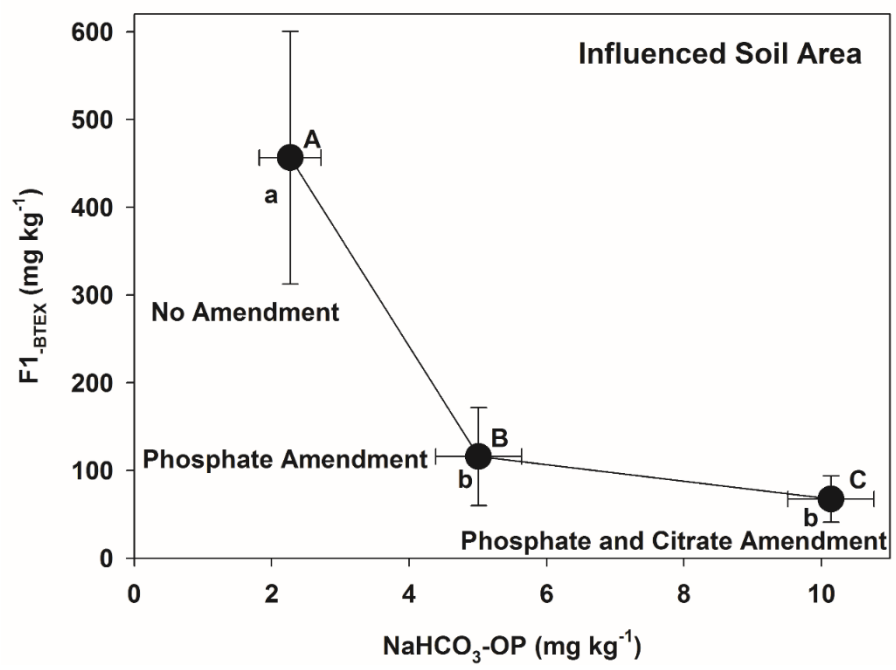

Fig. 5.1. Hydrocarbon ($F1_{-BTEX}$) and organic phosphorus ($NaHCO_3$-OP) in soil for different biostimulation treatments. Means with the same letter are not significantly different. Lowercase letters are for $F1_{-BTEX}$ and uppercase letters are for $NaHCO_3$-OP. Each point represents the average of 18 replicates and error bars represent the standard error of the mean. $F1_{-BTEX}$ refers to the concentration of hydrocarbons with an average effective carbon length of 6 to 12 with the concentration of benzene, toluene, ethylbenzene and xylenes subtracted from this concentration. $NaHCO_3$-OP refers to the organic phosphorus extracted with 0.5 M $NaHCO_3$.

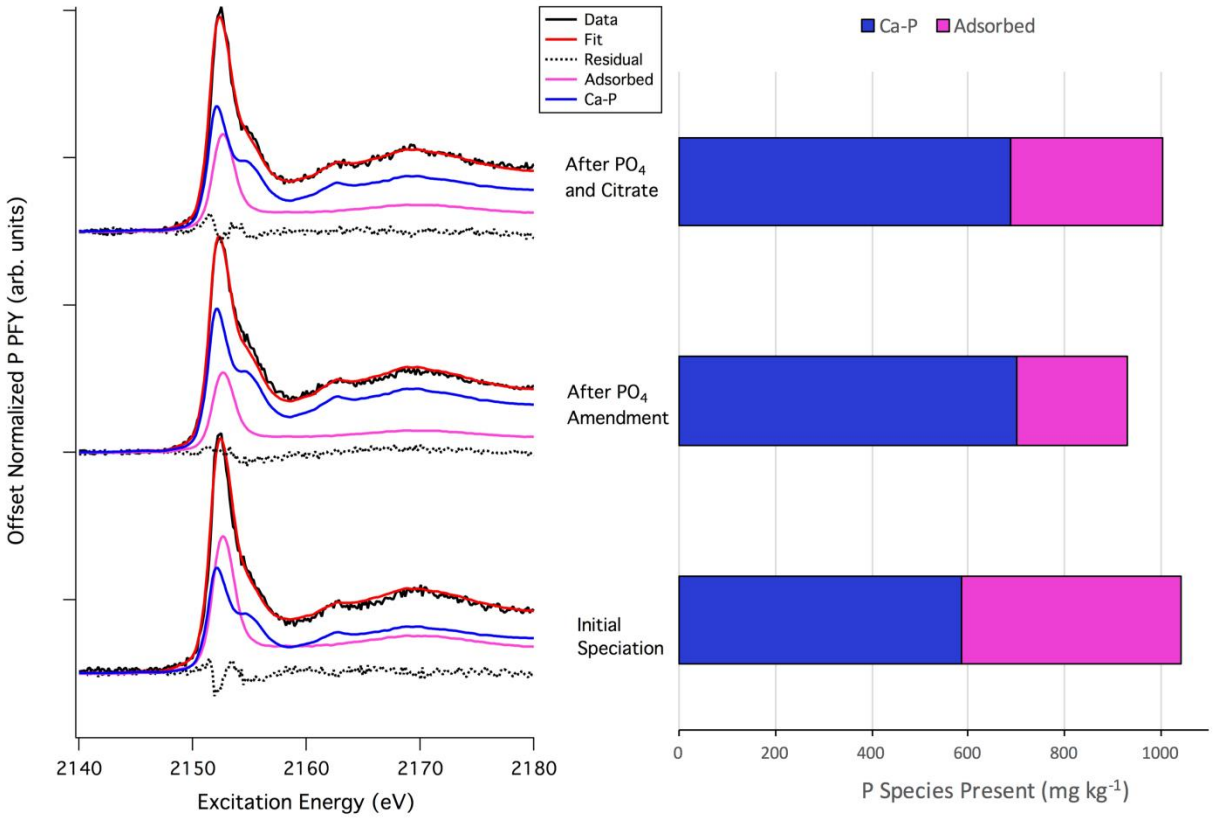

Fig. 5.2. Quantitative P speciation in soil samples via P K-edge XANES. Percent of linear combination fit (LCF) contribution multiplied with total P for three treatments are in the left panel. Relative phosphorus speciation in three samples was obtained by using a two component (adsorbed P in purple, Ca-P in blue) model in right panel.

5.5.2 Catabolic gene prevalence and most probable number

Citrate addition selectively stimulated hydrocarbon-degrading anaerobes containing the gene *bzdN* (Fig. 5.3). The log transformed *bzdN* gene copies per gram soil was 5.16 ± 0.59 for no amendment, 6.34 ± 0.22 for phosphate amendment, followed by 6.50 ± 0.21 for phosphate and citrate amendment. In contrast, citrate addition inhibited *bcrC*, decreasing from 9.71 ± 0.16 for no amendment to 8.15 ± 0.24 for phosphate amendment, then 8.10 ± 0.25 after citrate addition. Culturable facultative hydrocarbon degraders increased two orders of magnitude (increased from 1.9 ± 0.5 to 3.6 ± 0.6) after applying phosphate and citrate amendment in the site (Fig. 5.3).

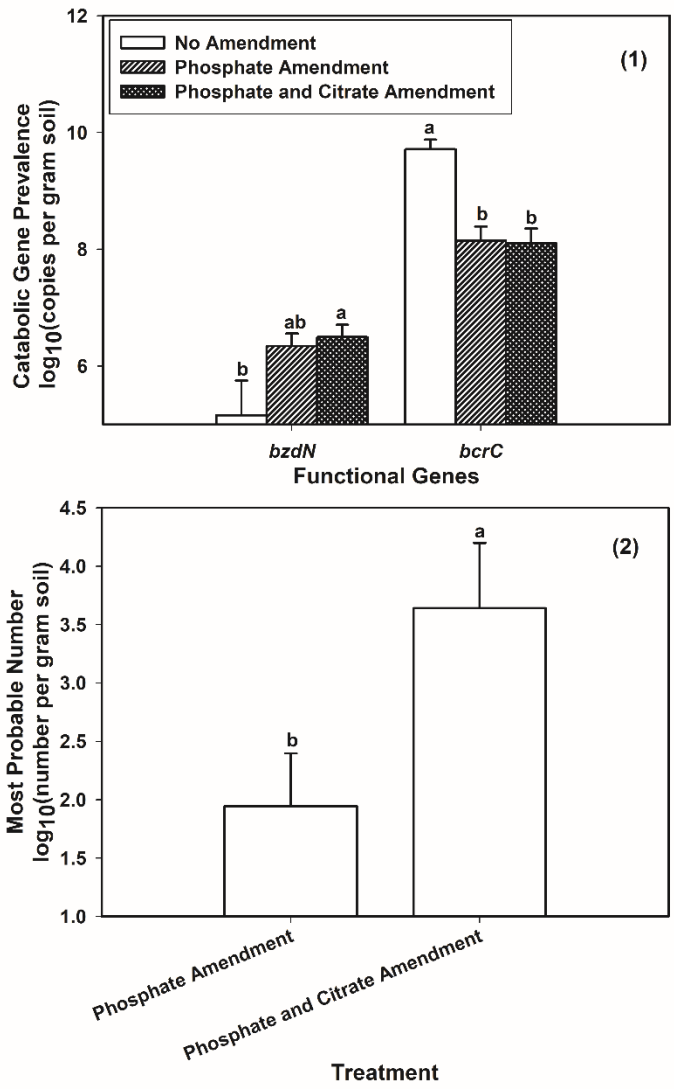

Fig. 5.3. Catabolic gene prevalence and most probable number soil area. (1) Catabolic gene prevalence of soil samples for different treatments (N = 18) (2) Most probable number (MPN, log10 transformed) for soil samples only during phosphate amendment (N = 16), phosphate and citrate amendment treatment (N = 18). Mean values are presented with standard error bars. Different letters indicate significant differences among groups.

5.5.3 Richness and evenness for bacterial community

The two phosphate amendment treatments increased the diversity of the bacterial community in the groundwater and soil, compared to the control (no amendment). In the groundwater, the Chao value, Simpson's index (D), Shannon-Weaver index (H), and E-evenness was higher after phosphate amendment, and citrate addition (Table A3.2). For example, the Chao richness estimator increased by about 100 species after phosphate amendment compared to the

control. In contrast, the diversity for soil samples was more sensitive to the phosphate amendment. The abundance of 100 rare OTUs for the no amendment increased after citrate addition (Fig. 5.4). Further, the citrate amendment caused a more substantial shift in microbial community richness compared to the phosphate amendment alone (see the tip of the abundance curve in Fig. 5.4).

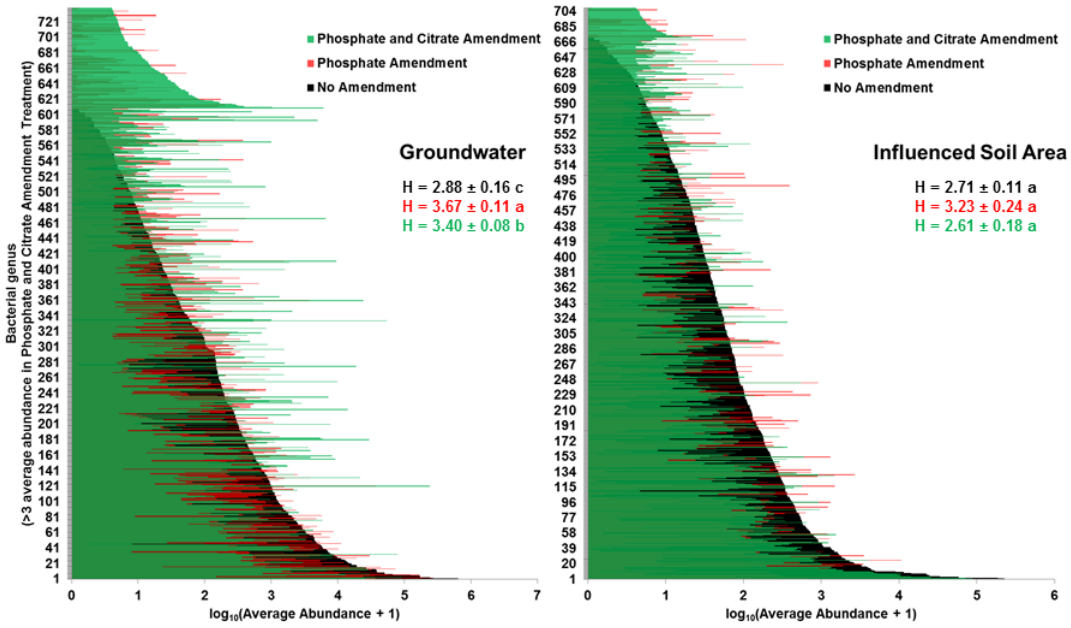

Fig. 5.4. Log-transformed mean abundance of bacterial genera ordered from least to most abundant in the no amendment treatment. This order is retained for the other treatments. Black bars represent for no amendment treatment. Red bars represent for the phosphate amendment, and the green bars represent for the phosphate and citrate amendment. The Shannon-Weaver index (H) value in the color correspond to the treatment shown in the same color for the abundance bars, and the same letters following H values indicate no significant differences between treatments.

5.5.4 Taxa summary

Citrate selectively increased anaerobic hydrocarbon degrader abundance but had a different effect in the soil compared to the groundwater. In groundwater, citrate amendment magnified the phosphate amendment effect, further increasing the relative abundance of *Chlorobi* (from 0.02% to 0.38%), *Firmicutes* (from 3.8% to 29.5%), *OP11* (from 0.2% to 0.4%), and *Spirochaetes* (from 0.02% to 0.7%) (Fig. A3.2). OTUs belong to *Geobacter*, had an absolute abundance of 2,200 for citrate addition (800 for no amendment and 2,500 for phosphate amendment). Citrate amendment selectively increased absolute abundance for OTUs within the

orders: *Bacteroidales*, *Lactobacillales*, *Clostridiales*, *Rhodocyclales*, and *Xanthomonadales*, especially *Desulfobacterales* and *Desulfovibrionales* (Fig. 5.5). The absolute abundance ratio for *Desulfobacterales* and *Desulfovibrionales* under different treatments (no amendment: phosphate amendment: phosphate and citrate amendment) was 2:3:53, and 1:8:102, respectively. For instance, the abundance for OTU1174 (belongs to *Desulfobacterales*) increased from 7 to 1,200 after citrate addition.

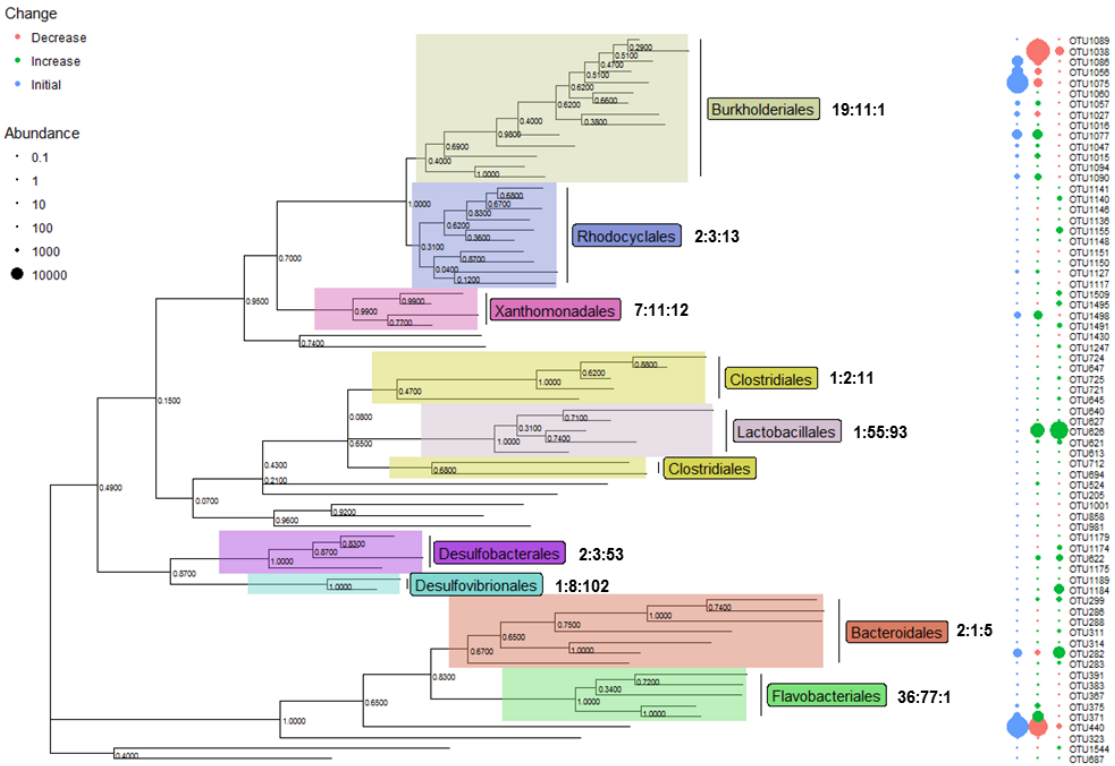

Fig. 5.5. Phylogenetic trees for 69 OTUs that changed significantly in response to different treatments in the groundwater. Symbol size indicates the OTU abundance for no amendment (first column), phosphate amendment (second column), and phosphate and citrate amendment (third column). Blue symbols represent the initial abundance for no amendment. For phosphate amendment treatment, green symbols indicate those OTUs abundance increased, and red symbols indicate abundance decreased, compared to no amendments. For the phosphate and citrate amendment, the color for the symbols is based on the comparison between phosphate treatment and citrate treatment. The node value on the tree is the bootstrap value and major clades are annotated with the corresponding order levels. The ratio beside the labeled order cluster is the total abundance for the related order ratio under different treatment (no amendment: phosphate amendment: phosphate and citrate amendment). The tree is drawn to scale, with branch lengths measured in the number of substitutions per site.

In contrast, within the soil, the citrate amendment reversed many of the changes seen after phosphate amendment by reducing the relative abundance of all phyla except *Proteobacteria*. For example, phosphate decreased relative abundance of *Proteobacteria* from 85% to 27%, but when citrate as added, this *Proteobacteria* abundance rebounded to 87% (Fig. A3.2). And the absolute abundance for *Proteobacteria* reduced from 700,000 to 28,000 by adding only phosphate, then recovered to 280,000 after citrate applied.

5.5.5 Analysis of the relationships between bacterial community composition and environment

Citrate continued to shift community structure in the groundwater further from the no-amendment and phosphorus only treatments. But in soil, citrate reversed the shift induced by phosphate to that more similar of the no-amendment control (Fig. 5.6). A transformed RDA, explained 81% of the community variance and with amendment treatments ($p = 0.005$) being the most significant factor explaining variation in bacterial community composition, followed by changes in log*bcrC* ($p = 0.01$) (Fig. A3.3).

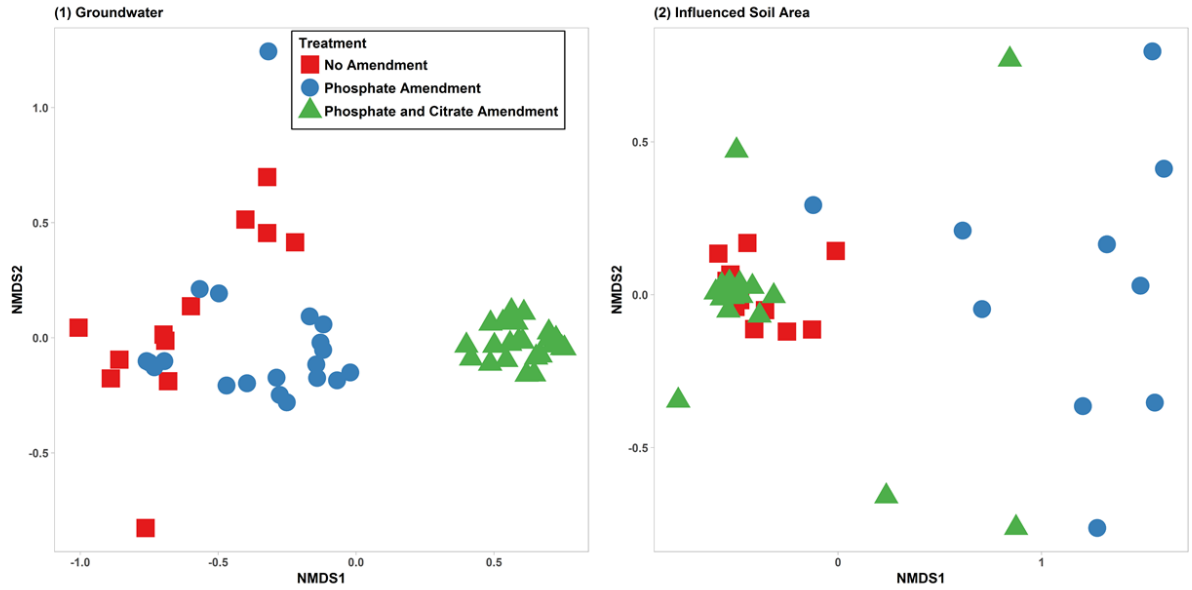

Fig. 5.6. Non-metric multi-dimensional scaling (NMDS) ordination biplot for bacterial community structure in groundwater (1) and influenced soil area (2). Red circle symbols represent samples for no amendment. Blue triangle symbols are samples for phosphate amendment. Green squares are samples for phosphate and citrate amendment. The stress is 0.09 for groundwater and 0.09 for influenced soil area. NMDS ordination was based on the 69 OTUs (significantly changed) abundance matrix for groundwater samples and 70 OTUs (most significantly changed) abundance matrix for influenced soil area samples.

5.6 Discussion

Over an 18-month period, citrate, combined with phosphate, increased the bioavailable organic P fraction and $F1_{-BTEX}$ degradation. Moreover, compared to phosphate only, citrate enhanced the efficiency of phosphate amendments. Using microcosms, others demonstrated the potential for citrate to induce labile organic P release from soil (Wei et al., 2010; Wang et al., 2015), and enhance hydrocarbon bioavailability (Gao et al., 2010a; d; Wang et al., 2015). Here, it was demonstrated that citrate also increased the culturable and total anaerobic hydrocarbon degrader population. For example, the highest pooled *bzdN* (*Azoarcus* type*)* gene copies were associated with citrate addition. However, this stimulation was selective for *bzdN*, with the citrate stimulation reducing the *bcrC* (*Thauera* type) gene copies. Changes in catabolic genes were linked to changes in phosphorus mineralogy, with increasing adsorbed phosphorus associated with increases in *bzdN* and inhibition of *bcrC*. A similar pattern was observed in a field microcosm experiment which manipulated phosphorus mineralogy (Siciliano et al., 2016). Bacterial community composition is likely driven by the adsorbed P fraction, which was depleted in the phosphate treatment due to the formation of hydroxyapatite, $Ca_{10}(PO_4)_6(OH)_2$, but increased with the addition of citrate. Thus, it appears that the selective stimulation of the hydrocarbon degrading microbial community is linked to changes in soil P mineralogy.

In addition to catabolic gene prevalence and culturable hydrocarbon degraders, anaerobic hydrocarbon degrading, iron-reducing, and nitrate-reducing bacteria, were also stimulated by citrate addition in the groundwater. Specific orders, known to contain hydrocarbon degraders, such as, *Clostridiales*, *Rhizobiales*, *Rhodospirillales*, *Rhodocyclales*, *Desulfobacterales*, *Desulfovibrionales*, and *Desulfuromonadales* (Edwards, 2003; Kasai et al., 2006; Robertson et al., 2007; Weelink et al., 2010; Zhang et al., 2012; van der Zaan et al., 2012; Kleinsteuber et al., 2012; Herbst et al., 2013; Luo et al., 2014; Zhang and Lo, 2015; Sheng et al., 2015; Quadros et al., 2016) were stimulated in groundwater. Phyla *Chlorobi*, *Firmicutes*, and *Spirochaetes* increased after phosphate amendment and citrate addition. *Firmicutes* is a dominant group of Fe(III)-reducers in hydrocarbon enrichment cultures (Li et al., 2011) and *Spirochaetes* are frequently found in anaerobic digesters (Lee et al., 2015). One specific OTU, OTU1195, was substantially increased by citrated amendment. OTU1195, which is affiliated to *Geobacter*, had a relative abundance of 0.21% for citrate addition (0.03% for no amendment and 0.17% for phosphate amendment). The stimulated iron-reducing bacteria in groundwater after citrate

addition corresponded to the increased iron(II) concentration (Chapter 4). Lovley (1997) reported that Fe(III) is the most abundant potential elector for anaerobic BTEX biodegradation. Despite the changes observed for *bzdN* and *bcrC*, the prevalence of *Thauera* and *Azoarcus*, were not significantly changed, thus, highlighting the importance of quantifying catabolic genes and culturable hydrocarbon degraders. Overall, the citrate amendment altered the groundwater community in a manner congruent with what one would expect for hydrocarbon degradation.

The use of the Bonferroni rule may have biased results against rare species that were stimulated by citrate addition. For example, the change for the abundance of OTU1178 in groundwater was not significant according to the Bonferroni rule. However, OTU1178 was undetectable during the first two amendments, and became present after citrate addition in groundwater. And OTU1178 belonging to the genus *Desulfocapsa,* which is mainly responsible for toluene metabolism coupled to sulfate reduction (Bombach et al., 2010). The same change occurred for other genera known to comprise toluene-degraders, such as *Desulfobacterium* and *Desulfovibrio* (Bombach et al., 2010). For total 1817 OTUs detected in soil, approximately 375 OTUs in the phyla *Caldithrix*, *Thermi*, *Actinobacteria*, *Armatimonadetes*, *AD3*, *Armatimonadetes*, *Bacteroidetes*, *BHI80-139*, *BRC1*, *Caldiserica*, *Chlorobi*, *Chloroflexi*, *Cyanobacteria*, *Fibrobacteres*, *Firmicutes*, *GAL15*, *Gemmatimonadetes*, *LD1*, *MAT-CR-M4-B07*, *NC10*, *Nitrospirae*, *NKB19*, *OP11*, *OP8*, *Planctomycetes*, *Proteobacteria*, *SAR406*, *SBR1093*, *Spirochaetes*, *Synergistetes*, *Tenericutes*, *TM6*, *Verrucomicrobia*, *WS3*, and *WS4*, had highest abundance after citrate addition. Despite that, these OTUs are rare (only occupied 0.04% for bacterial community). Thus, it may be that rare species are responsible for the continued hydrocarbon degradation in influenced soil rather than the dominant microbial community.

In contrast to the groundwater community, citrate addition reversed the enhancement of hydrocarbon degraders in the soil microbial community. For example, after phosphate amendment, increased abundance was observed for the phylum *Bacteroidetes*, *Chlorobi*, *Nitrospirae*, *OP11*, and *Spirochaetes*, and especially *Acidobacteria* and *Firmicute*. These changes were reversed after citrate addition. Further, based on the NMDS, the soil bacterial community after citrate addition was more similar to no amendment controls compared to the phosphate amendment. There are two factors explaining this: spatial and mineralogical. Spatially, the two soil samples closest to the phosphate amendment bacterial community were from borehole 16-01, which is the closest borehole to the infiltrators. The limited area of

influence from citrate is likely because the biological half-life for citrate in water is short and adsorption processes are rapid (Owen et al., 2001). The changes in the microbial community followed the changes in the soil mineralogy quite closely. As previously observed (Siciliano et al., 2016), adsorbed phosphate is tightly linked to soil microbial community composition. For example, some OTUs affiliated to phosphate solubilizing bacteria, increased after phosphate amendment and decreased after citrate addition in the groundwater and soil, such as *Pseudomonas* (OTU1430) and *Flavobacterium* (OTU375 and OTU371) (Rodríguez and Fraga, 1999). This may imply that citrate limits apatite formation, driving a higher fraction of the total soil P pool into not only the adsorbed but also the dissolved phase. This would reduce the need for solubilization mechanisms in the microbial community and would enhance the rate of biodegradation in groundwater (as observed).

5.7 Conclusion

Phosphate amendment and citrate addition selectively stimulated anaerobic hydrocarbon-degraders and altered bacterial community structure in the soil and groundwater. It found the amendment treatments, hydrocarbon levels, and catabolic gene prevalence constrained the bacterial community composition in the soil. In the groundwater the citrate addition promoted the influence of the phosphate amendment on the functional anaerobic hydrocarbon degraders in the phyla *Chlorobi, Firmicute* and well-known iron-reducing and sulfate reducing bacteria. Groundwater and soil microbial communities responded differently to biostimulatory treatments, largely because changes in phosphorus mineralogy dominated community response in soil, but not in groundwater.

6. TRAPPING CO_2 TO ASSESS PETROLEUM HYDROCARBONS BIODEGRADATION

6.1 Preface

Petroleum hydrocarbon (PHC) biodegradation is the major topic for this dissertation. The mineralization of ^{13}C-labeled PHC could release $^{13}CO_2$. Based on the $^{13}CO_2$ production from differently treated soils, it is possible to identify which situation has the highest degradation rate. This chapter developed and evaluated the use of $^{13}CO_2$ to assess PHC biodegradation, which can provide an efficient and low-cost method to assess different treatments for PHC biostimulation.

6.2 Abstract

Assessing remediation in small samples, or in samples that cannot be destructively sampled poses challenges during remediation technology development. One potential approach is to use ^{13}C-labelled contaminants and assess $^{13}CO_2$ production using cavity ring-down spectrometry. However, the application of cavity ring-down spectrometry technology in treatability microcosms has not been fully developed. Microcosm studies were conducted to develop a method that detected the biodegradation of mono- and polyaromatic hydrocarbons under aerobic and anaerobic conditions. Benzene or phenanthrene was added to the soil samples as ^{13}C-labelled substrate and normal substrate. Based on the $^{13}CO_2$ production between ^{13}C-labelled and normal substrate spiked groups, which was determined by gas chromatography-thermal conductivity detector and cavity ring-down spectrometry, it was possible to assess the mineralization rate of the compound of interest in the presence of other contaminants. This method, which used KOH traps to absorb produced CO_2, can condense CO_2 and remove the interference caused by H_2S, methanol, benzene, or methane on cavity ring-down detection of $^{13}CO_2$. This new approach is suitable to assess intrinsic biodegradation or biostimulation of petroleum hydrocarbons.

6.3 Introduction

Petroleum hydrocarbon (PHC) is one of the most widespread contaminants. In Canada, approximately 60% of 21,000 federal contaminated sites contain PHC (Canadian Council of Ministers of the Environment, 2008). The exploration, production, refining, transport, and storage of PHC regularly leads to leaks and accidental spills with an estimated seepage rate of 600,000 ± 200,000 metric tons per year (Das and Chandran, 2011). The release of PHC in the environment could cause serious damage to natural ecosystems and present risks for human health. For example, the chronic exposure of PHC may cause weariness, headaches, blood production malfunction, and irritation to eyes and lungs (Konečný et al., 2003). As a consequence, there are significant efforts underway to remediate PHC contaminated sites (Testa and Jacobs, 2014).

Contaminated sites can achieve optimum remediation through numerous avenues. Physical, chemical, and biological techniques, such as soil washing, chemical oxidation, and

phytoremediation, can reduce PHC contamination to acceptable levels (Wang et al., 2011). Bioremediation utilizes natural microbial activity to decrease the concentration of a pollutant. There are two main strategies for PHC bioremediation: (a) biostimulation which adds nutrients such as carbon, nitrogen, and phosphorus or other growth-limiting co-substrates to stimulate the growth of the indigenous PHC degrading organisms, and (b) bioaugmentation which increases the population of PHC degrading microorganisms. A quick and effective method to assess biodegradation activity is needed to assess if a treatment option is stimulating PHC bioremediation.

Accurate estimations of PHC bioremediation are difficult due to imprecisions associated with assessing PHC fate in soil. The fate of PHC in the soil involves several losses and movement processes such as dissolution, partitioning to solid matrices, volatilization, oxidation, and biodegradation (Dutta and Harayama, 2000; Coulon et al., 2010). Estimating only the biological loss fraction among these fate pathways is challenging. Techniques used to evaluate biodegradation include: determination of soil total PHC losses (Johnson et al., 2006), assessment of degrading microbial populations by most probable number (MPN) or genetic means (Bekins et al., 1999), and monitoring microbial respiration plus biogenic soil-gases including the measurement of O_2, CO_2, and CH_4 (Hinchee et al., 1991; Revesz et al., 1995; Sihota et al., 2011). A change in the PHC reflects total PHC loss; however, if assessed in water this change does not account for residual PHC that has not partitioned from the soil. Precisely assessing total PHC loss in soil is difficult due to high soil heterogeneity and from losses due to volatilization (Scherr et al., 2007; Modrzyński et al., 2016). Methods assessing the culturable degrading population typically detect less than 1% of microorganisms present and genetic methods suffer from primer bias (Kirk et al., 2004). Assessing biogenic soil gases has the advantage of directly determining activity without the partitioning effects occurring with PHC, but the natural soil respiration often makes the results ambiguous because separating natural soil respiration and the contaminant related soil respiration is difficult. Combining ^{14}C and ^{13}C for CO_2 monitoring can successfully characterize the natural attenuation of hydrocarbons on site (Conrad et al., 1997; Coffin et al., 2008; Höhener and Aelion, 2010; Sihota et al., 2011; Sihota and Ulrich Mayer, 2012). Yet, the detection of ^{14}C is typically performed using an accelerator mass spectrometer which are rare and typically, oversubscribed. In contrast, ^{13}C-based methods are widespread.

Isotope fractionation can complicate the use of isotopes to track bioremediation. The different zero-point energies between heavy and light isotopes results in differences during reactions (Meckenstock et al., 2004). Lighter isotopes form chemical bonds with higher zero-point energy than those formed by heavier isotopes, which means the lighter isotopes form weaker bonds compared to heavier isotopes. The activation energy for cleavage is also higher in heavier isotopes. Consequently, biological reactions lead to isotope fractionation. For example, the $^{13}C/^{12}C$ isotope ratio of the substrate's residual fraction is enriched in ^{13}C (Richnow et al., 2003a). Based on this, the isotope fractionation has been used to assess intrinsic biodegradation (Richnow et al., 2003a; b; Meckenstock et al., 2004; Hofstetter and Berg, 2011; Thullner et al., 2012).

Here, the intrinsic soil bacterial degradation potential of ^{13}C labeled PHC was assessed. Benzene and phenanthrene were chosen as representative contaminants at the PHC contaminated sites due to their toxic and widespread characteristics (Hunkeler et al., 2001; Mancini et al., 2008; Bahr et al., 2015). Most researchers using ^{13}C-based methods for biodegradation use the isotope composition of PHC to estimate loss (Aggarwal et al., 1997; Kelley et al., 1997; Conrad et al., 1999), or alternatively, only monitor isotope composition of CO_2 during the biodegradation process (Aggarwal and Hinchee, 1991; Kirtland et al., 2000; Morasch et al., 2007; Stelmach et al., 2016). This research developed a new method of trapping the CO_2 produced from mineralization of added benzene or phenanthrene to monitor the content and isotope composition of produced CO_2. In so doing, the breakdown rate was quantified by comparing the $^{13}CO_2$ production between ^{13}C enriched substance and a normal substance. Thus, this approach provides compound-specific information for mineralization rates under different conditions.

6.4 Materials and Methods

6.4.1 Soil sources and chemicals

We collected non-contaminated soil (clean soil) beside the General-Purpose Building at the University of Saskatchewan, Saskatoon, SK, Canada. Clean soil was stored at room temperature until processed. Contaminated soil samples for method development were collected from a soil core at a depth of 2.7 m to 3.2 m. The soil core (F1: 150-756 mg kg^{-1}; F2: 862-1400

mg kg^{-1}; F3: 30-254 mg kg^{-1}) was from a former gas station in Young, SK, Canada. Contaminated soil samples were collected for assessing anaerobic biodegradation of benzene and phenanthrene from a former gas station in an active urban area in Saskatoon, SK, Canada. Contaminated soil samples were stored at -20°C until processed. All chemicals used were of the highest available purity. Stable isotope enriched compounds benzene ($^{13}CC_5H_6$, 99 atom %) and phenanthrene ($^{13}C_2C_{12}H_{10}$, 99 atom %), both with a chemical purity > 99%, as well as normal benzene and normal phenanthrene were purchased from Sigma-Aldrich.

6.4.2 Method development

6.4.2.1 Identify filter material to remove H_2S

We observed H_2S production during the anaerobic biodegradation of benzene and phenanthrene, which interfered with the Picarro G2201-*i* Analyzer (Picarro Inc., CA, USA), a cavity ring-down spectrometer (CRDS), delta 13 carbon ($\delta^{13}C$) in CO_2 and CH_4 determinations. Two biogenic gas samples containing H_2S (1036 ppmv and 1102 ppmv) were collected from the incubation of *Desulfomonile tiedjei* 49306 using the ATCC Medium 1690 with 75 mM benzene and 75 mM sodium pyruvate as carbon sources. Activated carbon, steel wool and rusted steel wool were tested for their efficiency in removing H_2S in a filter. Two standard CO_2 gas samples, 1018 ppmv and 5000 ppmv, were used to test the recovery of CO_2 after being filtered. Gas Chromatography-Thermal Conductivity Detector (GC-TCD) analyzed the concentration of H_2S (Varian Micro-GC CP-2003, Varian Inc., CA, USA) and CO_2 (Bruker 450-GC, Bruker, MA, USA).

6.4.2.2 Comparison of trapped and headspace CO_2 determinations

Clean soils were sieved to 2 mm and homogenized. Treatments were done in quintuplicate with 5 g of soil incubated at room temperature in 160 mL serum bottles under aerobic and anaerobic conditions as treatments. Lab air was used as the headspace for the aerobic samples and mixed air containing 80% N_2, 15.5% Ar, and 4.5% CH_4 for the anaerobic samples. For the mixed air, the serum bottle headspace was rinsed with N_2 for 1 min at 100 kPa and then vacuumed for approximately 2 minutes to make the headspace pressure less than 7 Pa. After that, approximately 160 mL of mixed air was injected from a 1 L air bag. Two methods of sampling were used for each treatment: traps or no traps. Traps were built by smelting the end of a 1 mL

pipette tip as a trap which was filled with 0.5 mL of 1 M KOH (freshly made with deionized water). The serum bottle was capped with a gray butyl rubber septa and sealed with an aluminum crimp cap. The trap can absorb CO_2 released from the soil to form carbonate (Fig. 6.1). After incubation, the KOH solution in the trap was transferred to a pre-evacuated 12 mL vial, acidified with 1 mL of 1 M HCl to release CO_2 (Fig. 6.1), and 30 mL of N_2 was injected into the vial and mixed. Then, 15 mL of the sample was transferred to the second pre-evacuated 12 mL vial for further gas determinations. The second sampling method did not have traps, and 15 mL of headspace gas was directly collected and transferred to a pre-evacuated 12 mL vial for CO_2 measurement. The sampling points for aerobic and anaerobic were respectively days 0, 1, 3, 5, and days 0, 2, 4, 6, 8. CO_2 concentration of gas samples was determined by the GC-TCD.

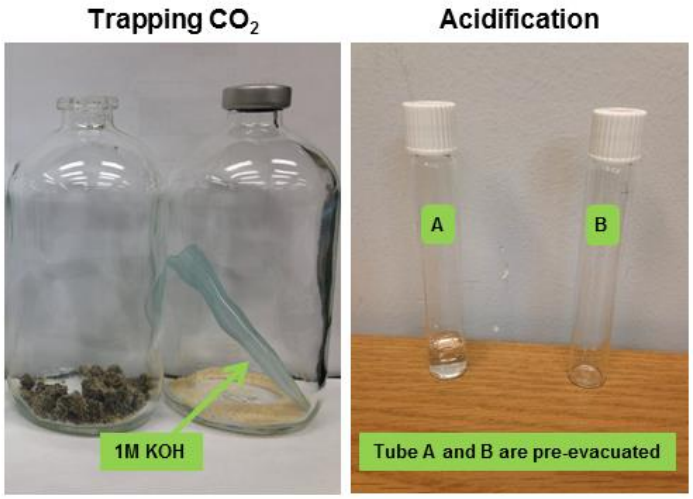

Fig. 6.1. Demonstration of the trapping and acidification process. In the left panel, the 1 mL blue trap in a 160 mL serum bottle was filled with 0.5 mL of 1 M KOH. In the right panel, pre-evacuated tube A contains the KOH solution transferred from the trap and 1 M HCl was added to release CO_2. Tube B was used to collect the released CO_2 for further gas determinations.

6.4.2.3 Evaluating different types of controls

Clean soils were sieved to 2 mm and homogenized. The working solution for phenanthrene was 1.5 g L^{-1} in toluene (enriched phenanthrene solution, containing 75% normal phenanthrene and 25% of $^{13}C_2C_{12}H_{10}$) and the solution for benzene was 75 mM in deionized water (enriched benzene solution, containing 96% normal benzene and 4% of $^{13}CC_5H_6$). Treatments were evaluated in triplicates at room temperature under aerobic and anaerobic conditions. For the phenanthrene spiked soil, 1 mL of phenanthrene solution was mixed with 1 g

of sand in a 160 mL serum bottle which was left to evaporate in the fume hood for two days. Then 5 g of soil and 1 mL of deionized water were added and mixed in the bottle. Lastly, the trap was added in the bottle before being sealed. For the benzene spiked soil, the order was (1) 5 g of soil was weighed in the bottle; (2) trap was added; (3) bottle was sealed; (4) 1 mL benzene solution was added by a syringe with a long needle; (5) the bottle was slightly shaken to mix well solution and soil.

There were two control treatments for the phenanthrene spiked soil. Only one step differed from the treated group: pure toluene was used instead of phenanthrene dissolved in toluene solution to soil for one (called substance control), while the other one had phenanthrene dissolved in toluene solution added without soil (called soil control). Similarly, two control treatments for the benzene spiked soil samples were set: (i) adding deionized water instead of benzene dissolved water solution to soil (substance control) and (ii) adding only the benzene dissolved water solution without soil (soil control). A 1 mL trap containing 0.5 mL of 1 M KOH was added to absorb produced CO_2. HCl (1 mL of 1 M) was used for acidification process. The sampling points for treatments were days 0, 1, 2, 3, 4, 5 for aerobic condition (only day 2 for controls), and days 0, 2, 4, 6, 8, 10, 12, 14 for anaerobic condition (only day 2 and day 14 for controls).

To test anaerobic benzene biodegradation, contaminated soil samples were used. This test also had a soil control, substance control (only benzene control), and substance spiked (benzene spike) treatments; empty serum bottles were used as an extra gas control (no soil, no substance, only gas to check the background headspace CO_2). The sampling points were days 0, 7, 14. The CO_2 concentration for gas samples was determined by GC-TCD. The $\delta^{13}C$ values were determined with the Picarro cavity ring-down spectrometry (CRDS).

6.4.3 Biodegradation assessment

6.4.3.1 Aerobic biodegradation of benzene and phenanthrene

To determine aerobic biodegradation of benzene and phenanthrene, five treatments of clean soil (5 g, 2 mm sieved) were tested in triplicates: (i) non-contaminant spiked (1 mL DI water, substance control), (ii) normal phenanthrene spiked, (iii) enriched phenanthrene (75% normal phenanthrene and 25% of $^{13}C_2C_{12}H_{10}$) spiked, (iv) normal benzene spiked, and (v)

enriched benzene (96% normal benzene and 4% of $^{13}CC_5H_6$) spiked. The working solution was 1.5 g L^{-1} for phenanthrene in toluene and 75 mM for benzene in deionized water. The 1 mL traps contained 0.5 mL of 1 M KOH, and 1 mL of 1 M HCl was used for the acidification process. The sampling points were days 0, 4, 8, and 12. CO_2 concentration and $\delta^{13}C$ values were determined at each sampling point.

6.4.3.2 Anaerobic biodegradation of benzene and phenanthrene

To determine anaerobic biodegradation of benzene and phenanthrene, four treatments were applied in triplicates: (i) normal phenanthrene spiked, (ii) enriched phenanthrene (normal phenanthrene: labelled $^{13}C_2C_{12}H_{10}$= 3:1) (iii) spiked, normal benzene spiked and (iv) enriched benzene (normal benzene: labelled $^{13}CC_5H_6$= 24:1) spiked. The working solution concentration and added amount were the same as aerobic biodegradation of benzene and phenanthrene treatments above. Contaminated soil (1 g) was incubated in a 12 mL vial for different treatments. A 0.2 mL trap containing 0.1 mL of 1 M KOH was set to absorb produced CO_2. Then, 0.2 mL of 1M HCl was added for acidification process. The headspace was composed of 80% N_2, 15.5% Ar, and 4.5% CH_4. CO_2 concentration and $\delta^{13}C$ values were determined for collected gas samples after a 14-day anaerobic incubation.

6.4.4 Calculation of breakdown rate

The breakdown rate was calculated as follows:

- Initially, the amount of CO_2 (N_{CO_2}, mmol) produced for a sample was calculated with the Eq. 6.1. V_i is the total volume for the gas sample, which was 0.0225 L for the method development. C_{CO_2} is the concentration for total CO_2 (mL L^{-1}). a is 1.977 mg mL^{-1}, the gas density of CO_2 at 1 atm at 0°C. b is 44.01 mg $mmol^{-1}$, the molar mass for CO_2.
- Secondly, the $\delta^{13}C$ value for CO_2 in the sample, $\delta^{13}C_{(sample)}$, needs to be converted to $^{13}C/^{12}C_{(sample)}$, which is the isotopic ratio of $^{13}C/^{12}C$ for CO_2 (Eq. 6.2) (Kleemann and Meckenstock, 2011). The R_{ref} is Pee Dee Belemnite (PDB) standard, 0.0112372.
- Thirdly, the $^{13}CO_2$ production was calculated in a sample, $(N_{^{13}CO_2})_{sample}$ (Eq. 6.3).

● Fourthly, the $^{13}CO_2$ production in the corresponding control group, $(N_{^{13}CO_2})_{control}$, was subtracted from $(N_{^{13}CO_2})_{sample}$ (If the control group is not the right one, the difference will be negative, which occurred during the right control set-up development). Then using the difference to divide the normality of spiked ^{13}C in the substance, which is $(N_{^{13}C})_{spiked}$, the substance breakdown rate was estimated during mineralization (Eq. 6.4).

$$N_{CO_2} = V_i \, C_{CO_2} \, a/b \quad \text{(Eq. 6.1)}$$

$$^{13}C/^{12}C_{(sample)} = [\delta^{13}C_{(sample)}/1000 + 1] \, R_{ref} \quad \text{(Eq. 6.2)}$$

$$(N_{^{13}CO_2})_{sample} = N_{CO_2} \, ^{13}C/^{12}C_{(sample)}/[^{13}C/^{12}C_{(sample)} + 1] \quad \text{(Eq. 6.3)}$$

$$Breakdown\ (\%) = [(N_{^{13}CO_2})_{sample} - (N_{^{13}CO_2})_{control}]/(N_{^{13}C})_{spiked} \times 100\% \quad \text{(Eq. 6.4)}$$

6.4.5 Statistical design and analysis

All statistical analyses were performed using R (R Core Team, 2016). Analysis of variance (ANOVA) and Kruskal-Wallis rank sum tests were used to determine the influence of treatment and time. The normality of residuals was tested using the Shapiro-Wilk statistic. When the data were significant and normally distributed, mean comparisons were made using Tukey's Honestly Significant Differences if the dataset was normal distributed. When the data were not normally distributed, a t-test compared different treatments. All tests were declared significant at $p<0.05$.

6.5 Results

6.5.1 Method development

6.5.1.1 Filter material for H_2S removal and CO_2 recovery

We found that rusted steel wool worked best to remove H_2S and recover CO_2 for filtration. The rusted steel wool and activated carbon had total removal of H_2S (Table 6.1), but the recovery for CO_2 for activated carbon was more variable. Because rusted steel wool needs a relatively large volume for a filter (about 5 mL), this resulted in a large volume of sample residual in the filter. The effective component in rusted steel wool is iron oxide. Thus, an

external filter with iron oxide powder (about 1 mL) was used for Picarro CRDS to remove H_2S produced in anaerobic biodegradation experiments. Picarro CRDS kept monitoring the H_2S concentration, and the filter would be changed when necessary to ensure the concentration of H_2S remained lower than 10 ppmv.

Table 6.1. The range of H_2S removal and CO_2 recovery for different materials used during filtration.

Material	H_2S removed (%)	CO_2 recovery (%)
Activated Carbon	100	81-128
Rusted Steel Wool	100	109-114
Steel Wool	92-100	108-116

6.5.1.2 Differences between trap CO_2 and headspace CO_2

The trap method increased the concentration of detected CO_2 compared to headspace samples. The concentration of CO_2 from the trap was 6.45 ± 0.40 (SE) times larger than the headspace under aerobic conditions, and 6.20 ± 0.30 larger under anaerobic conditions (Fig. 6.2). The amount of CO_2 (mmol) collected with the two methods was not significantly different under aerobic ($p = 0.14$) and anaerobic conditions ($p = 0.26$).

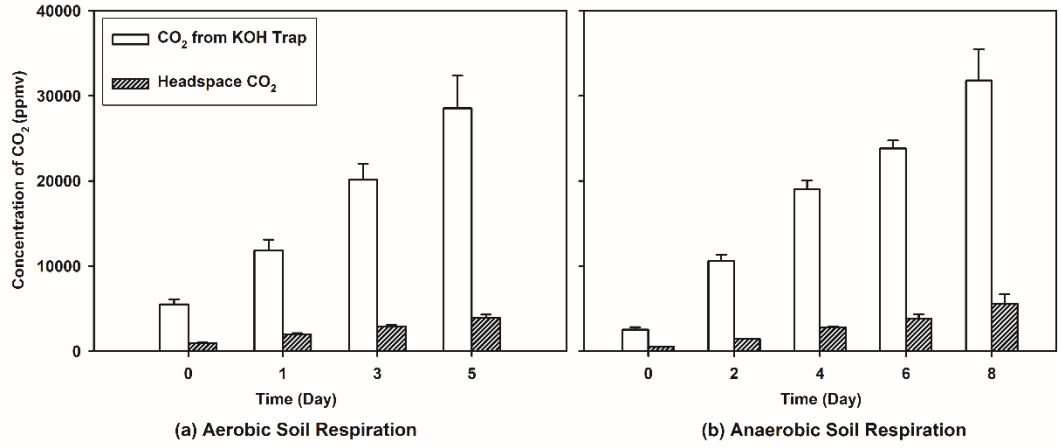

Fig. 6.2. Concentration of CO_2 under different conditions. (a) Aerobic soil respiration assessed by different methods (N =5) (b) Anaerobic soil respiration assessed by different methods (N = 5). Bars represent the average with error bars representing the standard error.

6.5.1.3 Appropriate controls

There are two potential controls: the enriched substance with no soil (**Soil Control**), and only soil with no enriched substance (**Substance Control**). The amount of $^{13}CO_2$ for substance control and substance spiked (adding benzene dissolved water solution or phenanthrene dissolved toluene solution in the soil) was always much higher than the soil control under both aerobic and anaerobic conditions (Fig. 6.3). The unusually low $\delta^{13}C$ values for treatment groups on day 2 were due to the limitations of the Picarro CRDS machine, which is designed for 300-2000 ppmv CO_2 concentration range. If the concentration is too low, as in this case (Fig. 6.3), the Picarro CRDS machine will produce inaccurate data with large deviations. In addition, the amount of $^{13}CO_2$ for soil control did not change when comparing day 2 and day 14 under anaerobic conditions. Thus, the soil control is likely not necessary.

The existence of benzene biodegradation under aerobic and anaerobic conditions was supported by $\delta^{13}C$ and $^{13}CO_2$ for collected CO_2. Under aerobic conditions, the initial $\delta^{13}C$ was -26.35 permil ± 1.17 permil (Fig. 6.4). For aerobic benzene biodegradation, the $\delta^{13}C$ for the benzene spiked treatment was -52.66 ± 1.58 permil, which was lower than the substance control (-26.68 ± 0.49) on Day 2, and consistently decreased to -57.39 ± 2.62 permil on Day 5. The produced amount of $^{13}CO_2$ kept increasing from 64 ± 17 to 3300 ± 240 nmol after five days. The $\delta^{13}C$ for the phenanthrene spiked treatment was similar to the substance control on day 2, and stayed around the initial aerobic $\delta^{13}C$ value for the duration of the experiment. The produced amount of $^{13}CO_2$ for the benzene spiked treatment was always higher than that of the phenanthrene spiked. The change of $\delta^{13}C$ and $^{13}CO_2$ demonstrated the occurrence for aerobic benzene biodegradation.

A similar situation happened for anaerobic benzene biodegradation. Under anaerobic conditions, the initial $\delta^{13}C$ was about -20.13 ± 0.67 permil (Fig. 6.4). The $\delta^{13}C$ for all treatments was similar at day 2 and day 14 (Fig. 6.3). The $\delta^{13}C$ for benzene spiked soil samples slightly decreased while $\delta^{13}C$ stayed at the same level for the phenanthrene spiked treatment. The amount of $^{13}CO_2$ for benzene spiked samples increased throughout the 14-day incubation (Fig. 6.4). The produced amount of $^{13}CO_2$ for benzene spiked samples was also higher when compared to phenanthrene spiked samples. The change in $\delta^{13}C$ and $^{13}CO_2$ indicates that the anaerobic benzene biodegradation occurred.

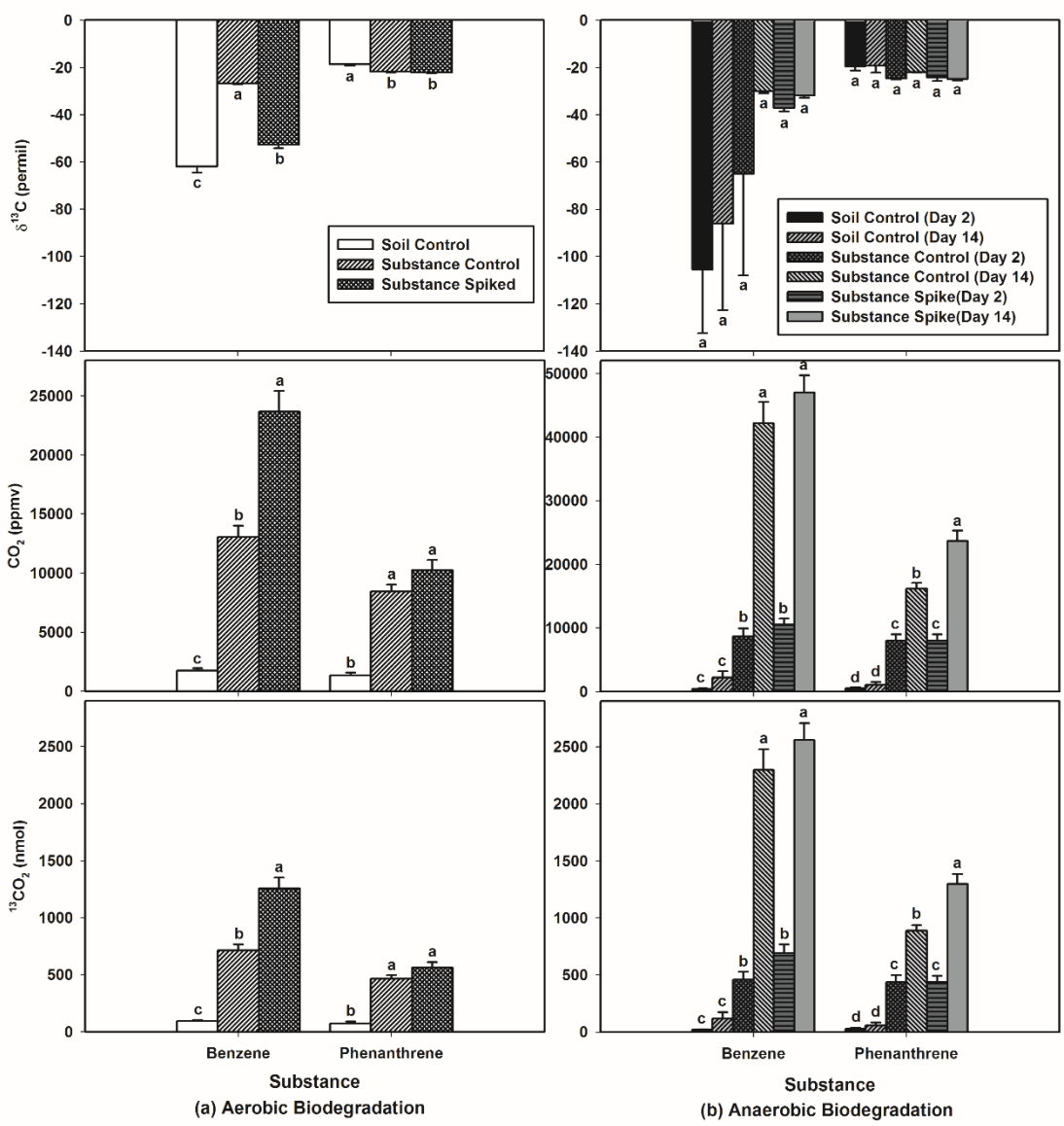

Fig. 6.3. The $\delta^{13}C$ for CO_2, CO_2 concentration, and $^{13}CO_2$ production for different treatments during (a) aerobic biodegradation on day 2, and (b) anaerobic biodegradation on day 2 and day 14, in clean soil. Bars represent averages (n = 3) with the standard error represented as error bars. Means with the same letter are not significantly different. Soil control represented the treatment of only adding the enriched benzene or phenanthrene solution with no soil; substance control was only soil added with no enriched substance solution. For substance spiked, benzene dissolved water solution or phenanthrene dissolved toluene solution was added to the soil sample.

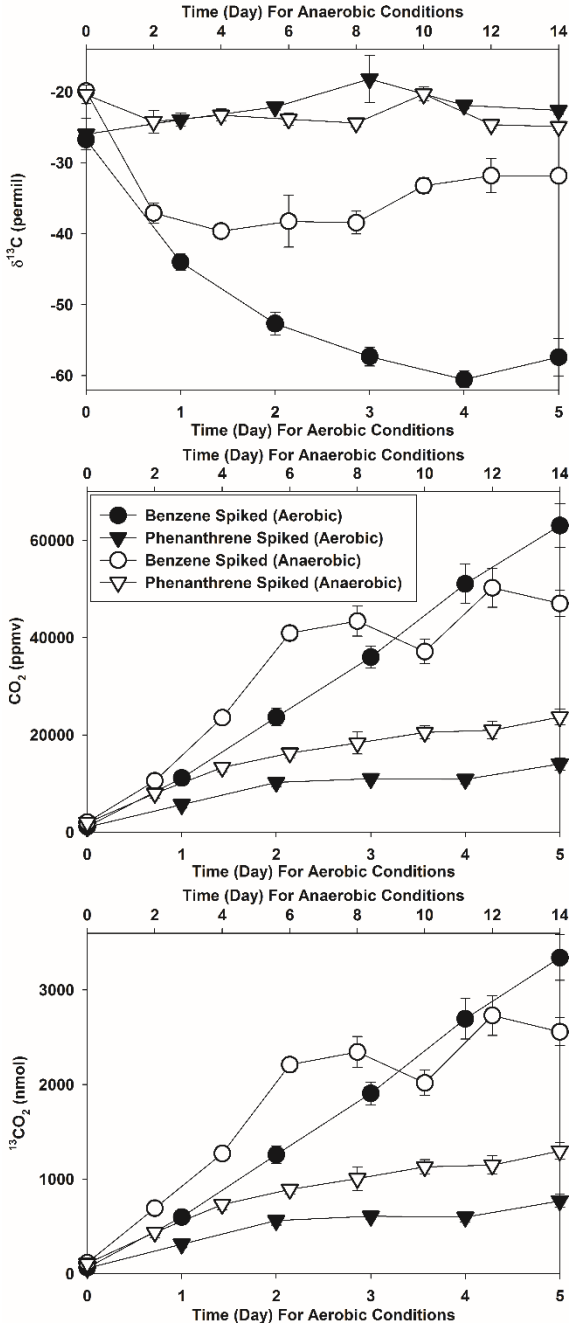

Fig. 6.4. The $\delta^{13}C$ value for CO_2 (top panel), CO_2 concentration (middle panel), and $^{13}CO_2$ content produced (bottom panel), during aerobic (black symbols) and anaerobic (white symbols) biodegradation of benzene (circles) and phenanthrene (triangles) in clean soil. Each point represents the average of three replicates and error bars represent the standard error of the estimate. The sampling period for aerobic biodegradation is on the bottom x-axis and anaerobic biodegradation is on the top x-axis.

The addition of benzene in the soil may inhibit biodegradation. A decrease of $\delta^{13}C$ and an increase of $^{13}CO_2$ were observed when the soil was spiked in both benzene dissolved water solution (**Benzene Spiked**) and deionized water (**Benzene Control**) (Fig. 6.5). However, the CO_2 concentration and $^{13}CO_2$ production, for benzene control treatment was higher than the benzene spiked treatment. The breakdown will be negative if calculation follows Eq. 6.1-6.4. Consequently, the benzene control needs to be adjusted from deionized water to the normal benzene solution (no enriched benzene added) to account for the possible inhibition on microbial activity from the addition of benzene. Similarly, the appropriate control set up for phenanthrene spiked treatment is to add normal phenanthrene toluene solution instead of solely toluene. In summary, to estimate mineralization rate the appropriate control to test an enriched substance is only a non-enriched substance spiked into soil, not the corresponding solvent.

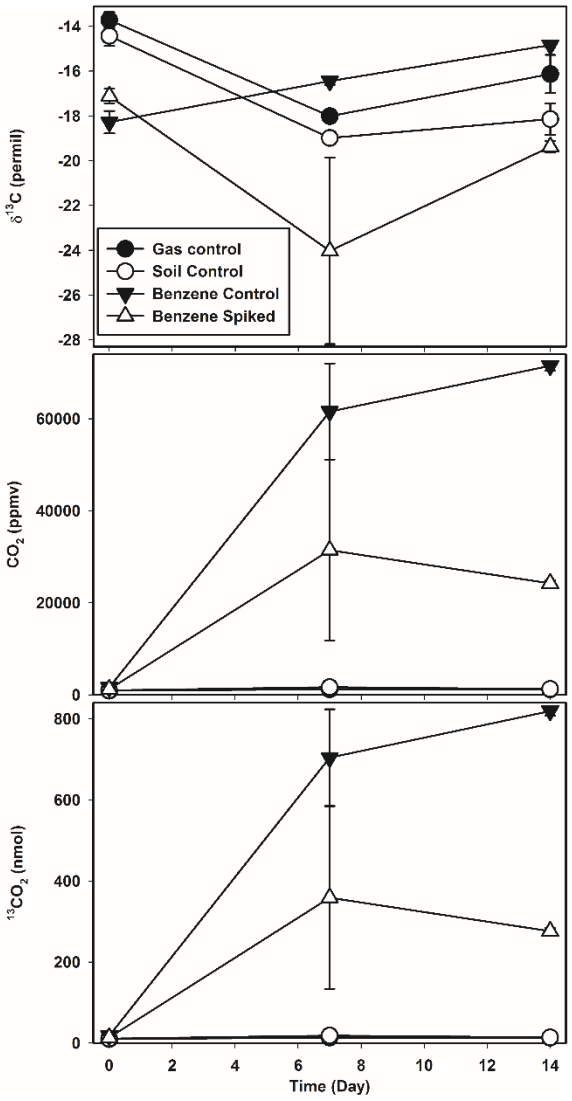

Fig. 6.5. The $\delta^{13}C$, concentration, and $^{13}CO_2$ content for CO_2 produced during the anaerobic biodegradation of benzene in contaminated soil. Each point represents the average of three replicates and error bars represent the standard error of the estimate. Treatments are denoted by the colour and shape of symbols.

6.5.2 Assessment of biodegradation

6.5.2.1 Aerobic biodegradation benzene and phenanthrene

We successfully evaluated aerobic biodegradation for benzene and phenanthrene in clean soil (Fig. 6.6). Initial $\delta^{13}C$ was from -14 to -18 permil. The change in $\delta^{13}C$ for normal benzene, enriched phenanthrene, normal phenanthrene and substance control treatments followed similar

trends. However, the enriched benzene spiked treatment had a lower and decreasing $\delta^{13}C$ trend line (-39.01 ± 0.05 at Day 12) compared to the other treatments. The breakdown (%) is 10.17 ± 5.10 for benzene and 8.72 ± 1.81 for phenanthrene in 12 days. Compared with normal benzene spiked treatment, the enriched benzene spiked treatment always had the lowest $\delta^{13}C$ value and highest CO_2 concentration.

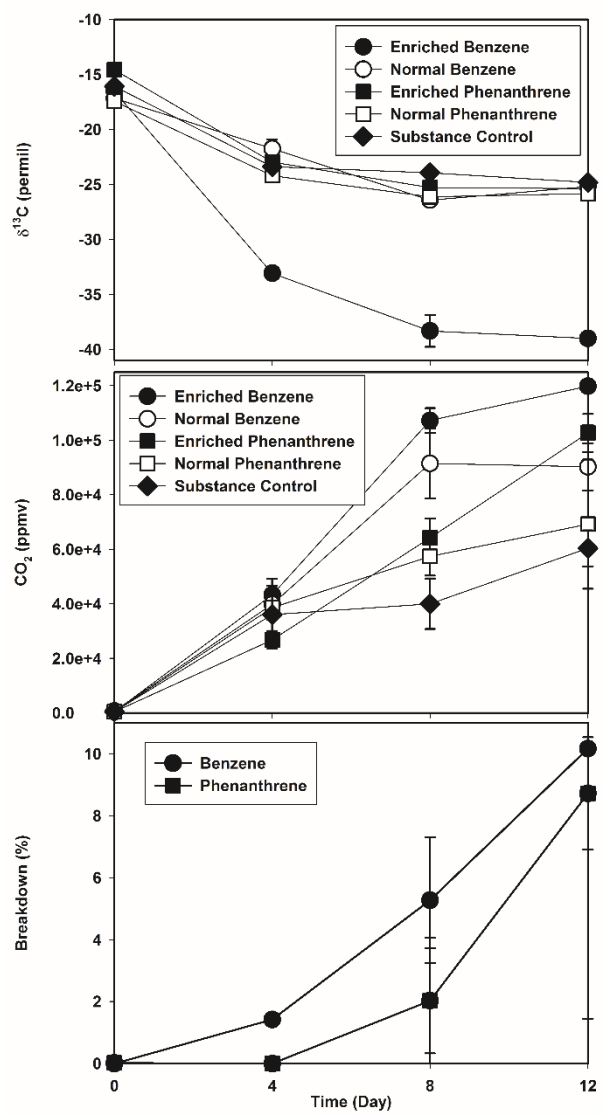

Fig. 6.6. Aerobic biodegradation assessment of benzene and phenanthrene. The top panel shows the $\delta^{13}C$ among different treatments, the middle panel shows the total CO_2 concentration in the serum bottle and the bottom panel shows the breakdown for biodegradation. Each point represents the average of three replicates and error bars represent the standard error of the estimate. Treatments are denoted by the colour and shape of symbols.

6.5.2.2 Anaerobic biodegradation benzene and phenanthrene

We assessed anaerobic biodegradation for phenanthrene with contaminated soil samples (Fig. 6.7). The $\delta^{13}C$ among normal benzene, enriched benzene, normal phenanthrene and enriched phenanthrene spiked treatments were not significantly different (p-value = 0.3193). The breakdown for benzene (%) in these soil samples approached zero (0.01 ± 0.01) after 14 days. There was 4.11 ± 0.84 % breakdown detected for anaerobic phenanthrene biodegradation. Interestingly, the enriched benzene group had the lowest production of CO_2 and enriched phenanthrene treatment had the highest value of CO_2 concentration.

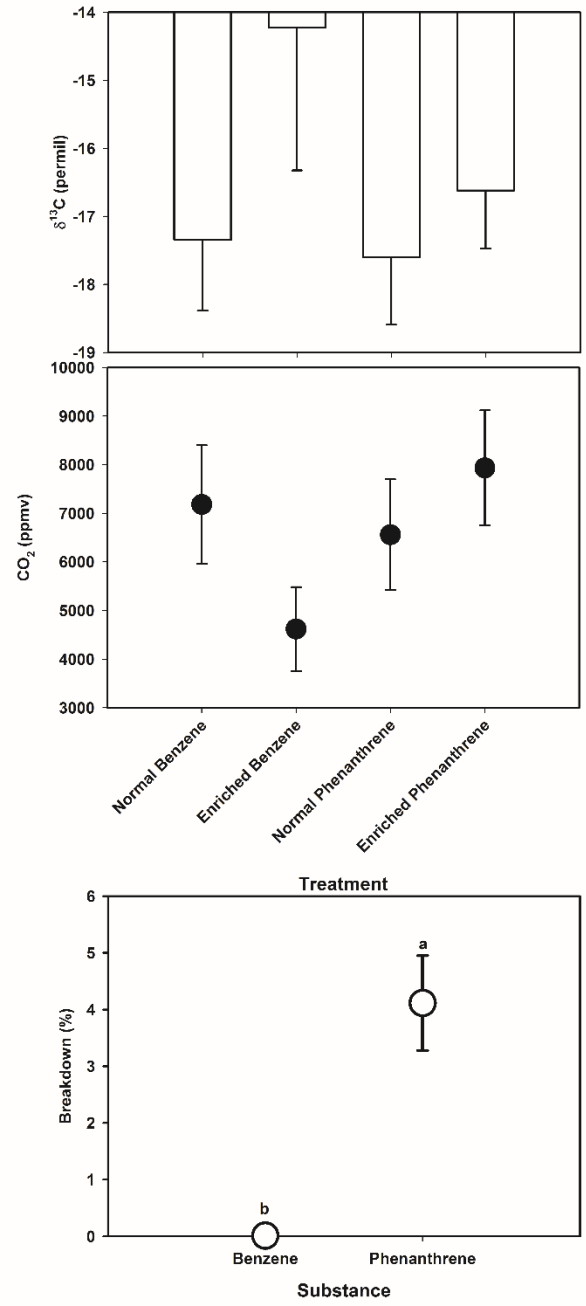

Fig. 6.7. Estimation for anaerobic biodegradation of benzene and phenanthrene with contaminated soil samples. Top panel shows the $\delta^{13}C$ among different treatments after 14 days. The concentration for CO_2 is in the middle panel and the bottom panel shows the breakdown of biodegradation in 14 days. Each bar or point represents the average of 18 samples and error bars represent the standard error of the estimate. Means with the same letter are not significantly different. In the bottom panel, the breakdown was compared with zero, which was assigned with 'b'.

6.6 Discussion

This study developed and validated a low-cost method to assess biodegradation in soil samples. Using a CO_2 trap method reduces the cost because only partially ^{13}C labeled compounds need to be used and detected by cavity ring-down spectrometer. In contrast, the other approach would be to use fully ^{13}C labeled compounds or isotope composition with compound-specific isotope analysis (CSIA) of carbon by the ratio mass spectrometry (IRMS). The condensing function for the trap method makes the storage and analytical dilution process for gas samples easier and the trap is much easier to use than other trapping methods (Usdowski and Hoefs, 1986; Mccoy et al., 2015). For example, a CO_2 trap developed recently, has upper and lower sorbent element held by stainless steel screens, a PVC tubular frame, glass wool packing, and rubber O-rings for sealing (Mccoy et al., 2015). At the same time, the trap prevents the interference for Picarro CRDS caused by the components in the headspace, such as, methanol, benzene, or methane. The external iron oxide filter for Picarro CRDS eliminated the disturbance from H_2S, guaranteeing the accurate determination for anaerobic samples. H_2S could also be removed by EDTA-Fe^{3+}, Cu^{2+}/Zn^{2+}/ Fe^{3+} ions, activated carbon, or ZnO (Qiu et al., 2011; Pouralhosseini, 2013; Liu et al., 2015) and since the Picarro CRDS is designed to analyze atmospheric gas samples with low H_2S, a filter will likely always be required for microcosm assessments. However, even with the trap and filter, the appropriate control is needed to target the $^{13}CO_2$ from PHC mineralization, not from the natural soil respiration.

Normally, the isotopic composition of CO_2 produced from mineralization is nearly the same as that of the source substance. Reported $\delta^{13}C$ values for PHC including benzene and phenanthrene are from -22 to -31 permil (Table 6.2). Atmospheric CO_2 has a $\delta^{13}C$ value from -7 to -10 permil (Aggarwal and Hinchee, 1991). In the study, the gas control was from -14 to -18 permil during the method development. The range of $\delta^{13}C$ value for CO_2 from PHC mineralization is from 10 to -37 permil (Table 6.2). For most of treatments, except enriched benzene, the $\delta^{13}C$ value for CO_2 was within this range. There are two reasons for this range. One is that the enriched substance spiked was not a high concentration relative to the total C in the headspace and the substance just had only one or two carbon atoms replaced with ^{13}C. Even though the enriched phenanthrene did not have isotope fractionation, the enriched CO_2 also would not have altered the delta value to a great degree. The other reason is that isotope

fractionation influenced the benzene biodegradation process, which resulted in even lower delta value for CO_2. The depleted ^{13}C-CO_2 for enriched benzene biodegradation indicated the presence for isotope fractionation, which may limit the accuracy of the benzene mineralization rate.

Table 6.2. The $\delta^{13}C$ value for CO_2 and petroleum hydrocarbons (PHC) from different sources.

Substance	Source	$\delta^{13}C$ (permil)	Reference
CO_2	Atmospheric	-7 ~ -10	Aggarwal and Hinchee (1991)
	Natural organic matter decay	-7 ~ -25	Aggarwal and Hinchee (1991)
	Uncontaminated soil gas (aerobic)	-18 ~ -25	Aggarwal and Hinchee (1991)
	Contaminated soil gas (aerobic)	-21 ~ -30	Aggarwal and Hinchee (1991)
	Uncontaminated soil gas	-23	Conrad et al. (1997)
	Contaminated soil gas	-19 ~ -28	Conrad et al. (1997)
	Biodegradation for diesel fuel	-10 ~ -31	Conrad et al. (1997)
	Aerobic phenol and benzoate biodegradation	-25 ~ -37	Hall et al. (1999)
	Aerobic & anaerobic benzene biodegradation	-17 ~ -25	Morasch et al. (2007)
	Contaminated soil gas for unsaturated zone	-21 ~ -27	Bouchard et al. (2008)
	PHC natural attenuation in the vadose zone	10 ~ -30	Coffin et al. (2008)
	Vadose zone PHC biodegradation	-16 ~ -32	Sihota and Ulrich Mayer (2012)
	Decomposition of gasoline	-22 ~ -30	Stelmach et al. (2016)
	Decomposition of diesel	-31 ~ -35	Stelmach et al. (2016)
PHC	Hydrocarbons	-22 ~ -30	Aggarwal and Hinchee (1991)
	JP-4	-26	Aggarwal and Hinchee (1991)
	Heavy oils	-26 ~ -29	Whittaker et al. (1996)
	crude oil (BAL 250)	-27 ~ -29	Mazeas et al. (2002)
	diesel and gasoline	-31	Stelmach et al. (2016)
Benzene	Monitoring wells in a contaminated site	-24 ~ -27	Kelley et al. (1997)
	Free products	-26 ~ -29	Dempster et al. (1997)
	Products from different suppliers	-24 ~ -29	Harrington et al. (1999)
	Hydrocarbon mixture	-27 ~ -29	Bugna et al. (2004)
Phenanthrene	Pure chemical or extracted contaminant	-24 ~ -26	O'Malley et al. (1994)
	from crude oil (BAL 250)	-25 ~ -27	Mazeas et al. (2002)

Isotope fractionation may be induced during: PHC mineralization, gaseous CO_2 absorption by KOH solution, and CO_2 release from acidification by HCl, because the kinetic processes can produce isotope fractionations (Hoefs, 2015). Previous studies demonstrated that the isotopic fractionation occurs during the CO_2 absorption by $Ba(OH)_2$, NaOH, or NH_3-NH_4Cl, and isotope fractionation may vary or stay constant (Usdowski and Hoefs, 1986, 1988). But in this study, it was verified that the isotope effect of KOH absorption of CO_2 was too small to be

detected. If the isotope fractionation occurred during the KOH absorption process, the $\delta^{13}C$ value would have kept decreasing in all the treatments (normal benzene, enriched phenanthrene, normal phenanthrene, and substance control groups) over the last eight days during the aerobic biodegradation assessment (Fig. 6.6). Only the $\delta^{13}C$ value for CO_2 from the enriched benzene spiked treatment kept decreasing, which suggests that isotope fractionation during aerobic benzene biodegradation cannot be neglected. To get more accurate breakdown rates for benzene biodegradation, it may need to estimate the isotope fractionation factor for substances with IRMS (O'Malley et al., 1994; Dempster et al., 1997; Kelley et al., 1997), or alternatively, a uniformly labelled benzene could be used (Morasch et al., 2007; Bahr et al., 2015) to prevent fractionation.

Since the isotope fractionation for phenanthrene biodegradation is negligible, the trap method successfully assessed the phenanthrene mineralization under aerobic and anaerobic conditions. The absence of stable carbon isotope fractionation of phenanthrene once was reported under aerobic condition (Mazeas et al., 2002). In addition, the aerobic mineralization rate of phenanthrene in 62 days was 14-33% (0.2-0.5% per day) in a laboratory microcosm study (Bahr et al., 2015), which was close to findings. Aerobic phenanthrene breakdown rate was 0.6-0.9% per day and the anaerobic breakdown rate was 0.2-0.4% per day.

6.7 Conclusion

This study developed and evaluated a trapping method based on ^{13}C-CO_2 analysis by GC and Picarro CRDS to assess benzene and phenanthrene biodegradation. The new approach investigated the intrinsic phenanthrene biodegradation potential under aerobic and anaerobic conditions for soil samples. This method can also provide semi-quantitative data when the isotope fractionation effect is significant, such as benzene biodegradation. For benzene, the use of a uniformly labelled benzene molecule may avoid the fraction artifacts that confounded observations in this study.

7. SYNTHESIS AND CONCLUSIONS

Unlike U.S. and Europe, which started implementing various policies and programs since the mid-1990s for brownfields redevelopment, Canada did not start working on its urban brownfields reclamation until mid-2000s (Sousa, 2006). As an environmental friendly, cost-effective, low labor intensive technique for petroleum hydrocarbons (PHC) remediation, bioremediation attracted more and more attention after its successful application for the Exxon Valdez oil spill in 1990s (Chandra et al., 2013). However, some factors, i.e., bioavailability of pollutants, nutrients, and PHC degrading microorganisms population, can limit bioremediation efficacy (McGuinness and Dowling, 2009; Schwitzguébel et al., 2011).

Low molecular weight organic acid anions (LMOAA), such as oxalate, citrate, succinate, malonate, fumarate, are produced from the decomposition of organic matter, dead plants or exudates of plants and microbes, ubiquitous in soil (Collins, 2004). Even though LMOAA may be not stable due to consumption by soil microbes as a carbon source (Fujii et al., 2013), which may stimulate microbial community, LMOAA play an important role in soil chemistry and biology (Bolan et al. 1994; Kpomblekou-A and Tabatabai 2003). Addition of LMOAA could disrupt the sequestering soil matrix to enhancing the desorption of PHC and P in soils (Ding et al., 2011; Martin et al., 2014). Whereas the vast majority of research on LMOAA has focused on one direction, either P speciation or PHC desorption. But researches that evaluate the influence of LMOAA on PHC biodegradation through different routes as a whole, have been relatively limited, especially under anaerobic conditions. The research presented in this dissertation filled some of the knowledge gaps.

The general goal for this research was to assess the influence of LMOAA combined with phosphate amendment on PHC bioavailability, P bioavailability, and active hydrocarbon-degraders community for anaerobic PHC biodegradation, with laboratory microcosm studies and field tests. In addition, the carbon-13 labeling technique was used to develop a cost-effective, quick approach to estimate the PHC biodegradation potential in soil samples.

7.1 Summary of Findings

One key factor for PHC biodegradation, contaminant bioavailability was affected by LMOAA plus phosphate biostimulation treatments (Chapter 3). Biostimulation treatments were evaluated with benzene and gasoline as representative PHC simple compounds and complicated

mixture. During mimicked *ex situ* PHC biodegradation process, low concentrations of citrate addition with low phosphate addition promoted anaerobic benzene and gasoline biodegradation at low temperature. But it was much lower than the reported range, 10-1000 mM, at which level LMOAA enhanced the bioavailability for some PHC compounds (Ling et al., 2009, 2015; Gao et al., 2010a, b; An et al., 2010, 2011). Based on the distribution factor analysis for PHC, it was confirmed 10-100 mM citrate addition did provide more bioaccessible PHC fractions under anaerobic conditions, for *ex situ* anaerobic gasoline biodegradation. But the best positive effect on PHC bioavailability did not lead to the best *ex situ* biodegradation, which was likely caused by the positive effect for citrate on phosphate bioavailability. Interestingly, for mimicked *in situ* PHC biodegradation, better positive effect on PHC bioavailability induced better biodegradation at ambient temperature. It is well known that various factors influence bioremediation success, not only PHC/P bioavailability (McGuinness and Dowling, 2009; Schwitzguébel et al., 2011). The effect of LMOAA on PHC biostimulation could be situation-specific. The combination of the combination for 1.0 mM phosphate plus 10 mM citrate may be a good option for *in situ* biostimulation application in gasoline contaminated site (Chapter 4 and Chapter 5), probably by increasing the bioavailability for gasoline or other approaches.

Chapter 4 addressed the ability of citrate to increase the P bioavailability for *in situ* bioremediation, with enhanced gasoline dissipation, such as, $F1_{-BTEX}$ in soil Area 2 and BTEX in groundwater monitoring wells. Quick increases in bioavailable P in groundwater after adding citrate was found in a gasoline contaminated site. And the increased bioavailable P fraction may be related the exchangeable organic P dissolution in soil. The resin- and $NaHCO_3$–extracted P has been shown to contribute to soluble and exchangeable P (Schoenau and O'Halloran, 2007; Tiessen and Moir, 2007), which was selectively increased in certain area. The organic P solubilizing effect of LMOA was proposed to be dependent on the level of soil organic P, and the dynamic flux of organic P may be more important than the increased amount of organic P (Wei et al., 2010). Citrate did not change the bulk speciation or mineralogy of P in the soil, but changed the groundwater iron(II) content that related to iron-reducing microbes. In this study, the increased organic P in extraction only accounted 2–6% of total P, which demonstrated a quite important role for groundwater microbial activity for *in situ* bioremediation.

Chapter 5 investigated how the microbial community changed by citrate addition, especially the anaerobic hydrocarbon-degraders, during the 18-month biostimulation period for

three treatments. Citrate selectively increased the culturable and total anaerobic hydrocarbon degrader population, which had an analogous pattern in a field microcosm experiment (Siciliano et al., 2016). And the selective stimulation of the hydrocarbon degrading microbial community was linked to changes in soil P mineralogy. The soil bacterial community composition was likely driven by the adsorbed P fraction in the soil, which was depleted in the phosphate treatment and was effectively reintroduced after adding citrate. However, it was not the case in groundwater. The population for anaerobic hydrocarbon degraders, especially iron-reducing and nitrate-reducing bacteria, was increased by citrate addition in the groundwater. While, citrate addition reversed the enhancement of hydrocarbon degraders in the soil microbial community. Citrate may limit apatite formation, driving a higher fraction of the total soil P pool into not only the adsorbed but also the dissolved phase. If combined with the P sequential extraction result, the microbial community in the groundwater is more likely linked to the increased bioavailable organic P, not the adsorbed fraction in soil. The pool for absorbed P in soil and dynamic flux for organic P in groundwater determine the function and composition in soil and groundwater, respectively.

Chapter 6 developed and validated a cost-effective method to estimate biodegradation potential in soil samples, with stable carbon techniques. This method used a CO_2 trap to collect the produced $^{13}CO_2$ from mineralization of partially enriched benzene or phenanthrene, and determined the stable isotope data by cavity ring down spectrometer (CRDS). This trapping method offered some advantages: could condense the CO_2 to makes the storage and following analytical dilution process for gas samples easier; can prevent the gas interference for CRDS caused by the components in the headspace; equipped with iron oxide filter, the method could remove the disturbance from H_2S. This trap method successfully assessed the phenanthrene mineralization under aerobic and anaerobic conditions, and provided limited accurate mineralization estimation for benzene biodegradation due to isotope fractionation, permitting us to investigate the intrinsic PHC biodegradation potential under aerobic and anaerobic conditions for soil samples.

In conclusion, LMOAA, such as citrate, enhanced anaerobic PHC bioremediation through: (1) promoting the PHC partition into water phase to increase PHC bioavailability; (2) increasing bioavailable organic P fraction to increase P bioavailability; (3) stimulating the

anaerobic PHC degrader, particularly iron reducers (Fig. 7.1). And the active microbial community was closely related to P speciation, in both soil and groundwater.

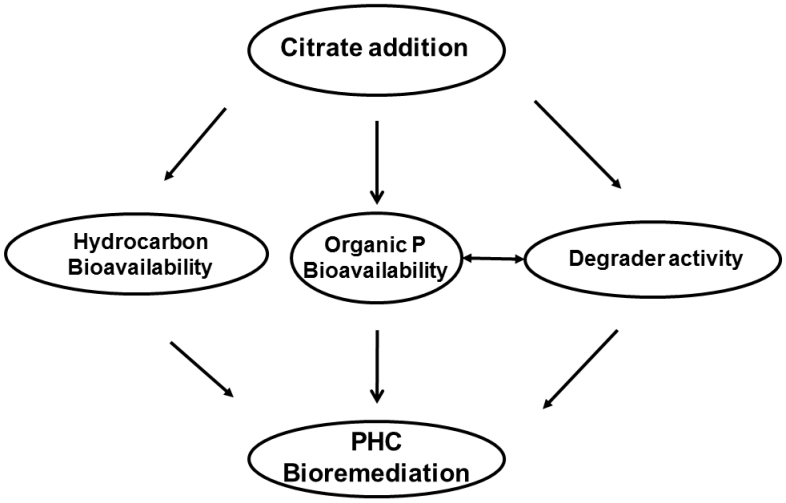

Fig. 7.1. Conceptual model of strategies by which citrate enhance PHC bioremediation.

7.2 Future Research

This research presented an integrated picture for the influence of citrate on PHC bioremediation through different strategies in the laboratory and in the field. Moreover, it provided insight into how to balance PHC bioavailability and P bioavailability for *in situ* and *ex situ* PHC biodegradation. LMOAA changed P mineralogy and P speciation in the soil, which were correlated to microbial community in soil and groundwater. A better understanding of P speciation, especially the organic P species and their role in microbial community composition and function will be important for PHC bioremediation application.

The positive effect of LMOAA on PHC bioavailability for PHC biodegradation was demonstrated in microcosm studies in Chapter 3. Different soil types, temperature, and microcosm slurry composition were tested. However, studying more parameters is required, particularly soil properties related to phase partition and mass transfer for PHC. In addition, the correlation among PHC bioavailability, P bioavailability, PHC biodegradation, and soil homogeneity was not clear. Studying P speciation in the soil and aqueous phase is therefore warranted, which supports better management for P amendment during PHC biostimulation process. The bioavailable organic P fraction was increased by citrate addition, based on

sequential extraction. It was unknown which kind of organic P was released, highlighting the need to combine other alternative analysis for organic P. Spectroscopic techniques offer a good potential for determining the speciation of organic P in soils (Doolette and Smernik, 2011). The three main spectroscopic techniques include solution 31P nuclear magnetic resonance (NMR) spectroscopy, solid-state 31P NMR spectroscopy and P XANES (X-ray absorption near-edge structure) spectroscopy, which can be applied in the future study.

Though the polyaromatic hydrocarbon compound-phenanthrene mineralization was successfully assessed, it was not able to accurately quantify the mineralization rate for monoaromatic hydrocarbon compound-benzene due to isotope fractionation. Determination of the isotope fractionation factor for substances with the isotope ratio mass spectrometry (IRMS), or using a uniformly labelled benzene to prevent fractionation, can be used for more accurate mineralization assessment.

8. REFERENCES

Abu Laban, N., D. Selesi, T. Rattei, P. Tischler, and R.U. Meckenstock. 2010. Identification of enzymes involved in anaerobic benzene degradation by a strictly anaerobic iron-reducing enrichment culture. Environ. Microbiol. 12(10): 2783–2796.

Aggarwal, P.K., M.E. Fuller, M.M. Gurgas, J.F. Manning, and M.A. Dillon. 1997. Use of stable oxygen and carbon isotope analyses for monitoring the pathways and rates of intrinsic and enhanced *in situ* biodegradation. Environ. Sci. Technol. 31(2): 590–596.

Aggarwal, P.K., and R.E. Hinchee. 1991. Monitoring *in situ* biodegradation of hydrocarbons by using stable carbon isotopes. Environ. Sci. Technol. 25(6): 1178–1180.

Aislabie, J., D.J. Saul, and J.M. Foght. 2006. Bioremediation of hydrocarbon-contaminated polar soils. Extremophiles 10(3): 171–179.

Amellal, N. 2001. Effect of soil structure on the bioavailability of polycyclic aromatic hydrocarbons within aggregates of a contaminated soil. Appl. Geochemistry 16(14): 1611–1619.

An, C., G. Huang, J. Wei, and H. Yu. 2011. Effect of short-chain organic acids on the enhanced desorption of phenanthrene by rhamnolipid biosurfactant in soil-water environment. Water Res. 45(17): 5501–5510.

An, C., G. Huang, H. Yu, J. Wei, W. Chen, and G. Li. 2010. Effect of short-chain organic acids and pH on the behaviors of pyrene in soil-water system. Chemosphere 81(11): 1423–1429.

Avanzi, I.R., L.H. Gracioso, M. dos P.G. Baltazar, B. Karolski, E.A. Perpetuo, and C.A.O. Nascimento. 2015. Aerobic biodegradation of gasoline compounds by bacteria isolated from a hydrocarbon-contaminated soil. Environ. Eng. Sci. 32(12): 990–997.

Bahr, A., A. Fischer, C. Vogt, and P. Bombach. 2015. Evidence of polycyclic aromatic hydrocarbon biodegradation in a contaminated aquifer by combined application of in situ and laboratory microcosms using ^{13}C-labelled target compounds. Water Res. 69: 100–109.

Barrera-Díaz, C.E., V. Lugo-Lugo, and B. Bilyeu. 2012. A review of chemical, electrochemical and biological methods for aqueous Cr(VI) reduction. J. Hazard. Mater. 223–224: 1–12.

Bekins, B.A., E.M. Godsy, and E. Warren. 1999. Distribution of microbial physiologic types in an aquifer contaminated by crude oil. Microb. Ecol. 37(4): 263–275.

Bento, F.M., F.A.O. Camargo, B.C. Okeke, and W.T. Frankenberger. 2005. Comparative bioremediation of soils contaminated with diesel oil by natural attenuation, biostimulation and bioaugmentation. Bioresour. Technol. 96(9): 1049–1055.

Bergelin, A., P.A.W. van Hees, O. Wahlberg, and U.S. Lundström. 2000. The acid–base properties of high and low molecular weight organic acids in soil solutions of podzolic soils. Geoderma 94(2–4): 223–235.

Bielská, L., I. Hovorková, K. Komprdová, and J. Hofman. 2012. Variability of standard artificial soils: Physico-chemical properties and phenanthrene desorption measured by means of supercritical fluid extraction. Environ. Pollut. 163: 1–7.

Birch, H., R. Hammershøj, M. Comber, and P. Mayer. 2017. Biodegradation of hydrocarbon

mixtures in surface waters at environmentally relevant levels – Effect of inoculum origin on kinetics and sequence of degradation. Chemosphere 184: 400–407.

Bisutti, I., I. Hilke, and M. Raessler. 2004. Determination of total organic carbon - An overview of current methods. TrAC - Trends Anal. Chem. 23(10–11): 716–726.

Bolan, N.S., R. Naidu, S. Mahimairaja, and S. Baskaran. 1994. Influence of low-molecular-weight organic acids on the solubilization of phosphates. Biol. Fertil. Soils 18(4): 311–319.

Boll, M., and G. Fuchs. 1995. Benzoyl-coenzyme A reductase (dearomatizing), a key enzyme of anaerobic aromatic metabolism: ATP dependence of the reaction, purification and some properties of the enzyme from *Thauera aromatica* strain K172. Eur. J. Biochem. 234(3): 921–933.

Boll, M., D. Laempe, W. Eisenreich, A. Bacher, T. Mittelberger, J. Heinze, and G. Fuchs. 2000. Nonaromatic products from anoxic conversion of benzoyl-CoA with benzoyl-coA reductase and Cyclohexa-1,5-diene- 1-carbonyl-CoA hydratase. J. Biol. Chem. 275(29): 21889–21895.

Boll, M., C. Löffler, B.E.L. Morris, and J.W. Kung. 2014. Anaerobic degradation of homocyclic aromatic compounds via arylcarboxyl-coenzyme A esters: Organisms, strategies and key enzymes. Environ. Microbiol. 16(3): 612–627.

Bombach, P., A. Chatzinotas, T.R. Neu, M. Kästner, T. Lueders, and C. Vogt. 2010. Enrichment and characterization of a sulfate-reducing toluene-degrading microbial consortium by combining *in situ* microcosms and stable isotope probing techniques. FEMS Microbiol. Ecol. 71(2): 237–246.

Boopathy, R. 2000. Factors limiting bioremediation technologies. Bioresour. Technol. 74(1): 63–67.

Bouchard, D., D. Hunkeler, P. Gaganis, R. Aravena, P. Höhener, M.M. Broholm, and P. Kieldsen. 2008. Carbon isotope fractionation during diffusion and biodegradation of petroleum hydrocarbons in the unsaturated zone: Field experiment at Værløse Airbase, Denmark, and modeling. Environ. Sci. Technol. 42(2): 596–601.

Bugna, G.C., J.P. Chanton, C.A. Kelley, T.B. Stauffer, W.G. MacIntyre, and E.L. Libelo. 2004. A field test of delta ^{13}C as a tracer of aerobic hydrocarbon degradation. Org. Geochem. 35(2): 123–135.

Burland, S.M., and E.A. Edwards. 1999. Anaerobic benzene biodegradation linked to nitrate reduction. Appl. Environ. Microbiol. 65(2): 529–533.

Canadian Council of Ministers of the Environment. 2001. Reference method for the Canada-wide standard for petroleum hydrocarbons in soil-Tier 1 Method. Can. Counc. Minist. Environ. https://www.ccme.ca/files/Resources/csm/phc_cws/final_phc_method_rvsd_e.pdf (accessed 4 Feb. 2013).

Canadian Council of Ministers of the Environment. 2008a. Canada-wide standard for petroleum hydrocarbons (PHC) in soil. Can. Counc. Minist. Environ. https://www.ccme.ca/files/Resources/csm/phc_cws/phc_standard_1.0_e.pdf (accessed 4 Feb. 2013).

Canadian Council of Ministers of the Environment. 2008b. Canada-wide standard for petroleum

hydrocarbons(PHC) in soil-User guildance. Can. Counc. Minist. Environ. https://www.ccme.ca/files/Resources/csm/phc_cws/pn_1398_phc_user_guide_1.1_e.pdf (accessed 4 Feb. 2013).

Canadian Council of Ministers of the Environment. 2008c. Canada-wide standard for petroleum hydrocarbons (PHC) in soil : Scientific rationale supporting technical document. Can. Counc. Minist. Environ. https://www.ccme.ca/files/Resources/csm/phc_cws/pn_1399_phc_sr_std_1.2_e.pdf (accessed 4 May 2013).

Canadian Real Estate Association. 2008. Redeveloping brownfields. Can. Real Estate Assoc. http://www.mah.gov.on.ca/AssetFactory.aspx?did=5248 (accessed 25 Feb. 2014).

Chandra, S., R. Sharma, K. Singh, and A. Sharma. 2013. Application of bioremediation technology in the environment contaminated with petroleum hydrocarbon. Ann. Microbiol. 63(2): 417–431.

Chatterjee, D., S.C. Datta, and K.M. Manjaiah. 2015. Effect of citric acid treatment on release of phosphorus , aluminium and iron from three dissimilar soils of India. Arch. Agron. Soil Sci. 61(1): 105–117.

Chen, T., C. Philips, J. Hamilton, B. Chartbrand, J. Grosskleg, K. Bradshaw, T. Carlson, K. Timlick, D. Peak, and S.D. Siciliano. 2017. Citrate addition increased phosphorus bioavailability and enhanced gasoline bioremediation. J. Environ. Qual. 46(5): 975–983.

Coates, J.D., R. Chakraborty, and M.J. McInerney. 2002. Anaerobic benzene biodegradation - A new era. Res. Microbiol. 153(10): 621–628.

Coffin, R.B., J.W. Pohlman, K.S. Grabowski, D.L. Knies, R.E. Plummer, R.W. Magee, and T.J. Boyd. 2008. Radiocarbon and stable carbon isotope analysis to confirm petroleum natural attenuation in the vadose zone. Environ. Forensics 9(1): 75–84.

Collins, R.N. 2004. Separation of low-molecular mass organic acid–metal complexes by high-performance liquid chromatography. J. Chromatogr. A 1059: 1–12.

Conrad, M.E., P.F. Daley, M.L. Fischer, B.B. Buchanan, T. Leighton, and M. Kashgarian. 1997. Combined ^{14}C and $\delta^{13}C$ monitoring of *in situ* biodegradation of petroleum hydrocarbons. Environ. Sci. Technol. 31(5): 1463–1469.

Conrad, M.E., A.S. Templeton, P.F. Daley, and L. Alvarez-Cohen. 1999. Isotopic evidence for biological controls on migration of petroleum hydrocarbons. Org. Geochem. 30(8): 843–859.

Conte, P., A. Zena, G. Pilidis, and A. Piccolo. 2001. Increased retention of polycyclic aromatic hydrocarbons in soils induced by soil treatment with humic substances. Environ. Pollut. 112(1): 27–31.

Corgié, S.C., T. Beguiristain, and C. Leyval. 2006. Differential composition of bacterial communities as influenced by phenanthrene and dibenzo[a,h]anthracene in the rhizosphere of ryegrass (*Lolium perenne* L.). Biodegradation 17(6): 511–521.

Coulon, F., M.J. Whelan, G.I. Paton, K.T. Semple, R. Villa, and S.J.T. Pollard. 2010. Multimedia fate of petroleum hydrocarbons in the soil: Oil matrix of constructed biopiles. Chemosphere 81: 1454–1462.

Cui, X., P. Mayer, and J. Gan. 2013. Methods to assess bioavailability of hydrophobic organic contaminants: Principles, operations, and limitations. Environ. Pollut. 172: 223–234.

Das, N., and P. Chandran. 2011. Microbial degradation of petroleum hydrocarbon contaminants: An overview. Biotechnol. Res. Int. 2011: 1–13.

Dempster, H.S., B.S. Lollar, and S. Feenstra. 1997. Tracing organic contaminants in groundwater: A new methodology using compound-specific isotopic analysis. Environ. Sci. Technol. 31(11): 3193–3197.

Díaz, E., J.I. Jiménez, and J. Nogales. 2013. Aerobic degradation of aromatic compounds. Curr. Opin. Biotechnol. 24(3): 431–442.

Ding, Q., H.L. Wu, Y. Xu, L.J. Guo, K. Liu, H.M. Gao, and H. Yang. 2011. Impact of low molecular weight organic acids and dissolved organic matter on sorption and mobility of isoproturon in two soils. J. Hazard. Mater. 190(1–3): 823–832.

Dong, X., J. Dröge, C. von Toerne, S. Marozava, A.C. McHardy, and R.U. Meckenstock. 2017. Reconstructing metabolic pathways of a member of the genus Pelotomaculum suggesting its potential to oxidize benzene to carbon dioxide with direct reduction of sulfate. FEMS Microbiol. Ecol. 93(3): 1–9.

Doolette, A.L., and R.J. Smernik. 2011. Soil organic phosphorus speciation using spectroscopic techniques. *In* Bünemann, E., Oberson, A., Frossard, E. (eds.), Phosphorus in action: Biological processes in soil phosphorus cycling. Springer Berlin Heidelberg, Berlin, Heidelberg. p. 3–36.

Duffner, A., E. Hoffland, and E.J.M. Temminghoff. 2012. Bioavailability of zinc and phosphorus in calcareous soils as affected by citrate exudation. Plant Soil (361): 165–175.

Duputel, M., F. Van Hoye, J. Toucet, and F. Gérard. 2013. Citrate adsorption can decrease soluble phosphate concentration in soil: Experimental and modeling evidence. Appl. Geochemistry 39: 85–92.

Dutta, T.K., and S. Harayama. 2000. Fate of crude oil by the combination of photooxidation and biodegradation. Environ. Sci. Technol. 34(8): 1500–1505.

Edwards, E.A. 2003. Physiological and molecular characterization of anaerobic benzene-degrading mixed cultures. Environ. Mcrobiology 5(2): 92–102.

Edwards, E.A., and D. Grbić-Galić. 1992. Complete mineralization of benzene by aquifer microorganisms under strictly anaerobic conditions. Appl. Environ. Microbiol. 58(8): 2663–2666.

Edwards, E.A., and D. Grbić-Galić. 1994. Anaerobic degradation of toluene and o-xylene by a methanogenic consortium. Appl. Environ. Microbiol. 60(1): 313–322.

Falciglia, P.P., M.G. Giustra, and F.G.A. Vagliasindi. 2011. Low-temperature thermal desorption of diesel polluted soil: Influence of temperature and soil texture on contaminant removal kinetics. J. Hazard. Mater. 185(1): 392–400.

Farhadian, M., C. Vachelard, D. Duchez, and C. Larroche. 2008. *In situ* bioremediation of monoaromatic pollutants in groundwater: A review. Bioresour. Technol. 99(13): 5296–5308.

Fathepure, B.Z. 2014. Recent studies in microbial degradation of petroleum hydrocarbons in hypersaline environments. Front. Microbiol. 5: 173.

Feenstra, S. 2005. Soil sampling in NAPL source zones: Challenges to representativeness. Environ. Forensics 6(1): 57–63.

Foght, J. 2008. Anaerobic biodegradation of aromatic hydrocarbons: Pathways and prospects. J. Mol. Microbiol. Biotechnol. 15(2–3): 93–120.

Fuchs, G., M. Boll, and J. Heider. 2011. Microbial degradation of aromatic compounds - from one strategy to four. Nat. Rev. Microbiol. 9(11): 803–816.

Fuentes, S., V. Méndez, P. Aguila, and M. Seeger. 2014. Bioremediation of petroleum hydrocarbons: Catabolic genes, microbial communities, and applications. Appl. Microbiol. Botechnology 98(11): 4781–4794.

Fujii, K., M. Aoki, and K. Kitayama. 2013. Reprint of "Biodegradation of low molecular weight organic acids in rhizosphere soils from a tropical montane rain forest." Soil Biol. Biochem. 56: 3–9.

Gan, W., B. Crozier, and Q. Liu. 2009a. Effect of citric acid on inhibiting hexadecane–quartz coagulation in aqueous solutions containing Ca^{2+} , Mg^{2+} and Fe^{3+} ions. Int. J. Miner. Process. 92(1–2): 84–91.

Gan, S., E. V. Lau, and H.K. Ng. 2009b. Remediation of soils contaminated with polycyclic aromatic hydrocarbons (PAHs). J. Hazard. Mater. 172(2–3): 532–549.

Ganesh, R., K.G. Robinson, G.D. Reed, and G.S. Sayler. 1997. Reduction of hexavalent uranium from organic complexes by sulfate- and iron-reducing bacteria. Appl. Environ. Microbiol. 63(11): 4385–4391.

Gao, Y., L. Ren, W. Ling, S. Gong, B. Sun, and Y. Zhang. 2010a. Desorption of phenanthrene and pyrene in soils by root exudates. Bioresour. Technol. 101(4): 1159–1165.

Gao, Y., L. Ren, W. Ling, F. Kang, X. Zhu, and B. Sun. 2010b. Effects of low-molecular-weight organic acids on sorption–desorption of phenanthrene in soils. Soil Chem. 74(1): 51–59.

Gao, Y., X. Yuan, X. Lin, B. Sun, and Z. Zhao. 2015. Low-molecular-weight organic acids enhance the release of bound PAH residues in soils. Soil Tillage Res. 145: 103–110.

Gardener, M. 2014. Community ecology: Analytical methods using R and Excel. Pelagic Publishing, Milton Keynes.

Gavrilescu, M., L.V. Pavel, and I. Cretescu. 2009. Characterization and remediation of soils contaminated with uranium. J. Hazard. Mater. 163(2–3): 475–510.

Gouliarmou, V., C.D. Collins, E. Christiansen, and P. Mayer. 2013. Sorptive physiologically based extraction of contaminated solid matrices: Incorporating silicone rod as absorption sink for hydrophobic organic contaminants. Environ. Sci. Technol. 47(2): 941–948.

Gouliarmou, V., and P. Mayer. 2012. Sorptive bioaccessibility extraction (SBE) of soils: combining a mobilization medium with an absorption sink. Environ. Sci. Technol. 46(19): 10682–10689.

Grimberg, S.J., W.T. Stringfellow, and M.D. Aitken. 1996. Quantifying the biodegradation of phenanthrene by Pseudomonas stutzeri P16 in the presence of a nonionic surfactant. Appl.

Environ. Microbiol. 62(7): 2387–2392.

Grossi, V., C. Cravo-Laureau, R. Guyoneaud, A. Ranchou-Peyruse, and A. Hirschler-Réa. 2008. Metabolism of n-alkanes and n-alkenes by anaerobic bacteria: A summary. Org. Geochem. 39(8): 1197–1203.

Halajnia, A., G.H. Haghnia, A. Fotovat, and R. Khorasani. 2009. Phosphorus fractions in calcareous soils amended with P fertilizer and cattle manure. Geoderma 150(1–2): 209–213.

Hall, J.A., R.M. Kalin, M.J. Larkin, C.C.R. Allen, and D.B. Harper. 1999. Variation in stable carbon isotope fractionation during aerobic degradation of phenol and benzoate by contaminant degrading bacteria. Org. Geochem. 30(8 A): 801–811.

Hamilton, J.G., D. Hilger, and D. Peak. 2017. Mechanisms of tripolyphosphate adsorption and hydrolysis on goethite. J. Colloid Interface Sci. 491: 190–198.

Haritash, A.K., and C.P. Kaushik. 2009. Biodegradation aspects of polycyclic aromatic hydrocarbons (PAHs): A review. J. Hazard. Mater. 169: 1–15.

Harrington, R.R., S.R. Poulson, J.I. Drever, P.J.S. Colberg, and E.F. Kelly. 1999. Carbon isotope systematics of monoaromatic hydrocarbons: Vaporization and adsorption experiments. Org. Geochem. 30(8 A): 765–775.

Hashim, M. a, S. Mukhopadhyay, J.N. Sahu, and B. Sengupta. 2011. Remediation technologies for heavy metal contaminated groundwater. J. Environ. Manage. 92(10): 2355–2388.

van Hees, P.A.W., K. Elgh-Dalgren, M. Engwall, and T. von Kronhelm. 2008. Re-cycling of remediated soil in Sweden: An environmental advantage? Resour. Conserv. Recycl. 52(12): 1349–1361.

van Hees, P.A.W., D.L. Jones, R. Finlay, D.L. Godbold, and U.S. Lundström. 2005a. The carbon we do not see—the impact of low molecular weight compounds on carbon dynamics and respiration in forest soils: A review. Soil Biol. Biochem. 37(1): 1–13.

van Hees, P.A.W., D.L. Jones, and D.L. Godbold. 2002. Biodegradation of low molecular weight organic acids in coniferous forest podzolic soils. Soil Biol. Biochem. 34(9): 1261–1272.

van Hees, P.A.W., D.L. Jones, L. Nyberg, S.J.M. Holmström, D.L. Godbold, and U.S. Lundström. 2005b. Modelling low molecular weight organic acid dynamics in forest soils. Soil Biol. Biochem. 37(3): 517–531.

van Hees, P.A.W., and U.S. Lundström. 2000. Equilibrium models of aluminium and iron complexation with different organic acids in soil solution. Geoderma 94(2–4): 201–221.

van Hees, P.A.W., S.I. Vinogradoff, A.C. Edwards, D.L. Godbold, and D.L. Jones. 2003. Low molecular weight organic acid adsorption in forest soils: Effects on soil solution concentrations and biodegradation rates. Soil Biol. Biochem. 35(8): 1015–1026.

Heider, J. 2007. Adding handles to unhandy substrates: Anaerobic hydrocarbon activation mechanisms. Curr. Opin. Chem. Biol. 11(2): 188–194.

Heider, J., A.M. Spormann, H.R. Beller, and F. Widdel. 1998. Anaerobic bacterial metabolism of hydrocarbons. FEMS Microbiol. Rev. 22(5): 459–473.

Hendershot, W.H., H. Lalande, and M. Duquette. 2008. Chapter 16 Soil reaction and exchangeable Acidity. *In* Soil sampling and methods of analysis. p. 173–178.

Herbst, F.A., A. Bahr, M. Duarte, D.H. Pieper, H.H. Richnow, M. von Bergen, J. Seifert, and P. Bombach. 2013. Elucidation of *in situ* polycyclic aromatic hydrocarbon degradation by functional metaproteomics (protein-SIP). Proteomics 13(18–19): 2910–2920.

Heyse, E., D. Augustijn, P.S.C. Rao, and J.J. Delfino. 2002. Nonaqueous phase liquid dissolution and soil organic matter sorption in porous media: Review of system similarities. Crit. Rev. Environ. Sci. Technol. 32(4): 337–397.

Hinchee, R.E., D.C. Downey, R.R. Dupont, P.K. Aggarwal, and R.N. Miller. 1991. Enhancing biodegradation products through soil venting. J. Hazard. Mater. 27: 315–325.

Hinsinger, P. 2001. Bioavailibility of soil inorganic P in the rhizosphere as effected by root-induced chemical changes: A review.pdf. Plant Soil 237: 173–195.

Hoefs, J. 2015. Stable Isotope Geochemistry. Seventh. Springer International Publishing, Cham.

Hofstetter, T.B., and M. Berg. 2011. Assessing transformation processes of organic contaminants by compound-specific stable isotope analysis. Trends Anal. Chem. 30(4): 618–627.

Höhener, P., and C.M. Aelion. 2010. 1. Fundamentals of environmental isotopes and their use in biodegradation. *In* Aelion, C.M., Höhener, P., Hunkeler, D., Aravena, R. (eds.), Environmental isotopes in biodegradation and bioremediation. CRC Press, Boca Raton. p. 3–23.

Höhener, P., D. Hunkeler, A. Hess, T. Bregnard, J. Zeyer, and P. Hohener. 1998. Methodology for the evaluation of engineered *in situ* bioremediation: Lessons from a case study. J. Microbiol. Methods 32(2): 179–192.

Huang, H., S. Wang, J. Lv, X. Xu, and S. Zhang. 2016. Influences of artificial root exudate components on the behaviors of BDE-28 and BDE-47 in soils : Desorption, availability, and biodegradation. Environ. Sci. Pollut. Res. Int. (23): 7702–7711.

Huling, S.G., and J.W. Weaver. 1992. Ground water issue: Dense nonaqueous phase liquids. USEPA. https://www.epa.gov/sites/production/files/2015-06/documents/dnapl_issue_paper.pdf (accessed 3 Jan. 2018).

Hunkelera, D., P. Höhenera, S. Bernasconib, and J. Zeyer. 1999. Engineered *in situ* bioremediation of a petroleum hydrocarbon-contaminated aquifer: Assessment of mineralization based on alkalinity, inorganic carbon and stable carbon isotope balances. J. Contam. Hydrol. 37(3–4): 201–223.

Hunkeler, D., N. Anderson, R. Aravena, S.M. Bernasconi, and B.J. Butler. 2001. Hydrogen and carbon isotope fractionation during aerobic biodegradation of benzene. Environ. Sci. Technol. 35(17): 3462–3467.

Illumina. 2013. 16S Metagenomic sequencing library preparation. Illumina. https://web.uri.edu/gsc/files/16s-metagenomic-library-prep-guide-15044223-b.pdf (accessed 2 Jan. 2017).

Indorante, S.J., L.R. Follmer, R.D. Hammer, and P.. Koenig. 1990. Particle-size analysis by a modified pipette procedure. Soil Sci. Soc. Am. J. 54(2): 560–563.

Jana, A.K., and P. Ghosh. 1995. Xanthan biosynthesis in continuous culture: Citric acid as an energy source. J. Ferment. Bioeng. 80(5): 485–491.

Jansa, J., R. Finlay, H. Wallander, F.A. Smith, and S.E. Smith. 2011. Role of mycorrhizal symbioses in phosphorus cycling. *In* Bünemann, E., Oberson, A., Frossard, E. (eds.), Phosphorus in action: Biological processes in soil phosphorus cycling. Springer Berlin Heidelberg, Berlin, Heidelberg. p. 137–168.

Ji, Y., G. Mao, Y. Wang, and M. Bartlam. 2013. Structural insights into diversity and n-alkane biodegradation mechanisms of alkane hydroxylases. Front. Microbiol. 4: 58.

Jiang, C., D. Wu, J. Hu, F. Liu, X. Huang, C. Li, and M. Jin. 2011. Application of chemical fractionation and X-ray powder diffraction to study phosphorus speciation in sediments from Lake Hongfeng, China. Chinese Sci. Bull. 56(20): 2098–2108.

Jiang, B., Z. Zhou, Y. Dong, W. Tao, B. Wang, J. Jiang, and X. Guan. 2015a. Biodegradation of benzene, toluene, ethylbenzene, and o-, m-, and p-xylenes by the newly isolated bacterium Comamonas sp. JB. Appl. Biochem. Biotechnol. 176(6): 1700–1708.

Jiang, B., Z. Zhou, Y. Dong, B. Wang, J. Jiang, X. Guan, S. Gao, A. Yang, Z. Chen, and H. Sun. 2015b. Bioremediation of petrochemical wastewater containing BTEX compounds by a new immobilized bacterium Comamonas sp. JB in Magnetic Gellan Gum. Appl. Biochem. Biotechnol. 176(2): 572–581.

Jin, S., and P.H. Fallgren. 2007. Site-specific limitations of using urea as a nitrogen source in biodegradation of petroleum wastes in soil. Soil Sediment Contam. 16(5): 497–505.

Johnson, S.E., and R.H. Loeppert. 2006. Role of Organic Acids in Phosphate Mobilization from Iron Oxide. Soil Sci. Soc. Am. J. 70: 222–234.

Johnson, P., P. Lundegard, and Z. Liu. 2006. Source zone natural attenuation at petroleum hydrocarbon spill sites - I: Site-specific assessment approach. Gr. Water Monit. Remediat. 26(4): 82–92.

Jones, D.L., and P.R. Darrah. 1994. Role of root derived organic acids in the mobilization of nutrients from the rhizosphere. Plant Soil 166: 247–257.

Jones, D.L., and P.R. Darrah. 1995. Influx and effiux of organic acids across the soil-root interface of Zea mays L . and its implications in rhizosphere C flow. Plant Soil 173: 103–109.

Jones, D.L., and E. Oburger. 2011. Solubilization of phosphorus by soil microorganisms. *In* Bünemann, E., Oberson, A., Frossard, E. (eds.), Phosphorus in action: Biological processes in soil phosphorus cycling. Springer Berlin Heidelberg, Berlin, Heidelberg. p. 169–198.

Jones, S.A., and V. Uddameri. 2004. Hazardous waste assessment, management, and minimization. Water Environ. Res. 76(6): 1857–1871.

Joshi-Tope, G., and A.J. Francis. 1995. Mechanisms of biodegradation of metal-citrate complexes by Pseudomonas fluorescens. J. Bacteriol. 177(8): 1989–1993.

Kamath, R., J.L. Schnoor, and P.J.J. Alvarez. 2004. Effect of root-derived substrates on the expression of nah-lux genes in Pseudomonas fluorescens HK44: Implications for PAH biodegradation in the rhiziosphere. Environ. Sci. Technol. 38(6): 1740–1745.

Kan, J., Y. Wang, A. Obraztsova, G. Rosen, J. Leather, K.G. Scheckel, K.H. Nealson, and Y.M. Arias-thode. 2011. Ecotoxicology and environmental safety marine microbial community

response to inorganic and organic sediment amendments in laboratory mesocosms. Ecotoxicol. Environ. Saf. 74(7): 1931–1941.

Kar, G., D. Peak, and J.J. Schoenau. 2012. Spatial distribution and chemical speciation of soil phosphorus in a band application. Soil Sci. Soc. Am. J. 76(6): 2297.

Kasai, Y., Y. Takahata, M. Manefield, and K. Watanabe. 2006. RNA-based stable isotope probing and isolation of anaerobic benzene-degrading bacteria from gasoline-contaminated groundwater. Appl. Environ. Microbiol. 72(5): 3586–3592.

Kelley, C.A., B.T. Hammer, and R.B. Coffin. 1997. Concentrations and stable isotope values of BTEX in gasoline-contaminated groundwater. Environ. Sci. Technol. 31(9): 2469–2472.

Khodaei, K., H.R. Nassery, M.M. Asadi, H. Mohammadzadeh, and M.G. Mahmoodlu. 2017. BTEX biodegradation in contaminated groundwater using a novel strain (*Pseudomonas* sp. BTEX-30). Int. Biodeterior. Biodegradation 116: 234–242.

Kirk, J.L., L.A. Beaudette, M. Hart, P. Moutoglis, J.N. Klironomos, H. Lee, and J.T. Trevors. 2004. Methods of studying soil microbial diversity. J. Microbiol. Methods 58(2): 169–188.

Kirtland, B.C., C.M. Aelion, and P.A. Stone. 2000. Monitoring anaerobic natural attenuation of petroleum using a novel *in situ* respiration method in low-permeability sediment. Bioremediat. J. 4(3): 187–201.

Kleemann, R., and R.U. Meckenstock. 2011. Anaerobic naphthalene degradation by Gram-positive, iron-reducing bacteria. FEMS Microbiol. Ecol. 78(3): 488–496.

Kleinsteuber, S., K.M. Schleinitz, J. Breitfeld, H. Harms, H.H. Richnow, and C. Vogt. 2008. Molecular characterization of bacterial communities mineralizing benzene under sulfate-reducing conditions. FEMS Microbiol. Ecol. 66(1): 143–157.

Kleinsteuber, S., K.M. Schleinitz, and C. Vogt. 2012. Key players and team play: Anaerobic microbial communities in hydrocarbon-contaminated aquifers. Appl. Microbiol. Biotechnol. 94(4): 851–873.

Kley, L.S.-V. der, J. de Fraye, R. Pentel, L. Buve, R. Jacquet, H.L.A. Slenders, I. Heasman, S. Wallace, and M. Ackermann. 2011. Dealing with contaminated sites: From theory towards practical application. *In* Swartjes, F.A. (ed.), Dealing with contaminated sites: From theory towards practical application. Springer Netherlands, Dordrecht. p. 1054–1077.

Knight, V., F. Caccavo, S. Wudyka, and R. Blakemore. 1996. Synergistic iron reduction and citrate dissimilation by *Shewanella alga* and *Aeromonas veronii*. Arch. Microbiol. 166(4): 269–274.

Konečný, F., Z. Boháček, P. Müller, M. Kovářová, and I. Sedláčková. 2003. Contamination of soils and groundwater by petroleum hydrocarbons and volatile organic compounds - Case study: ELSLAV BRNO. Bull. Geosci. 78(3): 225–239.

Kpomblekou-A, K., and M.A. Tabatabai. 2003. Effect of low-molecular weight organic acids on phosphorus release and phytoavailabilty of phosphorus in phosphate rocks added to soils. Agric. Ecosyst. Environ. 100: 275–284.

Kumar, S., G. Stecher, and K. Tamura. 2016. MEGA7: Molecular evolutionary genetics analysis version 7.0 for bigger datasets. Mol. Biol. Evol. 33(7): 1870–1874.

Kunapuli, U., C. Griebler, H.R. Beller, and R.U. Meckenstock. 2008. Identification of intermediates formed during anaerobic benzene degradation by an iron-reducing enrichment culture. Environ. Microbiol. 10(7): 1703–1712.

Kuntze, K., Y. Shinoda, H. Moutakki, M.J. McInerney, C. Vogt, H.-H. Richnow, and M. Boll. 2008. 6-Oxocyclohex-1-ene-1-carbonyl-coenzyme A hydrolases from obligately anaerobic bacteria: Characterization and identification of its gene as a functional marker for aromatic compounds degrading anaerobes. Environ. Microbiol. 10(6): 1547–1556.

Kuntze, K., C. Vogt.C., H.H. Richnow, and M. Boll. 2011. Combined application of PCR-based functional assays for the detection of aromatic-compound-degrading anaerobes. Appl. Environ. Microbiol. 77(14): 5056–5061.

Kuppusamy, S., T. Palanisami, M. Megharaj, K. Venkateswarlu, and R. Naidu. 2016a. *In-situ* remediation approaches for the management of contaminated sites: A comprehensive overview. *In* de Voogt, P. (ed.), Reviews of environmental contamination and toxicology. Springer International Publishing, Cham. p. 4–90.

Kuppusamy, S., M.P. Thavamani Megharaj, K. Venkateswarlu, and R. Naidu. 2016b. *Ex-situ* remediation technologies for environmental pollutants: A critical perspective. *In* de Voogt, P. (ed.), Reviews of environmental contamination and toxicology. Springer International Publishing, Cham. p. 120–164.

Lageman, R., R.L. Clarke, and W. Pool. 2005. Electro-reclamation, a versatile soil remediation solution. Eng. Geol. 77(3–4): 191–201.

Lam, E. 2004. Turning brownfields green: expertise is growing and municipalities are tapping into a wealth of redevelopment opportunities. Altern. J. 30(5): 24–26.

Lee, J.-F., M.-H. Hsu, H.-P. Chao, H.-C. Huang, and S.-P. Wang. 2004. The effect of surfactants on the distribution of organic compounds in the soil solid/water system. J. Hazard. Mater. 114(1–3): 123–130.

Lee, S.H., J.H. Park, S.H. Kim, B.J. Yu, J.J. Yoon, and H.D. Park. 2015. Evidence of syntrophic acetate oxidation by *Spirochaetes* during anaerobic methane production. Bioresour. Technol. 190: 543–549.

Lepleux, C., M.P. Turpault, P. Oger, P. Frey-Klett, and S. Uroz. 2012. Correlation of the abundance of betaproteobacteria on mineral surfaces with mineral weathering in forest soils. Appl. Environ. Microbiol. 78(19): 7114–7119.

Liang, Y., X. Zhang, D. Dai, and G. Li. 2009. Porous biocarrier-enhanced biodegradation of crude oil contaminated soil. Int. Biodeterior. Biodegrad. 63(1): 80–87.

Li, H., J. Peng, K.A. Weber, and Y. Zhu. 2011. Phylogenetic diversity of Fe(III)-reducing microorganisms in rice paddy soil: Enrichment cultures with different short-chain fatty acids as electron donors. J. Soils Sediments 11(7): 1234–1242.

Li, J., and Y. Zhang. 2012. Remediation technology for the uranium contaminated environment: a review. Procedia Environ. Sci. 13: 1609–1615.

Licht, L.A., and J.G. Isebrands. 2005. Linking phytoremediated pollutant removal to biomass economic opportunities. Biomass and Bioenergy 28(2): 203–218.

Liebeg, E.W., and T.J. Cutright. 1999. The investigation of enhanced bioremediation through the addition of macro and micro nutrients in a PAH contaminated soil. Int. Biodeterior. Biodegradation 44(1): 55–64.

Lin, T., P. Pan, and S. Cheng. 2010. *Ex situ* bioremediation of oil-contaminated soil. J. Hazard. Mater. 176: 27–34.

Ling, W., L. Ren, Y. Gao, X. Zhu, and B. Sun. 2009. Impact of low-molecular-weight organic acids on the availability of phenanthrene and pyrene in soil. Soil Biol. Biochem. 41(10): 2187–2195.

Ling, W., R. Sun, X. Gao, R. Xu, and H. Li. 2015. Low-molecular-weight organic acids enhance desorption of polycyclic aromatic hydrocarbons from soil. Eur. J. Soil Biol. 66(2): 339–347.

Liu, Z., D. Stromberg, X. Liu, W. Liao, and Y. Liu. 2015. A new multiple-stage electrocoagulation process on anaerobic digestion effluent to simultaneously reclaim water and clean up biogas. J. Hazard. Mater. 285: 483–490.

Löffler, C., K. Kuntze, J.R. Vazquez, A. Rugor, J.W. Kung, A. Böttcher, and M. Boll. 2011. Occurrence, genes and expression of the W/Se-containing class II benzoyl-coenzyme A reductases in anaerobic bacteria. Environ. Microbiol. 13(3): 696–709.

Love, M.I., W. Huber, and S. Anders. 2014. Moderated estimation of fold change and dispersion for RNA-seq data with DESeq2. Genome Biol. 15(12): 550.

Lovley, D. 1997. Potential for anaerobic bioremediation of BTEX in petroleum-contaminated aquifers. J. Ind. Microbiol. Biotechnol. 18(2): 75–81.

Lovley, D.R., S.J. Giovannoni, D.C. White, J.E. Champine, E.J.P. Phillips, Y.A. Gorby, and S. Goodwin. 1993. *Geobacter metallireducens* gen. nov. sp. nov., a microorganism capable of coupling the complete oxidation of organisc compounds to the reduction of iron and other metals. Arch. Microbiol. 159: 336–344.

Lovley, D.R., and D.J. Lonergan. 1990. Anaerobic oxidation of toluene, phenol, and para-cresol by the dissimilatorty iron-reducing organism, GS-15. Appl. Environ. Microbiol. 56(6): 1858–1864.

Lovley, D.R., and J.C. Woodward. 1996. Rapid anaerobic benzene oxidation with a variety of chelated Fe (III) forms. Appl. Environ. Microbiol. 62(1): 288–291.

Luo, F., C.E. Devine, and E.A. Edwards. 2016. Cultivating microbial dark matter in benzene-degrading methanogenic consortia. Environ. Microbiol. 18(9): 2923–2936.

Luo, F., R. Gitiafroz, C.E. Devine, Y. Gong, L.A. Hug, L. Raskin, and E.A. Edwards. 2014. Metatranscriptome of an anaerobic benzene-degrading, nitrate-reducing enrichment culture reveals involvement of carboxylation in benzene ring activation. Appl. Environ. Microbiol. 80(14): 4095–4107.

Luo, L., S. Zhang, X. Shan, and Y. Zhu. 2006. Oxalate and root exudates enhance the desorption of p,p'-DDT from soils. Chemosphere 63: 1273–1279.

Mancini, S.A., C.E. Devine, M. Elsner, M.E. Nandi, A.C. Ulrich, E.A. Edwards, and B.S. Lollar. 2008. Isotopic evidence suggests different initial reaction mechanisms for anaerobic benzene biodegradation. Environ. Sci. Technol. 42(22): 8290–8296.

Martin, B.C., S.J. George, C.A. Price, M.H. Ryan, and M. Tibbett. 2014. The role of root exuded low molecular weight organic anions in facilitating petroleum hydrocarbon degradation: Current knowledge and future directions. Sci. Total Environ. 472: 642–653.

Martin, B.C., S.J. George, C.A. Price, E. Shahsavari, A.S. Ball, M. Tibbett, and M.H. Ryan. 2016. Citrate and malonate increase microbial activity and alter microbial community composition in uncontaminated and diesel-contaminated soil microcosms. Soil 2(3): 487–498.

Masy, T., S. Demanèche, O. Tromme, P. Thonart, P. Jacques, S. Hiligsmann, and T.M. Vogel. 2016. Hydrocarbon biostimulation and bioaugmentation in organic carbon and clay-rich soils. Soil Biol. Biochem. 99: 66–74.

Mazeas, L., H. Budzinski, and N. Raymond. 2002. Absecence of stable carbon isotope fractionation of saturated and polycyclic aromatic hydrorcarbons during aerobic bacterial biodegradation. Org. Geochem. 33(11): 1259–1272.

Mbadinga, S.M., L.-Y.Y. Wang, L. Zhou, J.-F.F. Liu, J.-D.D. Gu, and B.-Z.Z. Mu. 2011. Microbial communities involved in anaerobic degradation of alkanes. Int. Biodeterior. Biodegradation 65(1): 1–13.

Mccoy, K., J. Zimbron, T. Sale, and M. Lyverse. 2015. Measurement of natural losses of LNAPL using CO_2 traps. Groundwater 53(4): 658–667.

McGuinness, M., and D. Dowling. 2009. Plant-associated bacterial degradation of toxic organic compounds in soil. Int. J. Environ. Res. Public Health 6(8): 2226–2247.

McIntyre, C.P., P.M.A. Harvey, S.H. Ferguson, A.M. Wressnig, H. Volk, S.C. George, and I. Snape. 2007. Determining the extent of biodegradation of fuels using the diastereomers of acyclic isoprenoids. Environ. Sci. Technol. 41(7): 2452–2458.

McMurdie, P.J., and S. Holmes. 2013. Phyloseq: An R package for reproducible interactive analysis and graphics of microbiome census data. PLoS One 8(4).

Meckenstock, R.U., B. Morasch, C. Griebler, and H.H. Richnow. 2004. Stable isotope fractionation analysis as a tool to monitor biodegradation in contaminated acquifers. J. Contam. Hydrol. 75(3–4): 215–255.

Megharaj, M., B. Ramakrishnan, K. Venkateswarlu, N. Sethunathan, and R. Naidu. 2011. Bioremediation approaches for organic pollutants: A critical perspective. Environ. Int. 37(8): 1362–1375.

Menendez-Vega, D., J.L.R. Gallego, A.I. Pelaez, G.F. de Cordoba, J. Moreno, D. Muñoz, and J. Sanchez. 2007. Engineered in situ bioremediation of soil and groundwater polluted with weathered hydrocarbons. Eur. J. Soil Biol. 43: 310–321.

Mills, S.A., and W.T. Frankenberger. 1994. Evaluation of phosphorus sources promoting bioremediation of diesel fuel in soil. Bull. Environ. Contam. Toxicol. 53(2): 280–284.

Mitchell, A., F. Bucchini, G. Cochrane, H. Denise, P. Ten Hoopen, M. Fraser, S. Pesseat, S. Potter, M. Scheremetjew, P. Sterk, and R.D. Finn. 2016. EBI metagenomics in 2016 - An expanding and evolving resource for the analysis and archiving of metagenomic data. Nucleic Acids Res. 44(Database issue): D595–D603.

Mitra, A., and S. Mukhopadhyay. 2016. Biofilm mediated decontamination of pollutants from the environment. AIMS Bioeng. 3(1): 44–59.

Modrzyński, J.J., J.H. Christensen, P. Mayer, and K.K. Brandt. 2016. Limited recovery of soil microbial activity after transient exposure to gasoline vapors. Environ. Pollut. 216: 826–835.

Morales, M., V. Sentchilo, C. Bertelli, A. Komljenovic, N. Kryuchkovc-Mostacci, A. Bourdilloud, B. Linke, A. Goesmann, K. Harshman, F. Segers, F. Delapierre, D. Fiorucci, M. Seppey, E. Trofimenco, P. Berra, A. El Taher, C. Loiseau, D. Roggero, M. Sulfiotti, A. Etienne, G.R. Buendia, L. Pillard, A. Escoriza, R. Moritz, C. Schneider, E. Alfonso, F. Ben Jeddou, O. Selmoni, G. Resch, G. Greub, O. Emery, M. Dubey, T. Pillonel, M. Robinson-Rechavi, and J.R. Van Der Meer. 2016. The genome of the toluene-degrading Pseudomonas veronii strain 1YdBTEX2 and its differential gene expression in contaminated sand. PLoS One 11(11).

Morasch, B., P. Höhener, and D. Hunkeler. 2007. Evidence for in situ degradation of mono-and polyaromatic hydrocarbons in alluvial sediments based on microcosm experiments with ^{13}C-labeled contaminants. Environ. Pollut. 148(3): 739–748.

Newell, C.J., S.D. Acree, R.R. Ross, and S.G. Huling. 1995. Ground water issue: Light nonaqueous phase liquids. USEPA. https://nepis.epa.gov/Exe/ZyPDF.cgi/10002DXR.PDF?Dockey=10002DXR.PDF (accessed 3 Jan. 2018).

O'Malley, V., T.A.A. Jr, and J. Hellou. 1994. Determination of the $^{13}C/^{12}C$ ratios of individual PAH from environmental samples: Can PAH sources be apportioned? Org. Geochem. 21(6/7): 809–822.

Oburger, E., D.L. Jones, and W.W. Wenzel. 2011. Phosphorus saturation and pH differentially regulate the efficiency of organic acid anion-mediated P solubilization mechanisms in soil. Plant Soil 341(1–2): 363–382.

Ortega-Calvo, J.J., M. Lahlou, and C. Saiz-Jimenez. 1997. Effect of organic matter and clays on the biodegradation of phenanthrene in soils. Int. Biodeterior. Biodegradation 40(2–4): 101–106.

Ouvrard, S., D. Lapole, and J.L. Morel. 2006. Root exudates impact on phenanthrene availability. Water, Air, Soil Pollut. Focus 6: 343–352.

Owen, A.G., D.L. Godbold, D.L. Jones, and L. Stro. 2001. Organic acid behaviour in a calcareous soil : Sorption reactions and biodegradation rates. Soil Biol. Biochem. 33: 2125–2133.

Paliwal, V., S. Puranik, and H.J. Purohit. 2012. Integrated perspective for effective bioremediation. Appl. Biochem. Biotechnol. 166(4): 903–924.

Pandey, J., A. Chauhan, and R.K. Jain. 2009. Integrative approaches for assessing the ecological sustainability of *in situ* bioremediation. FEMS Microbiol. Rev. 33(2): 324–375.

Parales, R.E., J.V. Parales, D.A. Pelletier, and J.L. Ditty. 2008. Chapter 1 Diversity of Microbial Toluene Degradation Pathways. *In* Gadd, G.M., Sariaslani, S. (eds.), Advances in applied microbiology. Elsevier, Amsterdam. p. 1–73.

Pérez-Pantoja, D., B. González, and D.H. Pieper. 2010. Aerobic degradation of aromatic hydrocarbons. *In* Timmis, K.N. (ed.), Handbook of Hydrocarbon and Lipid Microbiology. Springer Berlin Heidelberg, Berlin, Heidelberg. p. 799–837.

Phelps, C.D., and L.Y. Young. 1999. Anaerobic biodegradation of BTEX and gasoline in various aquatic sediments. Biodegradation 10(1): 15–25.

Philipp, B., and B. Schink. 2012. Different strategies in anaerobic biodegradation of aromatic compounds: Nitrate reducers versus strict anaerobes. Environ. Microbiol. Rep. 4(5): 469–478.

Philp, P., J.O.N. Allen, and J.T. Wilson. 2002. Biodegradation of MTBE in groundwater at a gasoline release. Environ. Sci. Technol. 36(23): 5139–5146.

Pignatello, J.J., and B. Xing. 1996. Mechanisms of slow sorption of organic chemicals to natural particles. Environ. Sci. Technol. 30(1): 1–11.

Polen, T., D. Schluesener, A. Poetsch, M. Bott, and V.F. Wendisch. 2007. Characterization of citrate utilization in Corynebacterium glutamicum by transcriptome and proteome analysis. FEMS Microbiol. Lett. 273(1): 109–119.

Pouralhosseini, S. 2013. Making ZnO adsorption more affordable to remove H2S by changing the catalysts regeneration method. Pet. Sci. Technol. 31(1): 62–67.

Powell, S.M., S.H. Ferguson, I. Snape, and S.D. Siciliano. 2006. Fertilization stimulates anaerobic fuel degradation of antarctic soils by denitrifying microorganisms. Environ. Sci. Technol. 40(6): 2011–2017.

Qian, P., J.J. Schoenau, and N. Ziadi. 2006. Chapter 13 Ion supply rates using ion-exchange resins. *In* Carter, M.R., Gregorich, E.G. (eds.), Soil sampling and methods of analysis. 2nd Edi. CRC Press, Boca Raton. p. 135–140.

Qiu, B., L. Han, J. Wang, L. Chang, and W. Bao. 2011. Preparation of sorbents loaded on activated carbon to remove H2S from hot coal gas by supercritical water impregnation. Energy and Fuels 25(2): 591–595.

Quadros, P.D. de, V.S. Cerqueira, J.C. Cazarolli, M. do C.R. Peralba, F.A.O. Camargo, A. Giongo, and F.M. Bento. 2016. Oily sludge stimulates microbial activity and changes microbial structure in a landfarming soil. Int. Biodeterior. Biodegrad. 115: 90–101.

Qu, D., Y. Zhao, J. Sun, H. Ren, and R. Zhou. 2015. BTEX biodegradation and its nitrogen removal potential by a newly isolated *Pseudomonas thivervalensis* MAH1. Can. J. Microbiol. 61(9): 691–699.

R Core Team. 2016. R: A language and environment for statistical computing. R Foundation for Statistical Computing, Vienna, Austria, Austria.

Rahman, K.S.M., J. Thahira-Rahman, P. Lakshmanaperumalsamy, and I.M. Banat. 2002. Towards efficient crude oil degradation by a mixed bacterial consortium. Bioresour. Technol. 85(3): 257–261.

Ramette, A. 2007. Multivariate analyses in microbial ecology. FEMS Microbiol. Ecol. 62(2): 142–160.

Ranck, J.M. 2003. BTEX removal from produced water using surfactant-modified zeolite.

Master's thesis, New Mexico Institute of Mining and Technology, Socorro.

Raynaud, X., B. Jaillard, P.W. Leadley, X. Raynaud, and P.W. Leadley. 2016. Plants may alter competition by modifying nutrient bioavailability in rhizosphere : A modeling approach. Am. Nat. 171(1): 44–58.

Rentz, J.A., P.J.J. Alvarez, and J.L. Schnoor. 2004. Repression of Pseudomonas putida phenanthrene-degrading activity by plant root extracts and exudates. Environ. Microbiol. 6(6): 574–583.

Revesz, K., T.B. Coplen, M.J. Baedecker, P.D. Glynn, and M. Hult. 1995. Methane production and consumption monitored by stable H and C isotope ratios at a crude oil spill site, Bemidji, Minnesota. Appl. Geochemistry 10(5): 505–516.

Richnow, H.H., E. Annweiler, W. Michaelis, and R.U. Meckenstock. 2003a. Microbial *in situ* degradation of aromatic hydrocarbons in a contaminated aquifer monitored by carbon isotope fractionation. J. Contam. Hydrol. 65(1–2): 101–120.

Richnow, H.H., R.U. Meckenstock, L.A. Reitzel, A. Baun, A. Ledin, and T.H. Christensen. 2003b. *In situ* biodegradation determined by carbon isotope fractionation of aromatic hydrocarbons in an anaerobic landfill leachate plume (Vejen, Denmark). J. Contam. Hydrol. 64(1–2): 59–72.

Robertson, S.J., W.B. McGill, H.B. Massicotte, and P.M. Rutherford. 2007. Petroleum hydrocarbon contamination in boreal forest soils: A mycorrhizal ecosystems perspective. Biol. Rev. 82(2): 213–240.

Rodríguez, H., and R. Fraga. 1999. Phosphate solubilizing bacteria and their role in plant growth promotion. Biotechnol. Adv. 17(4–5): 319–339.

Rohrbacher, F., and M. St-Arnaud. 2016. Root exudation: The ecological driver of hydrocarbon rhizoremediation. Agronomy 6(1): 19.

Rojas-Avelizapa, N.G., T. Roldán-Carrillo, H. Zegarra-Martínez, A.M. Muñoz-Colunga, and L.C. Fernández-Linares. 2007. A field trial for an *ex-situ* bioremediation of a drilling mud-polluted site. Chemosphere 66(9): 1595–1600.

Romero, A., A. Santos, T. Cordero, J. Rodríguez-Mirasol, J.M. Rosas, and F. Vicente. 2011. Soil remediation by Fenton-like process: Phenol removal and soil organic matter modification. Chem. Eng. J. 170(1): 36–43.

Safinowski, M., and R.U. Meckenstock. 2006. Methylation is the initial reaction in anaerobic naphthalene degradation by a sulfate-reducing enrichment culture. Environ. Microbiol. 8(2): 347–352.

Sarkar, D., M. Ferguson, R. Datta, and S. Birnbaum. 2005. Bioremediation of petroleum hydrocarbons in contaminated soils: Comparison of biosolids addition, carbon supplementation, and monitored natural attenuation. Environ. Pollut. 136(1): 187–195.

Sarkar, P., A. Roy, S. Pal, B. Mohapatra, S.K. Kazy, M.K. Maiti, and P. Sar. 2017. Enrichment and characterization of hydrocarbon-degrading bacteria from petroleum refinery waste as potent bioaugmentation agent for *in situ* bioremediation. Bioresour. Technol. 242: 15–27.

Sashidhar, B., and a R. Podile. 2010. Mineral phosphate solubilization by rhizosphere bacteria

and scope for manipulation of the direct oxidation pathway involving glucose dehydrogenase. J. Appl. Microbiol. 109(1): 1–12.

Saskatchewan Ministry of Environment. 2009. Risk-based corrective actions for petroleum hydrocarbon impacted sites. Saskatchewan Ministry of Environment. http://www.environment.gov.sk.ca/adx/aspx/adxGetMedia.aspx?DocID=582b2f98-f27d-43d7-8fb6-fa5b50523319&MediaID=1541&Filename=Risk+Based+Corrective+Actions+for+Petroleum+Hydrocarbon+Impacted+Sites.pdf&l=English (accessed 12 Feb. 2016).

Sato, S., and N.B. Comerford. 2006. Organic anions and phosphorus desorption and bioavailability in a humid brazilian ultisol. Soil Sci. 171(9): 695–705.

Scherr, K., H. Aichberger, R. Braun, and A.P. Loibner. 2007. Influence of soil fractions on microbial degradation behavior of mineral hydrocarbons. Eur. J. Soil Biol. 43(5–6): 341–350.

Schoenau, J.J., and I.P. O'Halloran. 2006. Chapter 8 Sodium bicarbonate-extractable phosphorus. *In* Carter, M.R., Gregorich, E.G. (eds.), Soil sampling and methods of analysis. 2nd Edi. CRC Press, Boca Raton. p. 89–94.

Schwab, A.P., J. Su, S. Wetzel, S. Pekarek, and M.K. Banks. 1999. Extraction of petroleum hydrocarbons from soil by mechanical shaking. Environ. Sci. Technol. 33(11): 1940–1945.

Schwitzguébel, J.-P., E. Comino, N. Plata, and M. Khalvati. 2011. Is phytoremediation a sustainable and reliable approach to clean-up contaminated water and soil in Alpine areas? Environ. Sci. Pollut. Res. Int. 18(6): 842–856.

Sheng, Y., X. Tian, G. Wang, C. Hao, and F. Liu. 2015. Bacterial diversity and biogeochemical processes of Oil-contaminated groundwater, Baoding, North China. Geomicrobiol. J. 33(6): 537–551.

Shi, W., H. Shao, H. Li, M. Shao, and S. Du. 2009. Progress in the remediation of hazardous heavy metal-polluted soils by natural zeolite. J. Hazard. Mater. 170(1): 1–6.

Siciliano, S.D., T. Chen, C.L. Phillips, J.G. Hamilton, D.M. Hilger, B. Chartrand, J. Grosskleg, K. Bradshaw, T. Carlson, and D. Peak. 2016. Total phosphate influences the rate of hydrocarbon degradation but phosphate mineralogy shapes microbial community composition in cold-region calcareous soils. Environ. Sci. Technol. 50(10): 5197–5206.

Siddique, T., P.M. Rutherford, J.M. Arocena, and R.W. Thring. 2006. A proposed method for rapid and economical extraction of petroleum hydrocarbons from contaminated soils. Can. J. Soil Sci. 86: 725–728.

Sihota, N.J., O. Singurindy, and K.U. Mayer. 2011. CO_2-Efflux measurements for evaluating source zone natural attenuation rates in a petroleum hydrocarbon contaminated aquifer. Environ. Sci. Technol. 45(2): 482–488.

Sihota, N.J., and K. Ulrich Mayer. 2012. Characterizing vadose zone hydrocarbon biodegradation using carbon dioxide effluxes, isotopes, and reactive transport modeling. Vadose Zo. J. 11(4).

Sims, R.C. 1990. Soil remediation techniques at uncontrolled hazardous waste sites. J. Air Waste Manage. Assoc. 40(5): 704–732.

Smets, W., J.W. Leff, M.A. Bradford, R.L. McCulley, S. Lebeer, and N. Fierer. 2016. A method for simultaneous measurement of soil bacterial abundances and community composition via 16S rRNA gene sequencing. Soil Biol. Biochem. 96: 145–151.

Sousa, C.A. De. 2006. Urban brownfields redevelopment in Canada : the role of local government. Can. Geogr. 50(3): 392–407.

Staunton, S., and F. Leprince. 1996. Effect of pH and some organic anions on the solubility of soil phosphate : implications for P bioavailability. J. Soil Sci. 47: 231–239.

Stelmach, W., P. Szarlip, A. Trembaczowski, A. Bieganowski, and Y. Kuzyakov. 2016. Suppression of soil organic matter decomposition by gasoline and diesel as assessed by ^{13}C natural abundance. Eur. J. Soil Biol. 73: 8–14.

Strobel, B.W. 2001. Influence of vegetation on low-molecular-weight carboxylic acids in soil solution—A review. Geoderma 99(3–4): 169–198.

Ström, L., A.G. Owen, D.L. Godbold, and D.L. Jones. 2005. Organic acid behaviour in a calcareous soil implications for rhizosphere nutrient cycling. Soil Biol. Biochem. 37(11): 2046–2054.

Su, X., H. Lv, W. Zhang, Y. Zhang, and X. Jiao. 2013. Evaluation of petroleum hydrocarbon biodegradation in shallow groundwater by hydrogeochemical indicators and C, S-isotopes. Environ. Earth Sci. 69(6): 2091–2101.

Subramaniam, K., C. Stepp, J.J. Pignatello, B. Smets, and D. Grasso. 2004. Enhancement of polynuclear aromatic hydrocarbon desorption by complexing agents in weathered soil. Enviromental Eng. Sci. 21(4): 515–523.

Sullivan, E., and M. Sylvester. 2006. The evolution of environmental risk management. Risk Manag. 53(1): 30–33.

Sun, T.R., L. Cang, Q.Y. Wang, D.M. Zhou, J.M. Cheng, and H. Xu. 2010. Roles of abiotic losses, microbes, plant roots, and root exudates on phytoremediation of PAHs in a barren soil. J. Hazard. Mater. 176(1–3): 919–925.

Sun, T.R., L.M. Ottosen, P.E. Jensen, and G.M. Kirkelund. 2012. Electrodialytic remediation of suspended soil--Comparison of two different soil fractions. J. Hazard. Mater. 203–204: 229–235.

Tamura, K., and M. Nei. 1993. Estimation of the number of nucleotide substitutions in the control region of mitochondrial DNA in humans and chimpanzees. Mol. Biol. Evol. 10(3): 512–526.

Testa, S.M., and J.A. Jacobs. 2014. Oil spills and gas leaks: Environmental response, prevention, and cost recovery. McGraw-Hill Education, New York City.

Thompson, L.M., C.A. Black, and J.A. Zoellner. 1954. Occurrence and mineralization of organic phosphorus in soils, with particular references and associations with nitrogen, carbon and pH.pdf. Soil Sci. 77(3): 185–196.

Thullner, M., F. Centler, H.H. Richnow, and A. Fischer. 2012. Quantification of organic pollutant degradation in contaminated aquifers using compound specific stable isotope analysis - Review of recent developments. Org. Geochem. 42(12): 1440–1460.

Tiehm, a, and S. Schulze. 2003. Intrinsic aromatic hydrocarbon biodegradation for groundwater remediation. Oil Gas Sci. Technol. L Inst. Fr. Du Pet. 58(4): 449–462.

Tierney, M., and L.Y. Young. 2010. Anaerobic degradation of aromatic hydrocarbons. *In* Timmis, K.N. (ed.), Handbook of hydrocarbon and lipid microbiology. Springer Berlin Heidelberg, Berlin, Heidelberg. p. 925–934.

Tiessen, H., and J.O. Moir. 2006. Chapter 25 Characterization of available P by sequential extraction. *In* Carter, M.R., Gregorich, E.G. (eds.), Soil sampling and methods of analysis. 2nd Edi. CRC Press, Boca Raton. p. 293–306.

Tong, M., and S. Yuan. 2012. Physiochemical technologies for HCB remediation and disposal: A review. J. Hazard. Mater. 229–230: 1–14.

Townsend, G.T., R.C. Prince, and J.M. Suflita. 2004. Anaerobic biodegradation of alicyclic constituents of gasoline and natural gas condensate by bacteria from an anoxic aquifer. FEMS Microbiol. Ecol. 49(1): 129–135.

Turner, B.L., B.J. Cade-Menun, L.M. Condron, and S. Newman. 2005. Extraction of soil organic phosphorus. Talanta 66(2): 294–306.

Tyagi, M., M.M.R. da Fonseca, and C.C.C.R. de Carvalho. 2011. Bioaugmentation and biostimulation strategies to improve the effectiveness of bioremediation processes. Biodegradation 22(2): 231–241.

Ulrich, A.C., H.R. Beller, and E.A. Edwards. 2005. Metabolites detected during biodegradation of $^{13}C_6$-benzene in nitrate-reducing and methanogenic enrichment cultures. Environ. Sci. Technol. 39(17): 6681–6691.

Un, J.L.I., J.O.J.P. Ignatello, B.A.F.S. Mets, D.O.G. Rasso, and E.S.M. Onserrate. 2005. Bench-scale evaluation of *in situ* bioremediation strategies for soil at a former manufactured gas plant site. Environ. Toxicol. Chem. 24(3): 741–749.

Usdowski, E., and J. Hoefs. 1986. $^{13}C/^{12}C$ partitioning and kinetics of CO_2 absorption by hydroxide buffer solutions. Earth Planet. Sci. Lett. 80(1–2): 130–134.

Usdowski, E., and J. Hoefs. 1988. $^{13}C/^{12}C$ fractionation during the chemical absorption of CO_2 gas by the NH_3-NH_4Cl buffer. Chem. Geol. Isot. Geosci. Sect. 73(1): 79–85.

Vasudevan, N., and P. Rajaram. 2001. Bioremediation of oil contaminated soil. Environ. Int. 26: 409–411.

Vogt, C., S. Kleinsteuber, and H.H. Richnow. 2011. Anaerobic benzene degradation by bacteria. Microb. Biotechnol. 4(6): 710–724.

Wang, Y., X. Chen, J.K. Whalen, Y. Cao, Z. Quan, C. Lu, and Y. Shi. 2015. Kinetics of inorganic and organic phosphorus release influenced by low molecular weight organic acids in calcareous, neutral and acidic soils. J. Plant Nutr. Soil Sci. 178(4): 555–566.

Wang, Y., L. Fang, L. Lin, T. Luan, and N.F.Y. Tam. 2014. Effects of low molecular-weight organic acids and dehydrogenase activity in rhizosphere sediments of mangrove plants on phytoremediation of polycyclic aromatic hydrocarbons. Chemosphere 99: 152–159.

Wang, J., X. Feng, C.W.N. Anderson, Y. Xing, and L. Shang. 2012a. Remediation of mercury contaminated sites - A review. J. Hazard. Mater. 221–222: 1–18.

Wang, C., Z. Wang, L. Lin, B. Tian, and Y. Pei. 2012b. Effect of low molecular weight organic acids on phosphorus adsorption by ferric-alum water treatment residuals. J. Hazard. Mater. 203–204: 145–150.

Wang, Z., Y. Xu, J. Zhao, F. Li, D. Gao, and B. Xing. 2011. Remediation of petroleum contaminated soils through composting and rhizosphere degradation. J. Hazard. Mater. 190(1): 677–685.

Weelink, S.A.B., M.H.A. van Eekert, and A.J.M. Stams. 2010. Degradation of BTEX by anaerobic bacteria: Physiology and application. Rev. Environ. Sci. Biotechnol. 9(4): 359–385.

Weelink, S.A.B., N.C.G. Tan, H. Ten Broeke, W. Van Doesburg, A.A.M. Langenhoff, J. Gerritse, and A.J.M. Stams. 2007. Physiological and phylogenetic characterization of a stable benzene-degrading, chlorate-reducing microbial community. FEMS Microbiol. Ecol. 60(2): 312–321.

Wei, L., C. Chen, and Z. Xu. 2010. Citric acid enhances the mobilization of organic phosphorus in subtropical and tropical forest soils. Biol. Fertil. Soils 46(7): 765–769.

Wentzel, A., T.E. Ellingsen, H.K. Kotlar, S.B. Zotchev, and M. Throne-Holst. 2007. Bacterial metabolism of long-chain n-alkanes. Appl. Microbiol. Biotechnol. 76(6): 1209–1221.

Weyers, E., D.G. Strawn, D. Peak, A.D. Moore, L.L. Baker, and B. Cade-Menun. 2016. Phosphorus speciation in calcareous soils following annual dairy manure amendments. Soil Sci. Soc. Am. J. 80: 1531–1542.

White, J.C., M.I. Mattina, W.Y. Lee, B.D. Eitzer, and W. Iannucci-Berger. 2003. Role of organic acids in enhancing the desorption and uptake of weathered *p,p*'-DDE by *Cucurbita pepo*. Environ. Pollut. 124(1): 71–80.

Whittaker, M., S.J.T. Pollard, A.E. Fallick, and T. Preston. 1996. Characterisation of refractory wastes at hydrocarbon-contaminated sites - II. Screening of reference oils by stable carbon isotope fingerprinting. Environ. Pollut. 94(2): 195–203.

Widdel, F., and R. Rabus. 2001. Anaerobic biodegradation of saturated and aromatic hydrocarbons. Curr. Opin. Biotechnol. 12(3): 259–276.

Wongbunmak, A., S. Khiawjan, M. Suphantharika, and T. Pongtharangkul. 2017. BTEX- and naphthalene-degrading bacterium *Microbacterium esteraromaticum* strain SBS1-7 isolated from estuarine sediment. J. Hazard. Mater. 339: 82–90.

Xu, R., C. Li, and G. Ji. 2004. Effect of low-molecular-weight organic anions on electrokinetic properties of variable charge soils. J. Colloid Interface Sci. 277(1): 243–247.

Yakubu, M. 2007. Biological approach to oil spills remediation in the soil. African J. Biotechnol. 6(24): 2735–2739.

Yang, S.-Z.Z., H.-J.J. Jin, Z. Wei, R.-X.X. He, Y.-J.J. Ji, X.-M.M. Li, and S.-P.P. Yu. 2009. Bioremediation of oil spills in cold environments: A review. Pedosphere 19(3): 371–381.

Yang, Y., D. Ratt, B.F. Smets, J.J. Pignatello, and D. Grasso. 2001a. Mobilization of soil organic matter by complexing agents and implications for polycyclic aromatic hydrocarbon desorption. Chemosphere 43(8): 1013–1021.

Yang, Y., D. Ratt, B.F. Smets, J.J. Pignatello, D. Grasso, D. Ratte, B.F. Smets, J.J. Pignatello, D. Grasso, D. Ratt, B.F. Smets, J.J. Pignatello, and D. Grasso. 2001b. Mobilization of soil organic matter by complexing agents and implications for polycyclic aromatic hydrocarbon desorption. Chemosphere 43(8): 1013–1021.

Yanhong, Z.H.U., Z. Shuzhen, H. Honglin, and W.E.N. Bei. 2009. Effects of maize root exudates and organic acids on the desorption of phenanthrene from soils. J. Environ. Sci. 21(7): 920–926.

Yao, Z., J. Li, H. Xie, and C. Yu. 2012. Review on remediation technologies of soil contaminated by heavy metals. Procedia Environ. Sci. 16: 722–729.

Yergeau, E., M. Arbour, R. Brousseau, D. Juck, J.R. Lawrence, L. Masson, L.G. Whyte, and C.W. Greer. 2009. Microarray and real-time PCR analyses of the responses of high-arctic soil bacteria to hydrocarbon pollution and bioremediation treatments. Appl. Environ. Microbiol. 75(19): 6258–6267.

Yli-Halla, M. 2016. Fate of fertilizer P in soils: Inorganic pathway. *In* Schnug, E., De Kok, L.J. (eds.), Phosphorus in agriculture: 100 % zero. Springer Netherlands, Dordrecht. p. 27–40.

Yu, G., D.K. Smith, H. Zhu, Y. Guan, and T.T.Y. Lam. 2017. ggtree: An R package for visualization and annotation of phylogenetic trees with their covariates and other associated data. Methods Ecol. Evol. 8(1): 28–36.

van der Zaan, B.M., F.T. Saia, A.J.M. Stams, C.M. Plugge, W.M. de Vos, H. Smidt, A.A.M. Langenhoff, and J. Gerritse. 2012. Anaerobic benzene degradation under denitrifying conditions: Peptococcaceae as dominant benzene degraders and evidence for a syntrophic process. Environ. Microbiol. 14(5): 1171–1181.

Zhang, T., T.S. Bain, K.P. Nevin, M.A. Barlett, and D.R. Lovley. 2012. Anaerobic benzene oxidation by Geobacter species. Appl. Environ. Microbiol. 78(23): 8304–8310.

Zhang, T., S.M. Gannon, K.P. Nevin, A.E. Franks, and D.R. Lovley. 2010. Stimulating the anaerobic degradation of aromatic hydrocarbons in contaminated sediments by providing an electrode as the electron acceptor. Environ. Microbiol. 12(4): 1011–1020.

Zhang, Z., and I.M.C. Lo. 2015. Biostimulation of petroleum-hydrocarbon-contaminated marine sediment with co-substrate: Involved metabolic process and microbial community. Appl. Microbiol. Biotechnol. 99(13): 5683–5696.

Zhang, X., and L.Y. Young. 1997. Carboxylation as an initial reaction in the anaerobic metabolism of naphthalene and phenanthrene by sulfidogenic consortia . Appl. Environ. Microbiol. 63(12): 4759–4764.

Zhao, Y., D. Qu, Z. Hou, and R. Zhou. 2014. Enhanced natural attenuation of BTEX in the nitrate-reducing environment by different electron acceptors. Environ. Technol. 36(5): 615–621.

Zhou, Q., C.E. Gibson, and Y. Zhu. 2001. Evaluation of phosphorus bioavailability in sediments of three contrasting lakes in China and the UK. Chemosphere 42(2): 221–225.

Zhou, Y.Y., H. Huang, and D. Shen. 2016. Multi-substrate biodegradation interaction of 1, 4-dioxane and BTEX mixtures by Acinetobacter baumannii DD1. Biodegradation 27(1): 37–46.

Zytner, R.G. 2002. Organic compounds in unsaturated soil. J. Soil Contam. 4: 123–135.

APPENDIX 1

Table A1.1. Correlation matrix of analyzed variables during anaerobic gasoline biodegradation (10°C).

	W_{BTEX}†	$W_{F1\text{-}BTEX}$	W_{F1}	S_{BTEX}	$S_{F1\text{-}BTEX}$	S_{F1}	T_{BTEX}	$T_{F1\text{-}BTEX}$	T_{F1}	$K_{SW\text{-}BTEX}$	$K_{SW\text{-}F1\text{-}BTEX}$	$K_{SW\text{-}F1}$
W_{BTEX}		0.89‡	0.94	-0.42	-0.48	-0.48	0.73	0.45	0.55	-0.53	-0.54	-0.56
$W_{F1\text{-}BTEX}$	0.00		0.99	-0.40	-0.48	-0.46	0.64	0.57	0.61	-0.50	-0.55	-0.56
W_{F1}	0.00	0.00		-0.42	-0.49	-0.48	0.68	0.55	0.61	-0.52	-0.56	-0.57
S_{BTEX}	0.00	0.00	0.00		0.94	0.96	0.29	0.46	0.42	0.90	0.72	0.79
$S_{F1\text{-}BTEX}$	0.00	0.00	0.00	0.00		1.00	0.19	0.44	0.38	0.86	0.77	0.83
S_{F1}	0.00	0.00	0.00	0.00	0.00		0.21	0.44	0.39	0.88	0.77	0.83
T_{BTEX}	0.00	0.00	0.00	0.00	0.01	0.00		0.84	0.91	0.07	-0.09	-0.05
$T_{F1\text{-}BTEX}$	0.00	0.00	0.00	0.00	0.00	0.00	0.00		0.99	0.25	0.11	0.16
T_{F1}	0.00	0.00	0.00	0.00	0.00	0.00	0.00	0.00		0.21	0.06	0.11
$K_{SW\text{-}BTEX}$	0.00	0.00	0.00	0.00	0.00	0.00	0.33	0.00	0.00		0.91	0.95
$K_{SW\text{-}F1\text{-}BTEX}$	0.00	0.00	0.00	0.00	0.00	0.00	0.20	0.11	0.39	0.00		0.99
$K_{SW\text{-}F1}$	0.00	0.00	0.00	0.00	0.00	0.00	0.49	0.02	0.11	0.00	0.00	

† Variables starting with W correspond to the concentration of the compound in the water phase. S means the concentration of the compound in the soil phase and T is for the total amount in the microcosm. Variables starting with K_{SW} represent the distribution factor for the compound between soil and water.

‡ The top right values are Pearson correlation coefficients and the left bottom values are the corresponding p-values for the correlation matrix.

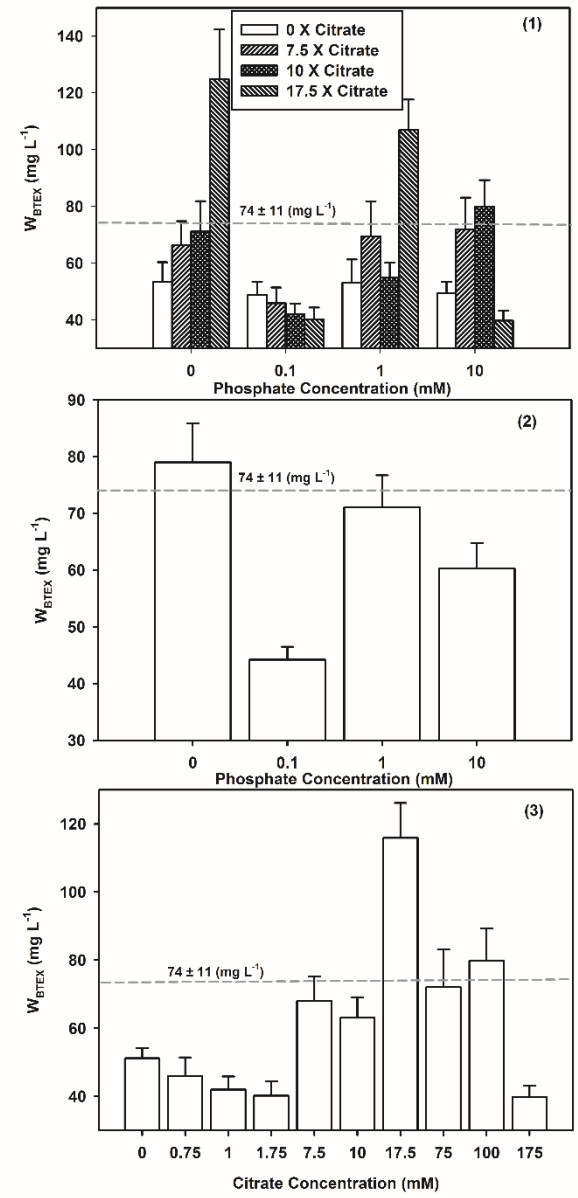

Fig. A1.1. The concentration of BTEX in the water phase (W_{BTEX}) in the microcosm, (1) for different amendment treatments, (2) for different phosphate addition, and (3) for different citrate addition, under anaerobic conditions at 10°C during a three-week incubation. For panel (1), averages of 12 replicates (three replicates per each soil, four soils) are denoted by bars with the error bars representing the standard error (SE) from the mean; the pattern of bars corresponds to the same ratio for citrate:phosphate (the 0 X citrate means 0 times of phosphate concentration for citrate added in that treatment) treatment. The grey dash line indicates the average benzene concentration in the abiotic control treatment (0.2% sodium azide, 1 mM phosphate, and 10 mM citrate, 12 replicates). Another abiotic control (amended with 1 mM phosphate and 10 mM citrate addition) was gamma irradiated, and had 75 ± 10 mg L^{-1} value for W_{BTEX}.

APPENDIX 2

Table A2.1. Total elemental concentrations of all borehole/soil samples.

Sample ID	Borehole Position	Treatment	Soil Zone	Total Elemental Concentration†				
				Fe	P	Ca	Mg	S
				mg kg^{-1}				
15-01-5	1 (in Area 2)	No Amendment	Saturated	35200	1040	27300	14400	-‡
15-10-5		Phosphate Amendment		37100	930	29400	12500	88
16-01-5		Phosphate and Citrate Amendment		43800	1000	12900	13500	34
15-02-2	2 (in Area 2)	No Amendment	Unsaturated	14100	1240	7610	7010	1830
15-11-2		Phosphate Amendment		35000	930	5640	8250	210
16-02-2		Phosphate and Citrate Amendment		12600	1210	5290	6960	1240
15-04-2	4 (in Area 1)	No Amendment	Unsaturated	26500	1160	10100	8230	70
15-13-2		Phosphate Amendment		26400	1030	7930	7030	150
16-04-2		Phosphate and Citrate Amendment		25200	1170	7950	6900	315
15-04-6		No Amendment	Saturated	30900	980	17600	15500	80
15-13-6		Phosphate Amendment		38900	970	21600	12000	120
16-04-6		Phosphate and Citrate Amendment		35300	1090	20900	12800	95

† Concentrations accurate within ±10%
‡ Element not detected

Table A2.2. The p-values from the Kruskal-Wallis rank sum test for the effect of treatment, area, and soil zone on soil properties.

Soil Property	Kruskal-Wallis rank sum test		
	Treatment	**Area**	**Soil Zone**
Resin-P	2.91E-01	1.42E-01	0.00E+00
$NaHCO_3$-IP	9.58E-01	1.80E-01	0.00E+00
$NaHCO_3$-OP	< 2.2E-16	7.90E-02	6.90E-02
NaOH-IP	2.89E-01	2.17E-01	0.00E+00
NaOH-OP	4.10E-02	9.84E-01	0.00E+00
Benzene	4.23E-01	0.00E+00	0.00E+00
Toluene	7.20E-02	0.00E+00	4.00E-03
Ethylbenzene	1.73E-01	2.00E-03	1.00E-03
Xylene	4.72E-01	0.00E+00	1.00E-03
$F1_{-BTEX}$	4.92E-01	2.00E-03	4.00E-03
BTEX	1.51E-01	0.00E+00	0.00E+00
F2	0.00E+00	1.20E-02	1.80E-01
F3	0.00E+00	3.52E-01	8.60E-01

Table A2.3. The p-values from the Kruskal-Wallis rank sum test for the influence of area and treatment on some groundwater properties.

Variables	Types	Area	Treatment
TDS	Normal water property	2.20E-16	3.85E-01
Conductivity		<2.2E-16	2.61E-01
Fluoride	Anion	6.93E-02	3.34E-02
Chloride		5.62E-04	7.24E-01
Bromide		1.94E-08	6.82E-03
Calcium (D)	Cation	1.23E-04	1.79E-02
Calcium (T)		1.26E-03	9.29E-01
Iron (D)		3.82E-04	7.07E-04
Iron (T)		3.06E-06	8.95E-03
Magnesium (D)		2.20E-16	1.20E-02
Magnesium (T)		4.70E-16	1.34E-01
Manganese (D)		1.43E-03	5.34E-02
Manganese (T)		3.15E-04	3.98E-01
Potassium (D)		4.29E-13	3.91E-01
Potassium (T)		1.16E-13	7.57E-01
Sodium (D)		2.20E-16	2.71E-01
Sodium (T)		2.20E-16	3.17E-03

Table A2.4. Soil particle size analysis and soil organic carbon (SOC) result in unsaturated and saturated zones for different soil areas.

Soil Zone	Soil Area	Clay Content (%)		Silt Content (%)		Sand Content (%)		SOC Content (%)	
		Mean	SE	Mean	SE	Mean	SE	Mean	SE
Unsaturated	Background	50.31	6.10	28.31	2.38	21.38	8.43	0.65	0.22
Saturated	Background	56.05	2.96	31.50	0.70	12.45	3.66	0.52	0.03
Unsaturated	Area 1	35.38	3.66	40.97	4.11	23.65	4.24	1.37	0.41
Saturated	Area 1	45.44	5.53	35.75	4.79	18.81	9.19	0.39	0.01
Unsaturated	Area 2	38.57	4.82	35.35	3.49	26.08	2.68	0.75	0.11
Saturated	Area 2	58.04	2.09	34.36	1.14	7.60	2.67	0.68	0.14

Table A2.5. Water Level Logger (Mini-Diver) data for monitoring wells from 2015 May 4th to 2016 March 4th by Amec Foster Wheeler (Saskatoon, Canada).

Monitoring well ID	Temperature (°C)	Water head (cm)	Level (m)	Conductivity (µS/cm)
10-02	10.486 (SE = 0.006)	618.79 (SE = 0.36)		
10-03	7.218 (SE = 0.003)		5.0649 (SE = 0.0021)	
13-01	8.794 (SE = 0.012)		2.5284 (SE = 0.0030)	
13-02	9.111 (SE = 0.010)		3.3429 (SE = 0.0019)	1953.61 (SE = 1.96)
13-05	10.341 (SE = 0.017)		2.6870 (SE = 0.0020)	
13-08	7.102 (SE = 0.006)		2.6732 (SE = 0.0008)	
East Infiltrator	14.005 (SE = 0.018)	392.49 (SE = 0.45)		
North Infiltrator	13.586 (SE = 0.025)		3.19179 (SE = 0.0034)	1497.97 (SE = 1.33)

Table A2.6. Soil pH after the two different amendment deliveries.

Soil Zone	Treatment	pH
Unsaturated	Phosphate Amendment	7.57 (SE = 0.07)
Unsaturated	Phosphate and Citrate Amendment	7.93 (SE = 0.05)
Saturated	Phosphate Amendment	7.74 (SE = 0.08)
Saturated	Phosphate and Citrate Amendment	8.04 (SE = 0.06)

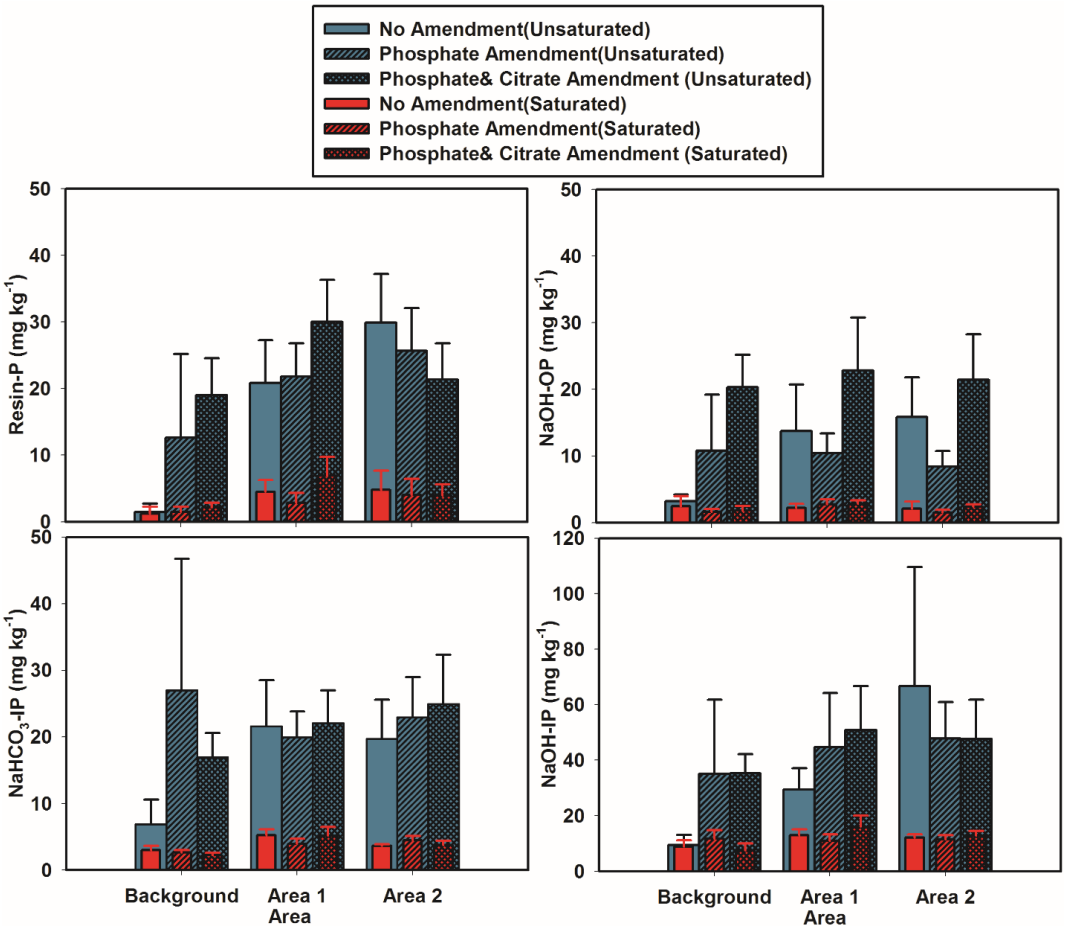

Fig. A2.1. Soil sequential extracted phosphorus forms in different soil zones across three site treatment areas. Averages for the unsaturated zone average are denoted by the dark cyan bars with the vertical bars marking the standard error from the mean. Values for the saturated zone are denoted by red bars with standard error vertical bars. Three treatments for the same zone are denoted with the black edge monochrome pattern for the same color.

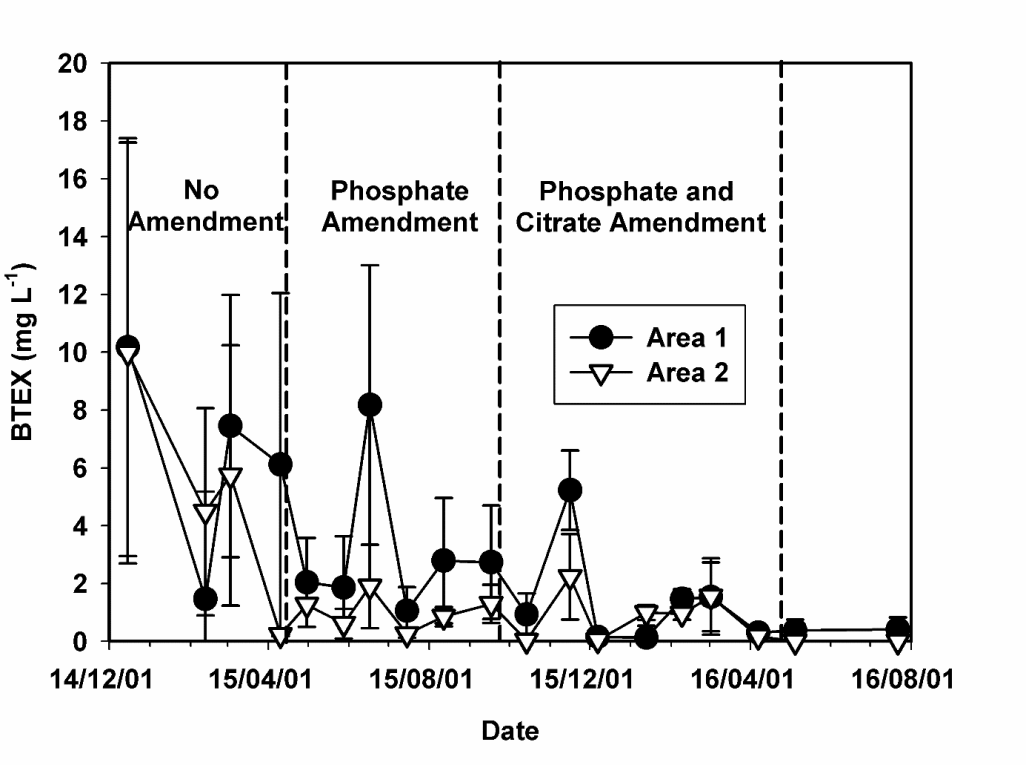

Fig. A2.2. Concentration of benzene, toluene, ethylbenzene and xylene (BTEX) in groundwater in Area 1 and Area 2 after subtracting the background concentration, during different biostimulation treatments. Values for Area 1 are denoted by dark circles with the vertical bars marking the standard error. Averages for Area 2 are denoted by white triangles with the vertical bars marking the standard error.

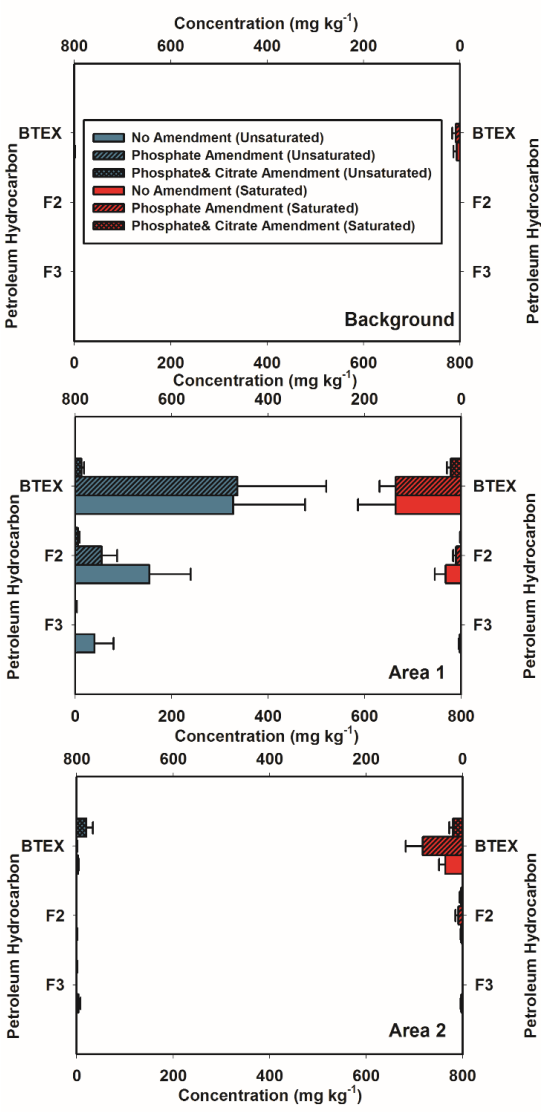

Fig. A2.3. Petroleum hydrocarbon fractions in different soil zones across three site treatment areas. Averages for the unsaturated zone average are denoted by the dark cyan bars with the vertical bars marking the standard error from the mean. Values for the saturated zone are denoted by red bars with standard error vertical bars. Three treatments for the same zone are denoted with the black edge monochrome patter for the same color.

APPENDIX 3

Table A3.1. Primers for the q-PCR to detect anaerobic biodegradation aromatic hydrocarbons.

Target gene	Primer or probe (5'–3' sequence)	Reference
bzdN	Forward (GAGCCGCACATCTTCGGCAT)	(Kuntze et al., 2011)
	Reverse (TRTGVRCCGGRTARTCCTTSGTCGG)	
bcrC	Forward (CGHATYCCRCGSTCGACCATCG)	
	Reverse (CGGATCGGCTGCATCTGGCC)	

Table A3.2. Diversity statistics for bacterial community in the groundwater and soil.

Sample Source	Treatment	N	Richness	Chao	D	Evenness (for Simpson)	H	E-evenness	J-evenness
Groundwater	No Amendment	12	341 ± 39 a†	760 ± 54 b	0.83 ± 0.04 b	0.023 ± 0.003 a	2.88 ± 0.16 c	0.059 ± 0.005 b	0.50 ± 0.02 b
	Phosphate Amendment	20	429 ± 27 a	982 ± 47 a	0.94 ± 0.01 a	0.063 ± 0.022 a	3.67 ± 0.11 a	0.125 ± 0.029 a	0.62 ± 0.02 b
	Phosphate and Citrate Amendment	24	409 ± 19 a	984 ± 41 a	0.90 ± 0.01 a	0.031 ± 0.003 a	3.40 ± 0.08 b	0.080 ± 0.006 a	0.57 ± 0.01 b
Influenced Soil Area	No Amendment	14	264 ± 27 a	813 ± 55 a	0.83 ± 0.01 a	0.026 ± 0.001 a	2.71 ± 0.11 a	0.062 ± 0.003 b	0.49 ± 0.01 ab
	Phosphate Amendment	10	288 ± 23 a	714 ± 58 a	0.84 ± 0.05 a	0.033 ± 0.006 a	3.23 ± 0.24 a	0.099 ± 0.012 a	0.57 ± 0.04 a
	Phosphate and Citrate Amendment	17	247 ± 25 a	799 ± 55 a	0.78 ± 0.04 a	0.028 ± 0.004 a	2.61 ± 0.18 a	0.067 ± 0.008 b	0.48 ± 0.06 b

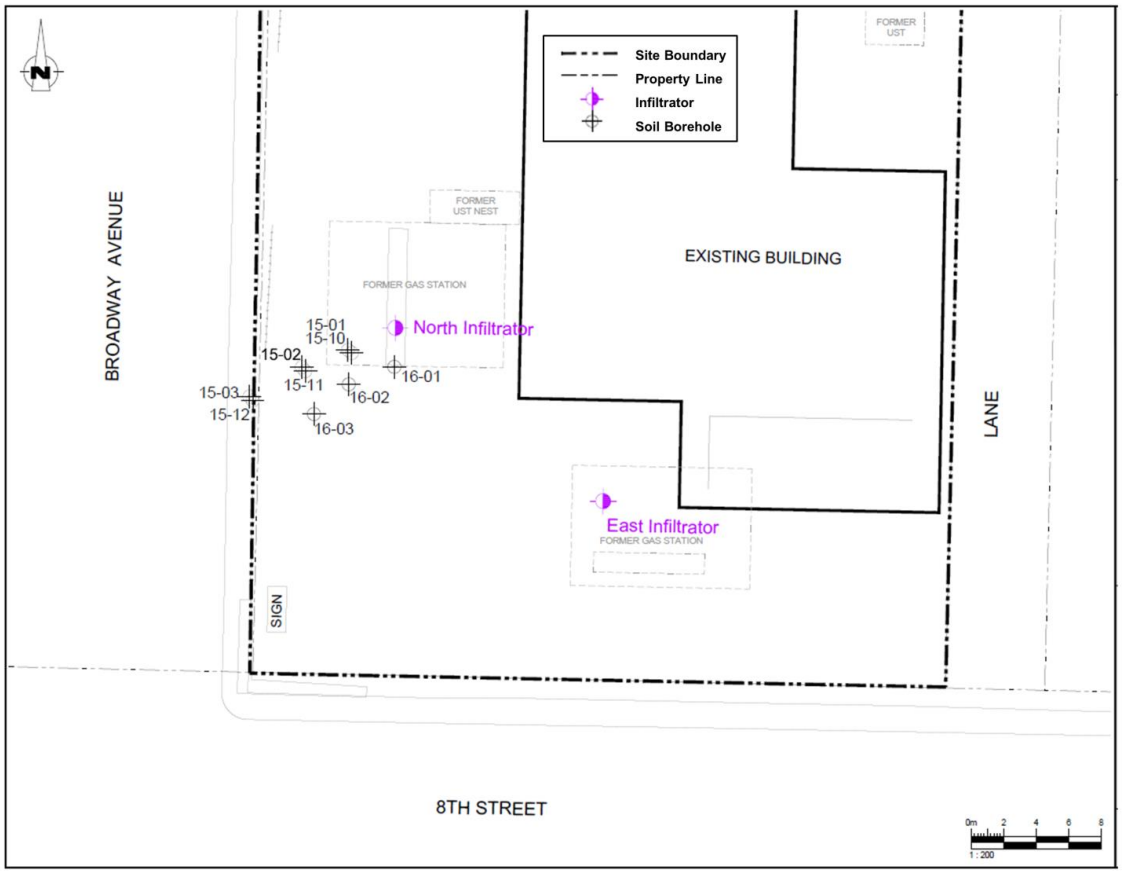

Fig. A3.1. Location of soil boreholes in the influenced soil area and infiltrators at Broadway and 8th street (adapted from a site map provide by Federated Co-operatives Limited). The scale is 1:200.

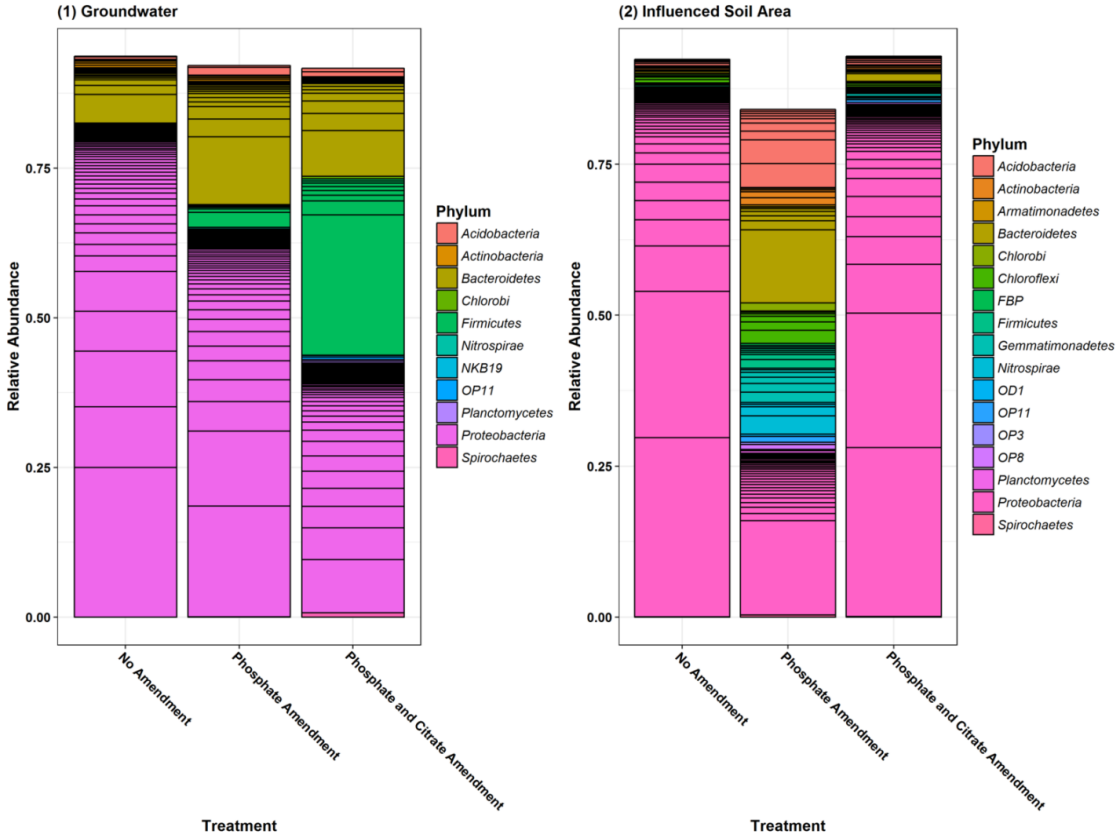

Fig. A3.2. Relative abundance for the top 100 most abundant OTUs in groundwater (1) and soil (2). The stacked bars represent the mean relative abundance (see Table A3.2 for the number of replicates for treatments). Each OTU was presented in a rectangular block with the relative abundance as the height, outlined by a thin black line and filled with the corresponding color for a phylum level.

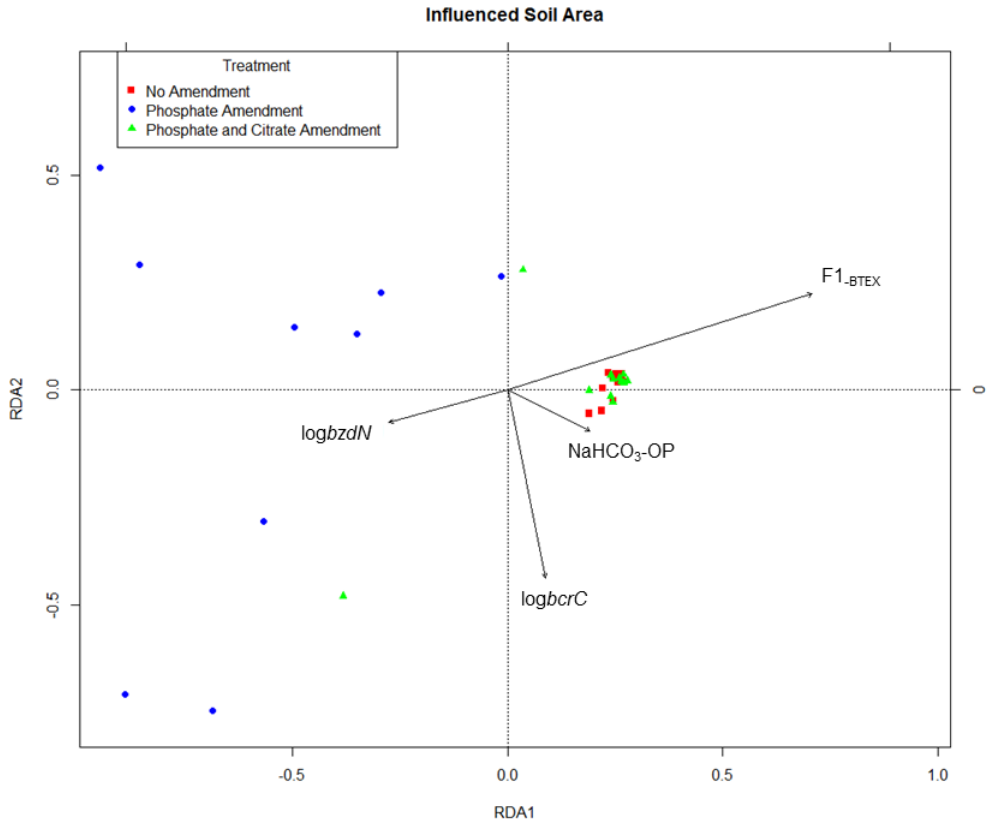

Fig. A3.3. Redundancy analysis (RDA) ordination of the bacterial community composition and other environmental properties. Red square symbols represent samples for no amendment. Blue circle symbols are samples for phosphate amendment. Green triangle symbols are samples for phosphate and citrate amendment. Catabolic gene prevalence for gene *brcC* and *bzdN* (log_{10} transformed copy numbers) are represented by log*brcC* and log*bzdN*. Hydrocarbon and organic phosphorus concentration are also represented by $F1_{-BTEX}$ and $NaHCO_3$-OP.